UNIVERSITY OF ZIMBABWE

FACULTY OF ENGINEERING

DEPARTMENT OF CIVIL ENGINEERING

ASSESSING THE RATE OF SEDIMENTATION OF THE LUBOVANE RESERVOIR AND THE IMPLICATIONS ON THE LIFESPAN OF THE LUSIP PROJECT IN SPHOFANENI, SWAZILAND

SITHEMBISO MKHONTA

MSc Thesis in IWRM

Harare, July 2016

UNIVERSITY OF ZIMBABWE

FACULTY OF ENGINEERING

CIVIL ENGINEERING DEPARTMENT

In collaboration with

ASSESSING THE RATE OF SEDIMENTATION OF THE LUBOVANE RESERVOIR AND THE IMPLICATIONS ON THE LIFESPAN OF THE LUSIP PROJECT IN SPHOFANENI, SWAZILAND

By:

SITHEMBISO MKHONTA

R156384X

Supervisors:

Dr. M.J. Tumbare (University of Zimbabwe)

Eng. A. Mhizha (University of Zimbabwe)

Prof. J. Matondo (University of Swaziland)

A thesis submitted in partial fulfillment of the requirements a Master of Science Degree in Integrated Water Resources Management at the University of Zimbabwe

July, 2016

DECLARATION

I, **Sithembiso Mkhonta**, declare that this research report is my own work. It is being submitted for the partial fulfillment of the degree of Master of Science in Integrated Water Resources Management (IWRM) at the University of Zimbabwe. It has not been submitted for any degree or any examination in any other University.

Date: ___________________________________

Signature: ______________________________

The findings, interpretations and conclusions expressed in this study do neither reflect the views of the University of Zimbabwe, neither the Civil Engineering Department nor the individual members of the MSc Examination Committee, nor their respective employer.

DEDICATION

This research work is dedicated to my lovely parents Sipho and Mirriam Mkhonta and also to my siblings who have supported me throughout my studying period.

ACKNOWLEDGEMENTS

I am thankful to the Lord for giving me strength and courage to conduct this research work with success. I am indebted to WaterNet for granting me this opportunity to study this wonderful programme and also for funding this research work

My sincere gratitude goes to my supervisors, Dr. M. J. Tumbare, Eng. A. Mhizha and Prof. J. Matondo for continuously giving me direction, encouragement and advice. Their support and guidance proved priceless for the entire duration of the research.

The author is also indebted to the Department of Water Affairs Swaziland, Swaziland Meteorological Services and Swaziland Water and Agricultural Development Enterprise (SWADE) for assisting with data and information whenever it was required.

Special thanks are forwarded to the Project Manager of Lower Usuthu Smallholder Irrigation Project Phase I (LUSIP I), Mr. S. Sithole and the Water Manager, Mr. M. Masilela for giving me office space and assisting with equipment that I used to carry out the research. Without their support, the research would not have been a success.

I am indebted to Zine Matshakeni for supporting me throughout this research work. Zine, your support is greatly appreciated.

Furthermore, I would like to thank Mr. Kevin, who assisted massively with the bathymetric survey and also allowed me to use his boat for the depth sounding.

I am also thankful to the University of Swaziland (UNISWA) for giving me working space to process my samples. Sincere gratitude is forward to Mr. S. Simelane who is a lab technician at UNISWA, for assisting me with processing my samples in the lab.

To the MSc IWRM 2015/16 Group, from the bottom of my heart, thank you. We were able to sail through it all. I have learnt a lot from you all and also from the different skills and abilities that each one of you possessed. Special thanks to Alfred Misi and Martin Kabantu for assisting with the GIS related work in my research.

ABSTRACT

An average of 19% of the reservoir storage volumes has been lost to sedimentation in Africa. The Lubovane reservoir in Swaziland, having been commissioned in 2009, is not an exception to sedimentation as all reservoirs globally lose about 1% of their storage due to sedimentation annually. The Lubovane reservoir was constructed as part of the Lower Usuthu Smallholder Irrigation Project (LUSIP) aimed at intensifying and commercializing agriculture for smallholder farmers. The study aimed at determining the rates of sedimentation of the Lubovane reservoir, with sediment deposited from Mhlatuzane River and a canal that conveys water from the Usutu River to the reservoir. Suspended sediment concentration was determined through grab sampling 300mm below the water surface in the canal and the river. The Revised Universal Soil Loss Equation (RUSLE) combined with GIS and remote sensing were used to predict sediment yield for the Mhlatuzane micro-catchment and it was validated using data that was collected from four erosion monitoring plots. A bathymetric survey was conducted in the Lubovane reservoir to determine the sediment that has already settled in the reservoir and the annual capacity loss due to deposition of sediment. The average sediment yield was found to be 26.8, 24.3, 8.83, 29.8 and 8.99 $t.ha^{-1}.yr^{-1}$ for years 1995, 2000, 2005, 2009 and 2015 respectively. Concentration of suspended sediment was found to be 2231 mg/l and 3436 mg/l for Mhlatuzane River and the Feeder canal respectively. The sediment yield of the Mhlatuzane River derived from the sediment concentration was 2.98 $t.ha^{-1}.yr^{-1}$ and the combined sediment yield from the sediment concentration monitoring, was $0.82x10^6$ m^3 leading to a 0.52% of storage capacity. The bathymetric survey data showed that there has already been $14.7x10^6$ m^3 of sediment that has settled in the reservoir to date, with an annual capacity loss of 1.36%. Suspended sediment monitoring underestimated the sediment loading in the reservoir since bedload was not sampled and hence, this method cannot be used to without sampling bedload to adequately monitor siltation of the reservoir. The study then concluded that if no measures are taken to reduce sedimentation and the sedimentation rates remain at this level, the reservoir life will be reduced from 100 years (design lifespan) to 81 years. The loss of storage capacity will lead to an annual loss in 20% yield of 1.23%.

Keywords: Reservoir, Sedimentation, LUSIP, RUSLE, Bathymetry, Yield

List of Abbreviations and Acronyms

DWA	Department of Water Affairs
GoS	Government of Swaziland
SWADE	Swaziland Water and Agricultural Development Enterprise
LUSIP	Lower Usuthu Smallholder Irrigation Project
EIA	Environmental Impact Assessment
WR	Water Resources
IWRM	Integrated Water Resources Management
FC	Feeder Canal
USLE	Universal Soil Loss Equation
RUSLE	Revised Universal Soil Loss Equation
SLEMSA	Soil Loss Estimation Model for Southern Africa
ILWIS	Integrated Land and Water Information Systems
GIS	Geographic Information Systems
NDVI	Normalized Difference Vegetative Index
DEM	Digital Elevation Model
ASTER	Advanced Space born Thermal Emission Radiometer
MDGs	Millennium Development Goals
SDGs	Sustainable Development Goals
GS	Gauging Station

Contents

List of Tables

List of Figures

CHAPTER ONE

1. INTRODUCTION

1.1 Background

Environmental degradation continues to escalate in African River systems and it has resulted in severe soil erosion especially in the tropical regions. Soil fertility loss, desertification and eventually sedimentation of rivers and reservoirs have been the observed results of the uncontrolled environmental degradation (Munthali *et al.*, 2011). According to Fox *et al*. (1997), reservoir sedimentation represents a major problem for the management of water supplies in many parts of the world and may have serious economic implications. All reservoirs will lose their water storage capacity, to a greater or lesser degree, due to sedimentation, and it is necessary to periodically update this information, generally by means of a bathymetric survey (Estigoni *et al.*, 2014). Siltation in reservoirs compromises the storage capacity hence reducing the annual yield that can be attained from the reservoir. In Africa, an average of 19% of the reservoir storage volumes are silted (Jebari *et al.*, 2010). In the Lower Usuthu Smallholder Irrigation Project (LUSIP), sedimentation of the Lubovane reservoir, if high, may lead to reduction of the water available for irrigation and domestic uses. Jain *et al*. (2002) pointed out that assessment of reservoir sedimentation is part of the basic information needed for the operation of any reservoir.

The Lubovane reservoir is the second largest water containment body in Swaziland after Maguga Dam and it is located in the lowveld of Swaziland in the Usuthu river basin. The capacity of the reservoir at full supply level standing at 224 meters above mean sea level, is 155 Mm^3 with 10% of it being dead storage (Mhlanga *et al.*, 2012). The reservoir was constructed upstream of the confluence of two rivers, Golome (ephemeral) and Mhlatuzane (perennial) rivers with tow embankments constructed across each river channel. It receives water mainly from the Mhlatuzane River and a Feeder Canal (FC) that diverts water from the Great Usuthu River. Apart from the two dam embankments (Golome and Mhlatuzane), the reservoir has one saddle dam on the south-east side. The Golome stream was a tributary to Mhlatuzane River and Mhlatuzane empties into the Great Usuthu River.

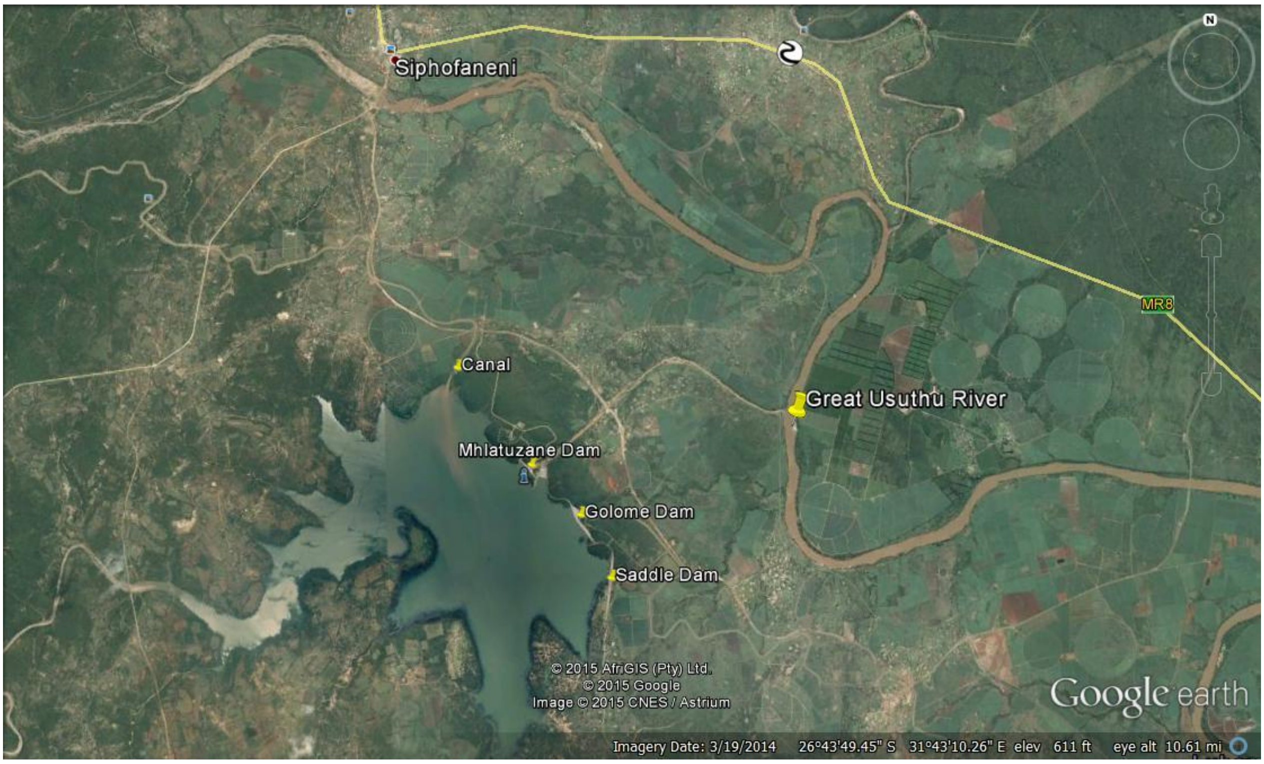

Figure 1-1: Locality map showing the Areas around the reservoir and part of the fields irrigated by the Lubovane reservoir (Accessed on 20 November, 2015)

Construction of the Lubovane reservoir started in 2006 and was completed in 2009. The dam spilled for the first time in 2011. It was constructed by Swaziland Water and Agricultural Development Enterprise (SWADE) as part of a project called the Lower Usuthu Smallholder Irrigation Project (LUSIP). SWADE was mandated by government to implement the project which would see the socio-economic improvement of livelihoods in the Siphofaneni and Matata areas in Swaziland (Figure 1-1). The Government of Swaziland (GoS) identified intensification of farming and commercialization of smallholder agriculture as the main element in its policy to alleviate poverty (Vasudeva, 2006). The smallholder farmers in the lower Usuthu basin were the poorest in the country before the LUSIP project. Evidence from surveys suggested that communities in the project area were very poor (US$ 96 per capita income per annum) compared to other rural areas of Swaziland (MNM-Consultants, 2002). The average per capita income of Swaziland is estimated at US$ 200 per annum.

The project has two phases, namely LUSIP I and LUSIP II. The first phase of the project constituted construction of the two dams, the intake structure, the canals, the pipelines and the balancing dams which would irrigate 6 500 ha in the Lubovane Block. This phase is almost complete the area has already been put under irrigation with the dam further supplying water to three treatment plants constructed strategically to benefit three chiefdoms in that area. Phase II is already under way as some of the funds required have already been sourced from donors and the resettlement process has already begun. The area to be irrigated in phase II is around 5 000 ha and it will get water from the Lubovane reservoir as well. Phase I of the project has already benefitted at least 2 000 farming households through increasing their income and their livelihoods. Livelihoods have also been improved in the aspect of health and safety as residents now have access to safe drinking water and improved sanitation. Due to projects like LUSIP, Swaziland is one of the best success stories of infrastructure's effect on water-related diseases in the rural areas and it is on track to achieve 100% water and sanitation services coverage by 2022 (Mwendera, 2006).

1.2 Problem statement

According to Vakakis-International (2000), during the design phase of the Lubovane reservoir, there were no accurate sediment data available for any rivers in Swaziland. As a result, regional estimates for design purposes, published in the WR90 Study by the South African Water Research Commission in 1990 (Midgley *et al.*, 1994) were used to design the reservoir. The regional estimates were based on field sediment data and reservoir bathymetric surveys done in South Africa and they were adopted in the feasibility study for sedimentation rates in Lubovane reservoir. For the Lubovane, the regional yield of the sub-catchment feeding to the reservoir was assumed at 6.24 $t.ha^{-1}.yr^{-1}$ (Vakakis-International, 2000).

After the Lubovane reservoir was commissioned, farming activities increased rapidly both downstream and upstream of the reservoir. The communities that were displaced by the project were relocated to areas that are upstream of the reservoir and that led to deforestation of large areas to allow construction of homesteads. These changes in land cover have an influence on the sediment yield of the Mhlatuzane micro-catchment. The regional estimates of sediment yields which were made had different land cover characteristics than the current one and there is currently no monitoring of sediment load in the River and the Feeder canal. The actual sediment yield of the sub-basin is thus currently not known.

The Swaziland IWRM Status report (Manyatsi and Brown, 2009) revealed that stakeholders are concerned that the business-as-usual approach to land management is adversely affecting both quantity and quality of water in the basin from sedimentation. Appendix 1 shows deposition of silt at the canal discharge point and at Othandweni Bridge upstream of Lubovane reservoir. This study assessed the sediment yield of the Mhlatuzane micro-catchment; hence the sedimentation rates of the Lubovane reservoir to determine the sustainability of the LUSIP project with respect to continued availability of water for irrigation and domestic use.

1.3 Justification of the Study

The Lubovane reservoir is the main pillar of the Lower Usuthu Smallholder Irrigation Project as it is the source of water for irrigation and domestic use. Development of new irrigation schemes and sustainability of the existing schemes developed in LUSIP I depends on the continued availability of water from the reservoir. The LUSIP was one of the major efforts the Government of Swaziland made to try and meet most of the then Millennium Development Goals (MDGs), now Sustainable Development Goals (SDGs), more especially MDG1 (now SDG 1 & 2) which was to eradicate extreme poverty and hunger (Vasudeva, 2006). The project also assists the country's efforts towards meeting other SDGs like promoting primary education, gender mainstreaming among others. The information that will be generated through this study will reveal the sediment yield of the catchment draining into the reservoir and the sediment loading from the canal. The information will then be used to inform decision makers whether soil conservation measures have to be put in place to reduce sediment yield or such is not necessary. Also, it will inform planners of the LUSIP II Project as to how much land they can develop in light of the annual reduction of the capacity of the reservoir due to sedimentation.

1.4 Objectives

1.4.1 General Objective

The project aimed at determining the sediment yield of the Mhlatuzane micro-catchment; hence the sedimentation rates of the Lubovane reservoir so as to determine its implications on the lifespan of the LUSIP with respect to continued availability of water for irrigation and domestic use.

1.4.2 Specific Objectives

1. To determine the land use and land cover changes in the Mhlatuzane micro-catchment before and after the LUSIP project implementation and to assess their contribution to sedimentation.

2. To assess the soil erosion potential of the Mhlatuzane catchment using the RUSLE model.

3. To estimate the annual rate of sedimentation of the reservoir, due to sediment load from the Mhlatuzane micro-catchment and the Feeder canal.

4. To extrapolate the reservoir water yield into the future with the current annual rates of sedimentation of the Lubovane reservoir.

1.5 Research questions

The research questions which lead to the achievement of the objective of this study were:

i. What is the annual sediment yield of the Mhlatuzane micro-catchment?

ii. What is the rate of sedimentation and sedimentation trends of the Lubovane reservoir?

iii. What are the implications of the sedimentation of Lubovane reservoir on the yields of the Lubovane reservoir?

1.6 Report Layout

The report of this study is presented in six chapters. The first chapter gives an introduction to the study by highlighting the background to the soil erosion problem and sedimentation of the Lubovane reservoir as well as the background of the LUSIP which led to the construction of the reservoir. The chapter also presents the problem statement, objectives and justification for carrying out the study.

Chapter 2 covers a review of literature on soil erosion and sedimentation and describes theoretical underpinnings of the methods. The chapter also discusses different methods and techniques of assessment of soil erosion and sediment deposition. Chapter 3 presents a description of the study area, showing the location of the study area, hydrological setup, climate, and soils. Materials and methods are covered in the fourth Chapter which consists of data collection, methods adopted to achieve objectives and the analysis procedures. Chapter 5 presents results and discussions for each objective. Finally the conclusion and recommendations derived from the study are presented in Chapter 6.

CHAPTER TWO

2. LITERATURE REVIEW

2.1 Introduction

Soil erosion is an environmental problem as it leads to removal of fertile topsoil, which is crucial for agriculture. One of the impacts of soil erosion that is even of much greater concern is increased rates of sedimentation in the rivers and reservoirs, causing capacity loss and also providing ingredients for water eutrophication as it carries pollutants (Wang *et al.*, 2009).

2.2 Reservoir Sedimentation

According to a UNESCO (2011) sediment comprises solid particles of both mineral and organic material and is widely referred by many authors as silt. This material is generated at catchment levels and transported by rainwater through drainage networks into rivers and eventually deposited on the river bed and in standing water bodies like lakes/reservoirs. Reservoir sedimentation, which decreases the useful life of the reservoir, is closely associated with soil and stream bed erosion in the corresponding basin (Hrissanthou, 2011). The river transports the soil, that is washed out from the catchment into the river, downstream until it reaches the impounded/still water where velocity decreases and hence deposition takes place and then it is said to be reservoir sedimentation. According to Lin *et al*. (2013) sediment transport and deposit within the catchment is an unavoidable natural process, but its impacts can be reduced by improving catchment management strategies. Reservoir sedimentation is a serious off-site consequence of soil erosion with large environmental and economic implications and on the other hand it also provides valuable information on erosion problems and sediment transport within a drainage basin. A reservoir can be considered as a large scale experiment, as the outlet of a giant erosion plot (de Vente *et al.*, 2011).

2.3 Causes of Reservoir sedimentation

De Vente et al (2011) conducted a study to determine the factors controlling sediment yield at the catchment scale in Northwest Mediterranean geo-ecosystems. In their study they used the Area Relief Temperature (ART) sediment delivery model and they found that Catchment area, catchment perimeter, stream length, relief ratio, Modified Fournier Index, the RUSLE's R factor, and catchments percentage with poor vegetation cover showed highest correlations with sediment yields of the catchment.

Overland flow is high on steep slopes, bare land or paved surfaces and also where ploughing up and down the slope is practiced. High overland flow increases chances of soil erosion where detached particles are transported down slope into rivers and eventually to reservoirs. Land use changes can also accelerate the rates and amount of sediment produced by a catchment as noticed in the Itaipu Lake in the Brazil-Paraguay border. According to (Norton *et al.*, 2001), sedimentation was not a threat to the Itaipu Hydro-electric Project initially and the project was expected to have a lifespan of more than 300 years but since the land use changed from forest to intense row crops, the lake started accumulating more sediment each year. Poorly managed catchments are bound to accumulate more sediment load as compared to properly managed catchments. In a study conducted in Brazil to link soil erosion to soil conservation practices, it was discovered that the elevated gross erosion values in the catchment were associated with areas of potentially high surface runoff. This was due to reduced infiltration resulting from poor soil management practices, evidenced by excessive compaction of the soils. (Didoné *et al.*, 2015).

2.4 Sedimentation and Climate Change

Mahabaleshwara and Nagabhushan (2014) have noted the growing body of evidence that the sediment loads of rivers and reservoirs will be affected by climate change mainly due to changes in rainfall and runoff. A study was conducted in Yan River in China by Wang *et al*. (2013) to analyze the changes in runoff and sediment loads over a 60 year period. The study found that a decrease in the runoff in the years led to an increase in sediment deposition which was articulated to the rivers losing the transport capacity as flow decreased. Runoff in the Usuthu basin in Swaziland was predicted to decrease by 4.8% by 2075 due to climate change and that will affect inflows into the Lubovane reservoir (Mhlanga *et al*., 2012).

The impacts of climate change will see an increase in rainfall intensity and runoff in some areas while others experience the opposite like the Usuthu Basin. The Arctic for instance has been predicted to experience major increases in runoff due to increase in rainfall and evaporation will also increase due to increase in global temperatures (Pohl *et al.*, 2006). This increase in rainfall and runoff will probably cause an increase in sedimentation in these areas compromising ability of reservoirs to function adequately, especially those for Hydro-power generation.

2.5 Impacts of Reservoir Sedimentation

Most rivers in the world are naturally occurring and transport of sediment by rivers is a natural process which is not a problem in itself (UNESCO, 2011). A proper balance between soil erosion and soil deposition is experienced in undisturbed systems and sediment is necessary for maintaining fluvial environments which include floodplains and channel systems. However, the anthropogenic activities in catchments have caused an increase in the sedimentation and soil erosion rates beyond the natural. The impacts of reservoir sedimentation as listed by UNESCO (2011) are categorized into those upstream and downstream of the reservoir.

2.5.1 Upstream Impacts of sedimentation

The most vital and devastating impact of sedimentation of reservoirs is the loss in storage capacity which affects the lifespan of the reservoir and the successive annual yields obtained from the reservoir (Carlos de Araujo *et al.*, 2006). Accumulated sediment in the world was estimated at 2000 million cubic metres in 2009 with an average annual capacity loss of 0.8% (ICOLD, 2009). The ICOLD report translated the loss of capacity to sedimentation to 0.6% reduction in power generation with replacement costs estimated at 13.6 billion U.S. Dollars per year. Dams are constructed at a cost, not only financial but, high social and environmental costs considering that an entire village can be resettled to pave way for a dam construction. If the sediment accumulation is high, the reservoir outlet works may also become clogged. Abrasion of hydraulic machinery may also occur, decreasing its efficiency and increasing maintenance costs.

2.5.2 Downstream Impacts of Reservoir sedimentation

The downstream impacts are quite different from the upstream as the problems result from shortage of sediment as most of the sediment is trapped by the dam. Stretching a dam structure across a river evidently creates a barrier preventing a portion of sediment from flowing downstream, depending on the trap efficiency of the dam. The construction of the Three Gorges Dam (TGD) in the Yangtze River caused major sediment shortage problems for downstream users of the river (Hu *et al.*, 2009). The sediment assessments conducted in the river showed that 172 million tonnes of sediment were trapped annually by the TGD and the impacts were reduction in yields due to decline in soil fertility which was previously recharged by sediment deposited during floods.

The proper functioning of wetlands and estuary areas around the globe is dependent on a reliable consistent supply of sediment. Such is necessary for the maintenance of their bio-diversity and proper functioning of their ecosystem (Suryawan *et al.*, 2015). Sediment loading therefore plays a vital role in these water systems as it supplies much needed nutrients for the fauna and flora existing in these ecosystems.

2.6 Methods of determining Soil Erosion and Subsequently Sedimentation

Assessment and estimation of soil erosion is often difficult due to the complex interplay of many factors, such as climate land cover, soil class, slope length and steepness as well as anthropogenic factors which involve activities that escalate soil erosion and those that aim at reducing it (Wordofa, 2011). There are various methods around the world of determining the rates of soil loss in a catchment and sedimentation of rivers and reservoirs. Such methods include models such as the Pan-European Soil Erosion Risk Assessment (PESERA), Universal Soil Loss Equation (USLE), Revised Universal Soil Loss Equation (RUSLE), Modified Universal Soil Loss Equation MUSLE, and Soil Loss Estimation Model for Southern Africa (SLEMSA) among many. The most common method for soil erosion assessment is the use of Universal Soil Loss Equation (USLE). Many authors have proposed modifications to the USLE but all circle around the concept where rainfall erosivity, soil erodibility, slope class, land cover and land management factors are taken as directly proportional to the rate of annual soil loss (Wijesekera and Samarakoon, 2001). However, for the purposes of this research, SLEMSA and RUSLE were discussed in detail as SLEMSA is a model that was generated for Southern African conditions and RUSLE is a widely used model especially where remote sensing and GIS is involved.

2.6.1 The Universal Soil Loss Equation for Sediment yield determination

The Universal Soil Loss Equation (USLE) was developed by Wischmeier and Smith (1978) as an empirical model useful in predicting long-term average annual soil erosion rates. The model integrates the effects of rainfall erosivity, slope, soil erodibility, crop management and support practices to predict the potential of soil erosion. It is a conservation planning tool that has been demonstrated to do a reasonably good job of estimating erosion for many disturbed-land uses (Renard *et al.*, 2010). However, the predictions of the model are limited to erosion resulting from sheet or rill erosion and not erosion by wind or gully erosion.

Stone and Hilborn (2012) have found that even though the USLE model was developed for use in agricultural plots with selected cropping and management systems, the improved RUSLE model can be applied to areas that are non-agricultural, like construction sites and settlements with bare soil. According to Breetzke *et al*. (2013), the USLE has been used in South Africa in comparison with SLEMSA and it proved to work better in modeling soil loss in the province of KwaZulu Natal.

Parameters of the USLE Model

The input data is divided into five different factors; rainfall erosivity, soil erodibility, topography, crop management and conservation practice (Andersson, 2010). The factors of the USLE vary over different storm events but tend to average out over long-term conditions, which explains why the equation is applicable in these actual conditions. Equation 2-1 below is used for the prediction of the annual soil loss from an area using the USLE model (Stone and Hilborn, 2012).

$$A = R \times K \times LS \times C \times P \qquad \textit{Equation 2-1}$$

Where:

A = Annual soil loss ($t.ha^{-1}.yr^{-1}$)

R = Rainfall runoff factor ($MJ.mm.ha^{-1}\ h^{-1}$)

K = Soil erodibility factor ($t.ha^{-1}.MJ^{-1}.mm^{-1}$)

LS = Topographic factor (dimensionless)

C = Cover and management factor (dimensionless)

P = Support practice factor (dimensionless)

The Rainfall Erosivity (R-factor)

This is the rainfall and runoff factor by geographic location and it is a measure of the potential of rainfall to cause detachment of soil particles and runoff (Arnoldus *et al.*, 1980). The kinetic energy of the rain can be considered as the potential rainfall energy available to be transformed into erosion. The erosivity of a single raindrop is naturally described as the droplet kinetic energy *E*; the mass of the droplet multiplied by the square of the velocity at impact divided by two; $E=m.V^2/2$ (Wall *et al.*, 2002a). However, if the rainfall intensity and storm kinetic energy data are not available at meteorological stations which is usually the case in developing countries, the usually available annual and monthly rainfall data available can be used to estimate R (Mbugua, 2009).

Soil erodibility (K-factor)

The soil erodibility factor is a measure of the vulnerability of the soil to erosion at each spatial location as a function of its texture, structure, permeability and organic matter content, with soil texture being the principal factor (Vaezi *et al.*, 2010). The K-factor can be determined for each spatial location through the use of erosion plots measuring soil loss per spatial location for each storm event. Such a study to determine the spatial variability of K through the use of grid plots was conducted successfully in North West Iraq. The soil erodibility values found estimated in the study were based on the original USLE monograph (Whichmeier and Smith, 1978) and equation 2-2.

$$100K = 2.1M1.1410–4(12–a) + 3.25(b – 2) + 2.5(c – 3) \qquad \text{Equation 2-2}$$

Where:

K = Soil erodibility factor in t h MJ^{-1} mm^{-1}

M – Expresses the effect of topsoil texture and is calculated as (% silt + % silty sand) × (100% -% clay)

a – % of topsoil organic matter (humus)

b – Class of topsoil structure

c – Class of soil profile permeability

However, in cases where it is not possible to determine the erodibility of soils in an area, look-up tables can be used to determine the K factor for each class with the corresponding organic matter content of the soil (Stone and Hilborn, 2012). In a GIS environment, a soil map (shapefile) is required to generate the K values for each soil type. The K factor ranges from 0.02 – 0.80 with high values associated with soils with high silt percentage. Coarse sandy soils have low erodibility because even though the particles are loose, they encourage infiltration thus reducing overland flow which is the driver for soil transportation after detachment by rainfall. Clay soils also have low erodibility due to the fact that the particles are cohesive hence not susceptible to detachment by raindrop impact.

Slope length-gradient (LS-Factor)

The slope and slope length factors (*S* and *L*, respectively) account for the effect of topography on soil erosion. The LS-factor is usually presented as a ratio of soil loss under specific conditions of the study site. It can be estimated through field measurement or from a digital elevation model (DEM) (Esther, 2009).

Crop/Vegetation and management (C-factor)

This is the crop/vegetation and management factor. It is used to determine the relative effectiveness of soil and crop management systems in terms of preventing or reducing soil loss. It is determined by the vegetative cover on that particular site and in an agricultural set-up, it is determined by the crop type and tillage method. It is expressed as a ratio comparing the soil eroded under a specific crop and management system to continuous fallow conditions (Wall *et al*., 2002a).

Support Practice (P-Factor)

The conservation practice factor P, in the Universal Soil Loss Equation is the ratio of soil support practice to the corresponding loss with up and down slope culture (Stone and Hilborn, 2012). The practices induced in this term are contouring, strip cropping (alternate crops on a given slope established on the contour), and terracing. The value of P ranges from 1.0 for up and down cultivation to 0.25 for contour strip cropping of gentle slope. It is basically an indication of the type of practices that will reduce runoff amount and rates and subsequently soil erosion (Collins *et al.*, 1996).

2.6.2 The Revised Universal Soil Loss Equation

The Revised Universal Soil Loss Equation (RUSLE) was developed as an interim improvement on the USLE and was intended to bridge the gap between what is now outdated technology (i.e. the USLE) and the new generation of process-based models (Renard *et a*l., 2010). The RUSLE is the newest improved version of USLE and could be considered as a transition from the empirical to the physically-based models (Hrissanthou, 2011) and it utilizes the same empirical equation used in the USLE. However, in the RUSLE, new methods have been introduced for the estimation of the values of the various factors of the USLE. These new methods allow for inclusion of quantitative information regarding seasonal variation of soil erodibility factor (K), irregular slopes (LS) and crop and management relationships (C) and the effect on erosion. Unlike the USLE, RUSLE's calculations are computerized as are the databases, which include information on soil erodibility (K) and climate (R) data for all major soils (Wall *et al.*, 2002b). Remote sensing and GIS tools can be used to generate the inputs of the RUSLE model.

2.6.3 Soil Loss Estimation for Southern Africa (SLEMSA)

The SLEMSA model was a result of an effort by Elwell (1978) to localize and adapt the United States developed RUSLE to southern African environments. According to Breetzke et al. (2013) this model was developed to estimate to predict soil loss resulting from sheet erosion on arable land for a long-term basis. It is widely used in African environments and it should be seen as a modelling technique as opposed to mechanistic description of the soil erosion system. One of the problems with the use of SLEMSA is the lack of literature for the estimation of regional input parameters (Breetzke *et al.*, 2013). SLEMSA is structured differently from RUSLE as it integrates only four systems which include crop, climate, soil and topography. The SLEMSA equation 2-3 is represented as follows

$$Z = K \times C \times X \qquad \textit{Equation 2-3}$$

Where:

Z = Mean annual soil loss ($t.ha^{-1}.yr^{-1}$)

K = Soil factor ($t.ha^{-1}.yr^{-1}$)

C = Crop Management factor

X = Topographic/Slope factor

Erodibility (K) Factor

Soil's vulnerability to erosion is mainly a function of its texture and type. Loose soils with smaller particles are easily eroded as they lack cohesion and reduce infiltration thus causing overland flow. K in the SLEMSA model is determined using the exponential relationship:

$$lnK = blnE + a \qquad \textit{Equation 2-4}$$

Where:

E = Raindrop kinetic energy ($J.m^{-2}$)

a and b = soil erodibility factor functions specific to the region being studied

$$E = 15.16MAP - 1517.67 \qquad \textit{Equation 2-5}$$

Where:

E = Kinetic energy of the raindrops ($J.m^{-2}.annum^{-1}$)

MAP = mean annual precipitation (mm)

Slope factor (X)

This factor is composed of basically two factors which are the slope length and the slope steepness (gradient) just like in the USLE model. Slope length and Slope steepness can be measured on site or calculated in a GIS environment then incorporated in equation 2-6 by Elwell (1978).

$$X = \frac{\sqrt{(L \times (0.76 + 0.53 \times S + 0.076 \times S^2)}}{25.65} \qquad \textit{Equation 2-6}$$

Where:

X = topographic ratio

L = slope length (m)

S = Slope steepness (%)

Crop factor (C)

The crop factor in the SLEMSA model is calculated based on a method developed by Elwell and Stocking (1976) for Zimbabwean grasslands since the model is Zimbabwean based and it is calculated using equations 2-7 and 2-8, depending on the interception of rainfall energy by the crop in that spatial location.

$C = e^{(-0.06i)}$, *When* i < 50% *Equation 2-7*

And

$C = \frac{2.3-0.01i}{30}$, *When* i > 50% *Equation 2-8*

Where;

C = Ratio of soil loss at interception level, *i*

i = interception of rainfall energy by the crop (%)

2.6.4 Bathymetric Surveys

McPherson *et al.* (2011) defined bathymetry as the measurement of the depth of the wetted reservoir bed below the water surface. These surveys are often supplemented with some type of topographic survey to obtain land-surface altitude data, above those determined from the bathymetric survey to the spillway crest altitude or higher. Sophisticated Bathymetry survey of a reservoir bed was conducted in Loch Lomond Reservoir, Santa Cruz County, California in 2009 by using boat-mounted SEA Swath Plush interferometry bathymetric multibeam-sidescan sonar (McPherson *et al.* 2011). Topographic data were collected with a boat-mounted mobile laser scanning system (Light Detection and Ranging, or LiDAR). The LiDAR survey provided highly detailed land-surface coverage of the areas seasonally exposed during dry periods, thereby producing a more accurate bathymetric map and storage-capacity table that could otherwise be obtained only when the reservoir is at or near maximum capacity.

This method was also carried out in 2012 in Mutangi catchment area of Chivi district a semi-arid area in the southern part of Zimbabwe by Chitata *et al*. (2014). The dam capacity was determined using the hydrographic surveys, grab sampling and the water depth-capacity method. Sedimentation rate and capacity loss in a decade (2000-2012) was determined by comparing the 2000 capacity to the present capacity at 2012.

2.6.5 Remote Sensing and GIS based Methods

2.6.5.1 Using Remote Sensing and GIS to determine Catchment Sediment Yield

The use of Remote Sensing (RS) and Geographic Information Systems (GIS) tools to estimate sediment yields of catchments and to estimate reduction in reservoir capacity have increased in the last decade. Jain and Kothyari (2015) used a GIS based method to identify sediment source areas and predict storm sediment yield of Nagwa and Karso catchments in Bihar, India. In their study, Integrated Land and Water Information System (ILWIS), was used for discretizing the catchments into grid cells and the ERDAS IMAGINE image processor used for processing satellite data related to land cover and soil characteristics. The gross surface erosion was calculated by assigning values to the various parameters of the USLE in individual cells.

Munthali *et al.* (2011) conducted a study that showed that GIS combined with the Pan-European Soil Erosion Risk Assessment (PESERA) model can be used to estimate sediment generated in a catchment and transportation of the sediment in a river system downstream. This model integrated land use data, climatic, physiographic and topographic information in a GIS for the Songwe River to determine critical sediment generating areas and hence the risk of reservoir sedimentation. In Zimbabwe, a study was conducted using the SLEMSA model combined with RS and GIS to assess the spatial erosion hazard in the Mbire District (Dube, 2011). The study found that SLEMSA and GIS can be used successfully to estimate potential soil erosion hazard in the District but not the occurrence of gully erosion.

2.6.5.2 Using Remote Sensing and GIS for Bathymetric Surveys

Geographical Information System (GIS) is also used to model bathymetry and the spatial distribution of sediments (Evans *et al.*, 2002). The Satellite Remote Sensing (SRS) method for assessment of reservoir sedimentation uses the fact that the water spread area of reservoirs at various elevations keeps on decreasing due to sedimentation. Narasayya et al. (2002) used this method to determine dam capacity for Srisailam Dam in Nandikotkur taluka of Kurnool District of Andhra Pradesh State of India. They noticed that for determination of sediment using the bathymetric surveys, a longer period is required for comparison because if the period is short, there might not be a significant change in the capacity since sedimentation is a gradual process. The capacity estimation of Srisailam Reservoir using Remote Sensing technique was carried out for the year 2004 in order to know deposition of sediment and the reduction in capacity since 1976 in the reservoir.

A study was conducted by Estigoni *et al*. (2014) to assess the accuracy of reservoir volume calculations based on different standard methods for determining reservoir capacity and sedimentation. The volume was calculated based on a digital terrain model according to the usual model, triangular irregular network (TIN), and according to the insertion of mesh points (IMP) method. This was then compared with the reference volume, and the accuracy of each survey was determined. The TIN method was found to have limitations in representing regions near shores, producing incorrect shallow depth readings, resulting in a lower calculated volume than the real volume. The study concluded that even surveys following the widely accepted standards contain errors of a magnitude that cannot be ignored.

2.7 Sediment Delivery Ratio (SDR)

Sediment delivery ratio (SDR) is traditionally defined as the fraction of upland gross erosion that is transported out of a defined area, e.g., a plot or catchment. It is, effectively, an index of sediment transport efficiency. Previously, it was treated as an empirically-lumped parameter used as a mechanism for compensating for sediment deposition within a catchment area (Lu *et al.*, n.d.). The SDR is presented as a fraction from 0 – 1.0 and when SDR = 1.0, the transport capacity of the sediment flow is not exceeded and at that point the sediment delivery is directly related to soil erosion. If the SDR < 1.0, the sediment delivery is limited by transport capacity because erosion exceeds the capacity of flow to transport the eroded material (Kinnell, 2004). Kinnell (2004) further mentioned that at SDR < 1.0, reducing the erosion rate will not necessarily result in a reduction in the amount of sediment delivered from the hill slope. It may just simply increase the value of the SDR.

2.8 Trap Efficiency of Reservoirs

The trap efficiency (TE) as defined by Mulu and Dwarakish (2015) is the ratio of sediment that has been deposited in a reservoir to the total inflow for a given period within the reservoir's economic lifetime. It is basically an indication of the sediment that is trapped against that sediment that passes the reservoir and flows to downstream. Sediment can leave the reservoir through the spillway when the reservoir is spilling and also during outflows. One method that is widely used for determining the TE of a reservoir is the Brune's curve established by Brune

(1953). The Brune's curve is widely used in estimating the sedimentation (Revel *et al.*, 2013) of reservoirs and it relates TE to capacity (V) and annual average inflow (I) ratio (Figure 2-1). It can also be presented as an equation that is an alternative to the curve (equation 2-9). Other localized methods include the Zimbabwean trap efficiency curve which assumes that above storage ratio of 0.1, the trap efficiency of the reservoir is 100% (Tumbare, 2013).

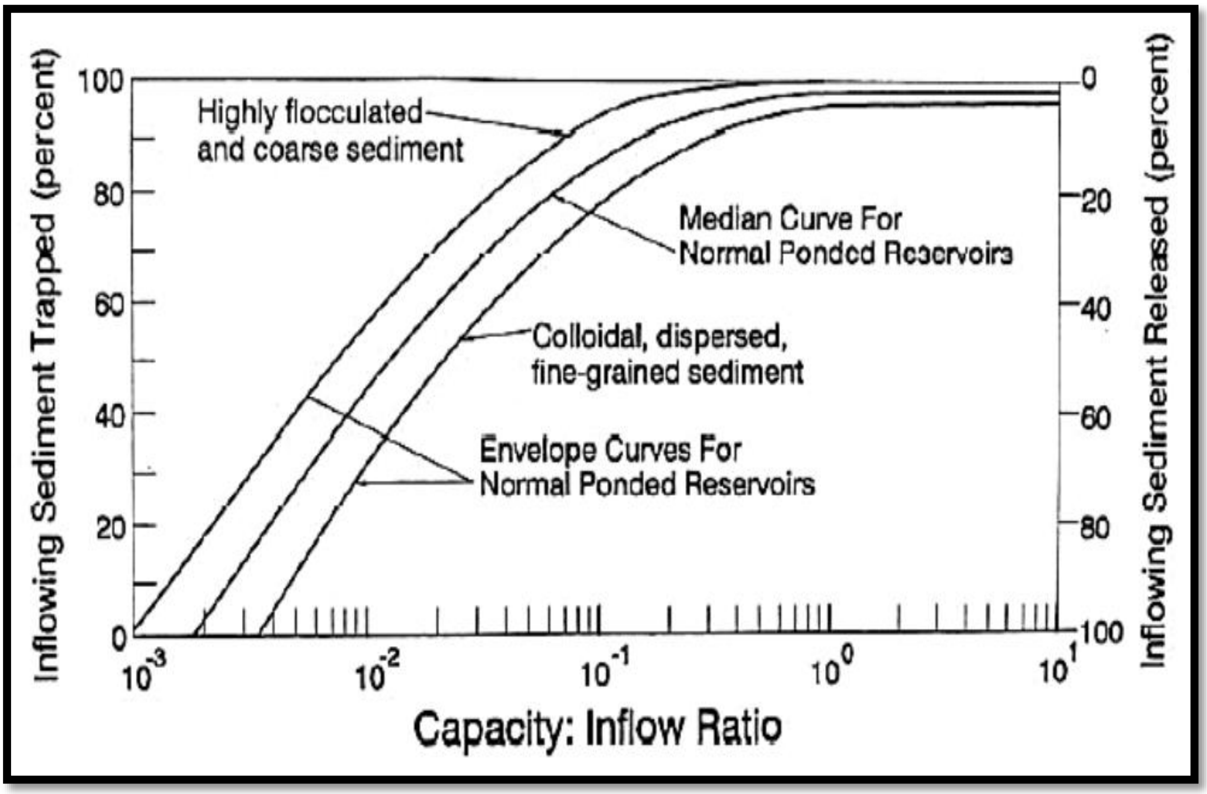

Figure 2-1: The Brune's curve for estimating Trap Efficiency (Brune, 1953)

$$TE = 100 \times 0.97^{0.19^{log\left[\frac{V}{I}\right]}}$$ *Equation 2-9*

Where:

TE = Trap Efficiency for Normal Ponded Reservoirs (%)

V = Reservoir capacity (m^3)

I = annual average inflow (m^3)

2.9 Sedimentation and yield of reservoirs

Most rivers are usually balanced in terms of sediment inflow and outflow at each particular point or section of the river. Stretching a dam across a river however, alters that balance since the water depth is increased and the velocity of flow reduced which then encourages settling as the sediment transport capacity of the river is compromised (Sumi and Hirose, 2010). Lizewski and Bellack (2007), adopted the Army Corps of Engineers' definition of reservoir yields, where they define it as the volume or schedule of supply at a specified location in a water body in a given specified period, usually over a year. The factors that affect reservoir yields include runoff, precipitation, Evapo-transpiration and seepage losses, initial volume of water in the reservoir, Surface and subsurface inflow and these can be looked at as inputs or determinants of the water budget. Figure 2-2 shows a typical set up of a water budget.

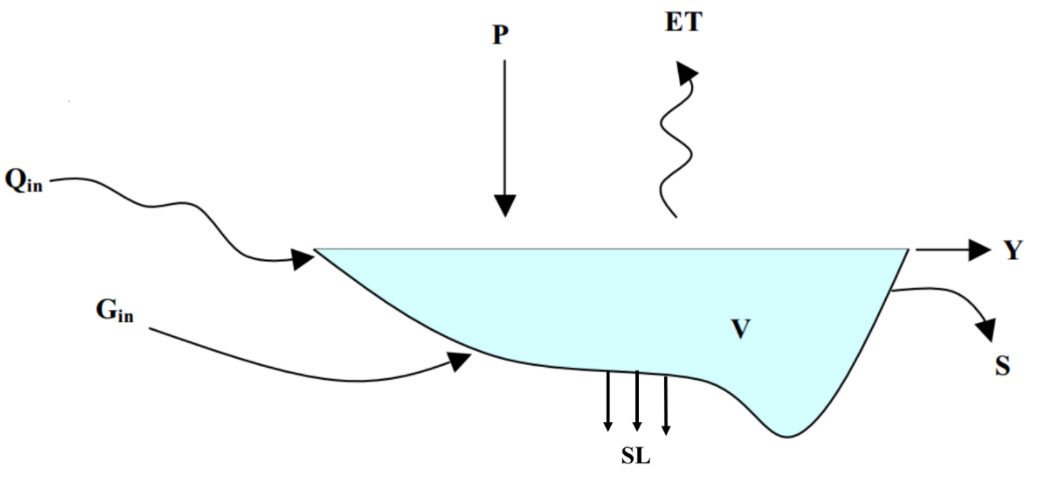

Figure 2-2: A typical set up of a water budget in a reservoir system (adopted from, Lizewski and Bellack (2007)

The water budget can be presented in an equation to determine the yield of a reservoir (Y) as follows.

$$Y = V + P + Q_{in} + G_{in} - ET - S - SL \qquad \text{Equation 2-10}$$

Where:

Y = Yield of reservoir

V = Initial volume of the reservoir

P = Precipitation

Q_{in} = Surface inflow (Runoff)

G_{in} = Groundwater inflow

ET = Evapo-transpiration

S = Uncontrolled Spillages

SL = Seepage Losses

A study was conducted in Zimbabwe by Tundu (2015) to assess the sedimentation of rivers and reservoirs in Zimbabwe, focusing on the Mazowe catchment. The study found that sediment load in the rivers ranged between 16 – 24 $t.ha^{-1}.yr^{-1}$. The Chimhanda dam was selected for analysis in the study and it was found to have lost 38.6% of its capacity due to sedimentation, and it had been in operation for 27 years which means annual loss in capacity was 1.43%. The study did not analyze the impact of storage loss on yields but it is expected to be significant considering the high sedimentation rates. In Malawi, a study was also conducted to determine the investigate the impacts of sedimentation on water availability of small dams with a case study on Chamakala dam (Kamtukule, 2008). The study found that the dam had lost 39% of its capacity in just 6 years and yield projections due to the loss in capacity showed that by 2017 the useable will have diminished if no measures were implemented to reduce sedimentation. The high sedimentation rates were attributed to poor catchment practices and that the dam was small in a large catchment.

CHAPTER THREE

3 DESCRIPTION OF STUDY AREA

This chapter details on the description of the study site where the research was carried out.

3.1 Geographic Location

The Lubovane reservoir surface area covers 13.9 km^2 at full supply level and is situated in the lowveld of Swaziland, in the Lubombo region. It sits on the Lower parts of the Usuthu basin. Geographically, it is located between Latitudes 26°46'57.60"S and 26°43'46.28"S and Longitudes 31°38'42.52"E and 31°42'54.45"E, about ten kilometers from the town of Siphofaneni. The Mhlatuzane river originates in the mountains around Hlatikhulu in the Shiselweni region and flows north-east into the Lubombo region (Figure 3-1). The Mhlatuzane micro-catchment sits in the Lower Usuthu sub-basin and the Usuthu Basin within Swaziland covers about 12700 km^2 (Mhlanga et al., 2012).

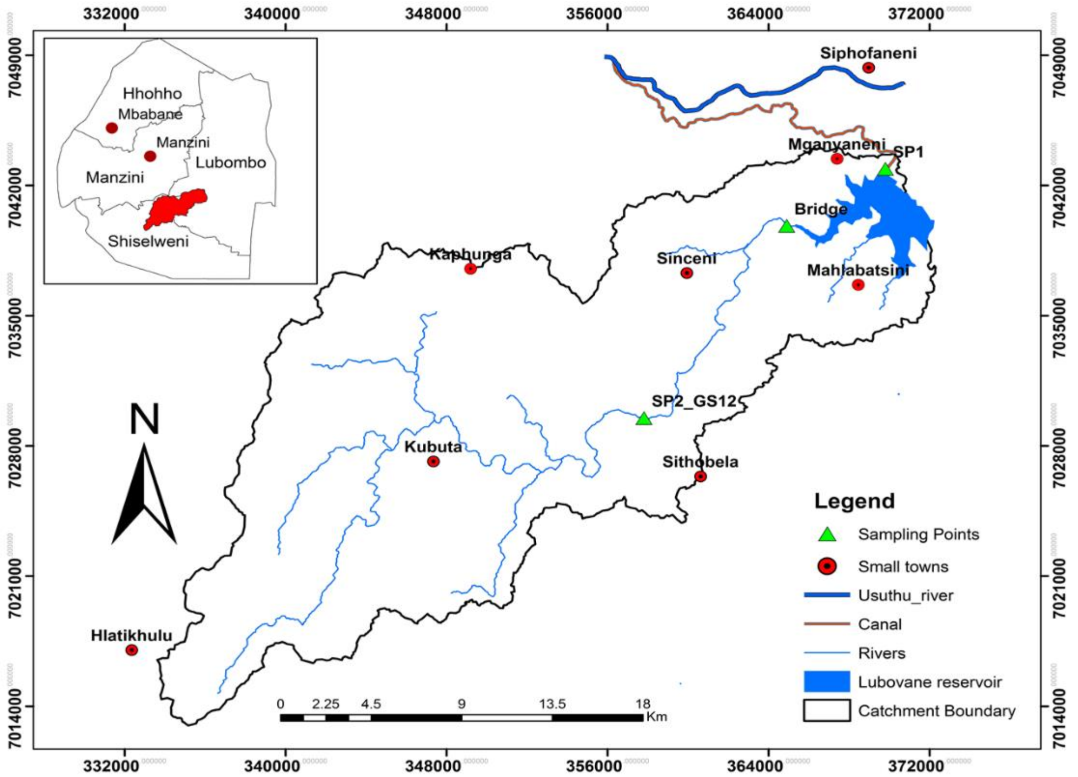

Figure 3-1: Location of the Lubovane reservoir and Mhlatuzane Micro-catchment

3.2 Hydrology

The Lubovane reservoir is one of many water impoundment bodies in the Usuthu basin. The catchment area of the reservoir is around 524 square kilometres. The Mhlatuzane catchment has a Mean Annual Runoff (MAR) of $70x10^6$ m^3 with a slightly high coefficient of variation of 98% (Vakakis-International, 2000). The reservoir receives water through the Mhlatuzane River as well as a feeder canal (FC) that diverts water from the Great Usuthu River at Bulungapoort weir. The MAR of the Usuthu River at Bulungapoort is $1400x10^6$ $m^{3.}$ The FC was designed to convey a maximum of 13.5 m^3/s of which is usually achieved only during the wet season. The general agreement in the Memorandum of Understanding (MOU) between Swaziland, South Africa and Mozambique was that the Lubovane reservoir was going to abstract water from the Usuthu River during high flows in the rainy season when flows exceed 10.8 m^3/s (Blackhurst, 2008). This period is when the power of the river to transport sediment is highest hence the FC transports silt from the Usuthu river to the Mhlatuzane micro-catchment. Sediment is generated in the reservoir catchment and transported through the Mhlatuzane River and other drainage networks into the reservoir.

3.3 Land use

Dominant land uses in the Lubovane dam catchment is agriculture and rural settlements. There are various farms both for subsistence and commercial purposes within the catchment. The areas around Khubutha are characterized by large fruit tree plantations with the main products being banana and oranges. There are noticeable spots of sand mining both for coarse grained sand from the streams and also fine grained plaster sand on the mainland. This poses a great risk of soil erosion in the micro-catchment and subsequently sedimentation as the sand is left bare and uncovered.

3.4 Climate

Average temperatures range from 19^0 C to 30^0 C, with maximum temperatures reaching 40^0 C usually around December and January. The annual rainfall in the basin ranges from 600 to 1000 mm with the lower parts of the basin receiving the least rains (Manyatsi and Brown, 2009). The lowveld of Swaziland is characterized by prolonged dry spells and high temperatures. Rainfall usually falls over a short period of time, with high intensities so it encourages the need for storage, if water is to be used, hence the reservoir (Mhlanga et al., 2012).

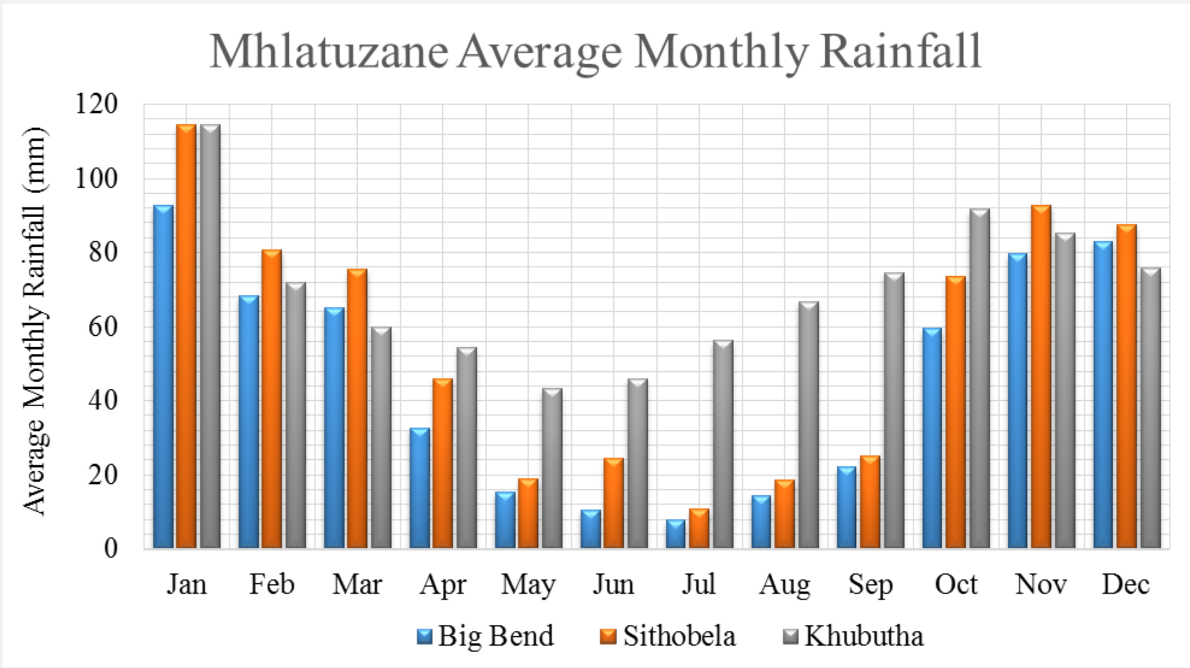

Figure 3-2: Average Monthly Rainfall (1981 – 2015) measured at 3 stations in and around the Mhlatuzane catchment area

The high temperatures in the lowveld of Swaziland have led to relatively high evaporation rates observed in the micro-catchment. The daily evaporation rates data for each month, used in this study, were obtained from the Big Bend weather station and it showed that high evaporation is experienced between December and January (see Appendix 3). Both these months have an evaporation rate of 5.8 $mm.d^{-1}$ with June in winter having the lowest evaporation rate of 1.9 $mm.d^{-1}$ (Figure 3-3). The annual evaporation rates are around 1390 mm meaning the reservoir loses over 15 Mm^3 of water to evaporation annually. Loss in capacity of the reservoir due to sedimentation, coupled with such high evaporation losses, will greatly compromise the ability of the reservoir to supply adequate water for irrigation and domestic use.

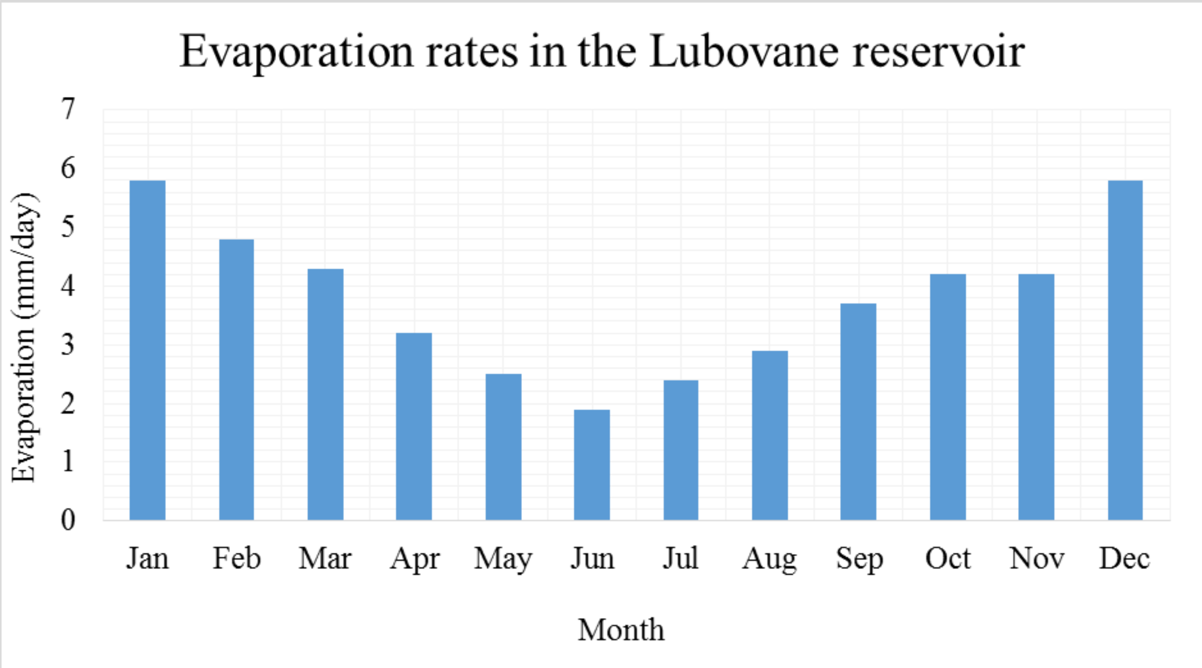

Figure 3-3: Monthly evaporation rates in the Lubovane reservoir area (obtained from the Big Bend Met Station)

3.5 Geology, Soils and vegetation in the Mhlatuzane Catchment

The overall geology of the LUSIP Project Area is characterized by the formations of the Karroo super-group, as well as by dolerite intrusions. The majority of the soils are deep, mostly poorly drained. There are also occurrences of very dark grey to black strongly cracking clay soils, which are moderately deep, moderately well to imperfectly drained dark reddish brown clayey soils (Fatoyinbo *et al.*, 2011). The soils reflect the transition from the acidic granites and sandstones of the western Lowveld to the more basic basalts and the dolerites of the eastern part. The west is characterized by soils ranging from sandy loams and the east contains red and black clays in the east which are some of the most naturally fertile soils in the country. The Mhlatuzane catchment falls in the lowveld, or Bushveld of the country in generally undulating lowland with isolated knolls and ridges. This region, in its undisturbed state, is vegetated largely with the typical African savanna (Swaziland, 2015).

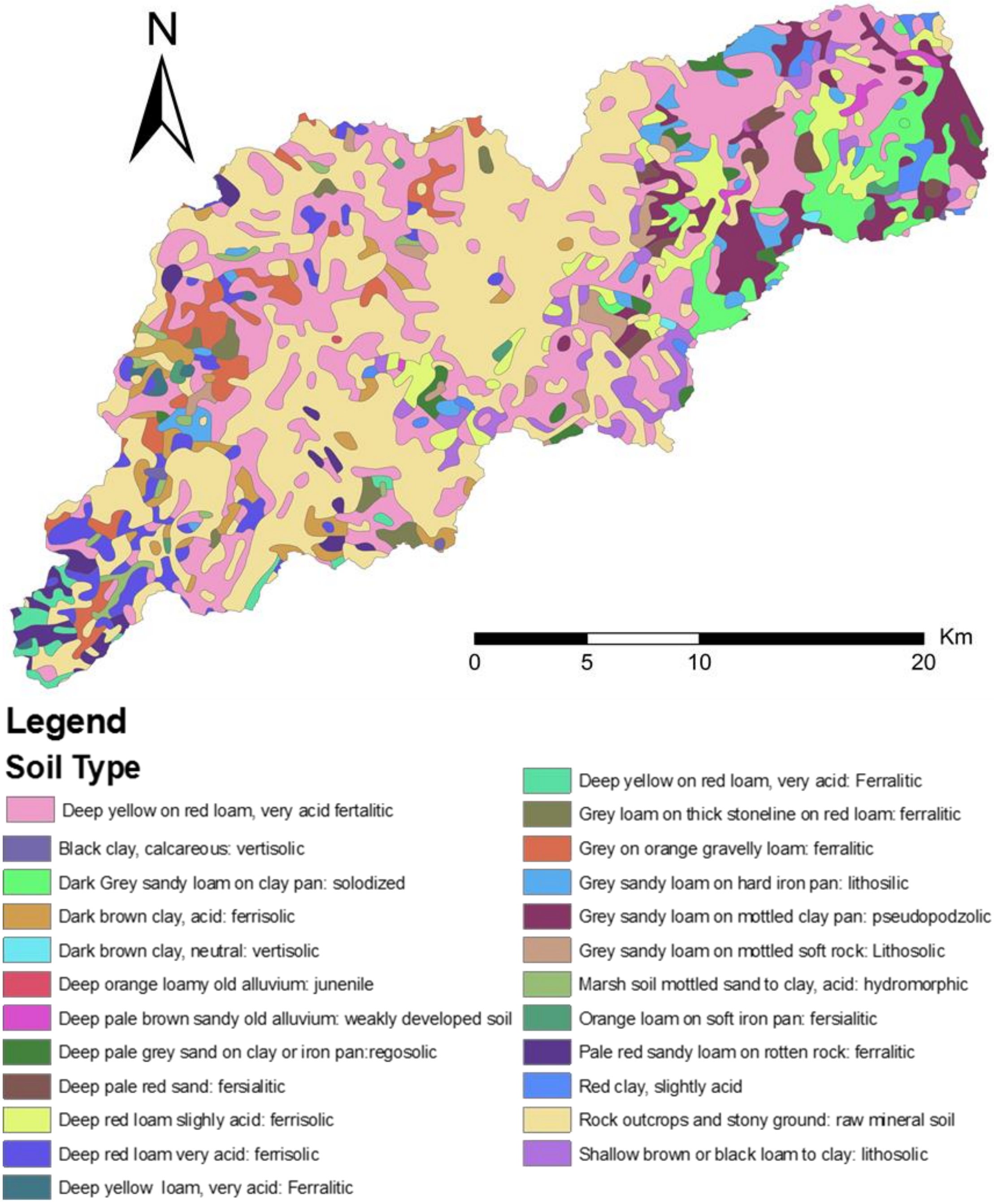

Figure 3-4: Spatial distribution of soils in Mhlatuzane

3.6 Elevation and Topography

The elevation in the Lubovane reservoir catchment ranges from 170 to 1253 metres above mean sea level with the highest areas observed in Mpompotha, Hlatikhulu, Kaphunga and Khubutha where there are large fruit plantations. Areas of low altitude are those closer to the reservoir towards the North-east and they include Mahlabatsini and Mganyaneni (see Figure 3-1 for locations).

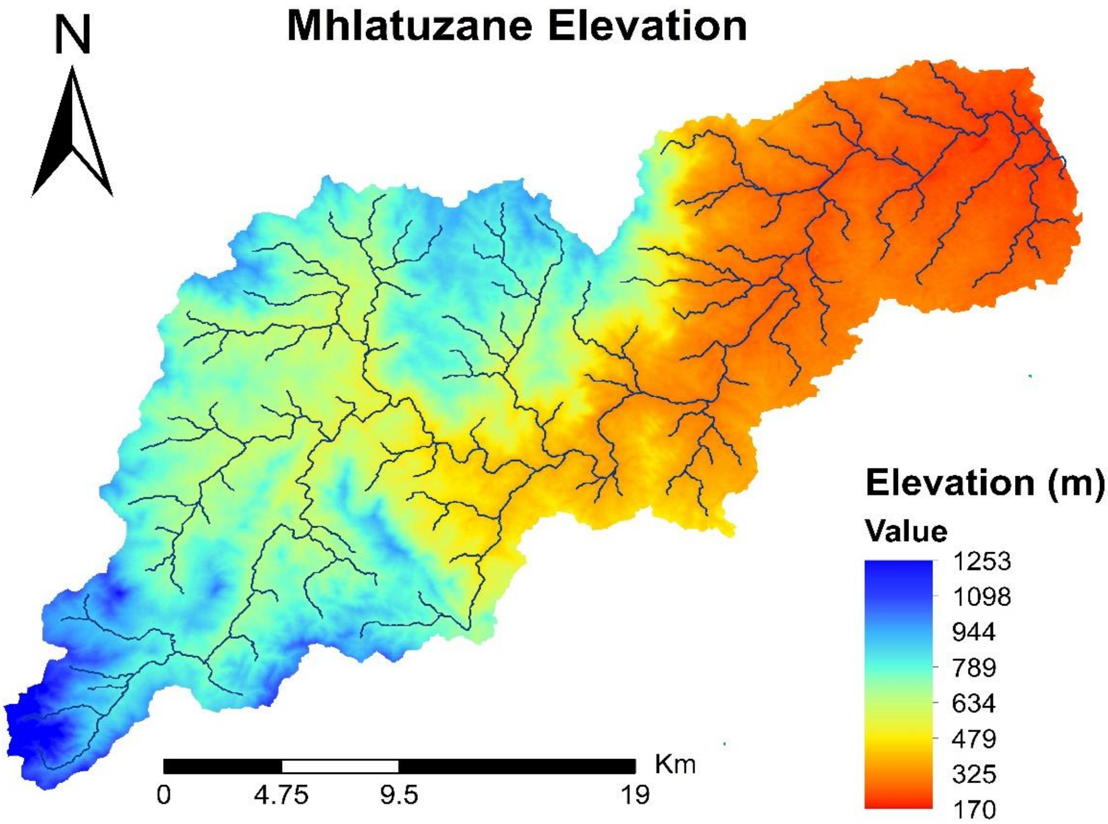

Figure 3-5: Topography and elevation in the Mhlatuzane micro-catchment

CHAPTER FOUR

4 MATERIALS AND METHODS

4.1 Data Requirements and acquisition

Data required for this study included rainfall data (1995 - 2015), slope and elevation maps, land cover/land use changes from the year 1995 to 2015 as well as data on the type of soils in the study area. This period was chosen in order to cover the period before the construction of the reservoir, resettlement period which saw a lot of deforestation around the water body, during the construction and after the reservoir was commissioned. The study also required bathymetry data of the reservoir to calculate the current capacity of the reservoir and hence its current yield. Such data was necessary to validate the RUSLE model used in the study to model soil erosion yields of the reservoir catchment.

4.1.1 Meteorological and Hydrological data Acquisition and Processing

Data for rainfall from the period 1995 to 2015 was acquired from the Swaziland Meteorological Services for three (Big Bend, Sithobela and Khubutha) stations falling in and closest to the study area. Coordinates for the stations were collected using a GPS and then the stations were overlain on the map for the study area to show their spatial distribution. The Thiessen polygon method in GIS was used to determine the areas of influence of each station and the rainfall for each location was the resultant rainfall from the influence of the interpolated stations.

Flow data was collected from the Department of Water Affairs (DWA) for Gauging Station 12 (GS12) which is a gauging station for Mhlatuzane River upstream of the Lubovane reservoir. Flow data for the Feeder canal (from January 2010 – March 2016) was collected from SWADE’s Water Management Unit as well the original Area – elevation – capacity relationships from the designs of the reservoir. Coordinates of the gauging stations were also collected using a GPS to determine its relative location to the reservoir.

4.1.2 Satellite data acquisition and processing

For Digital Elevation Modeling (DEM) hydro-processing, an ASTER DEM covering the study area was retrieved from the Global ASTER GDEM website (http://gdem.ersdac.jspacesystems.or.jp/). This was used to create a sub-catchment map of the

Lubovane reservoir to delineate the area that drains into the reservoir. The elevation and slope factors were also determined from the Digital Elevation Model (DEM). Landsat TM images were downloaded from the United States Geological Survey website (http://www.glovis.usgs.gov) for the years 1995, 2000, 2009 and 2015, all in the dry month of August in order to avoid excessive cloud cover in the images. The land cover maps were necessary for mapping land use changes in the reservoir catchment from 1995 to 2015 and also for producing the crop factor (C-factor) and support practice factor (P-factor) maps used in Soil erosion prediction in GIS. These Landsat satellite images and were processed using the Integrated Land and Water Information System (ILWIS) open source software (http://52north.org/communities/ilwis/ilwis-open) and ArcGIS to produce the desired outcomes.

4.2 Delineation of the catchment boundaries

The DEM hydro-processing was performed in ILWIS in order to obtain the boundary of the Lubovane catchment area which enclosed all points draining into the reservoir. A larger area was first digitized in Google Earth to produce a polygon (shapefile). This shapefile was then used to select the tile that covered the Lubovane reservoir and its catchment area, from the ASTER website. After downloading the tile (raster), the DEM hydroprocessing was performed from flow determination to network and catchment extraction as outlined in several manuals prepared by various authors (Gumindoga, 2015); (Daffi and Ohuchaogu, 2015). The catchment was then extracted from the other micro-catchments in the tile using the mask function. Shapefiles for rivers and small streams were extracted using the Digital Network Ordering (DNO) function in DEM-Hydro-processing.

4.3 Historical Rainfall in Mhlatuzane

The rainfall data obtained from the Swaziland Meteorological Station was analysed to determine trends in the data. Coordinates of the rainfall measuring stations were collected using a Global Positioning System (GPS) receiver to determine their location with relation to the study area. A point map was then created in ArcMap 10.2 where the points were displayed spatially as shown in the rainfall distribution map in Appendix 2. At this point, all three stations (Khubutha, Sithobela and Bigbend were considered. Thiessen polygons were created in ArcMap 10.2 using the spatial analyst tool to determine the areal influence of the rainfall stations in the study area. Weights were then assigned to each rainfall station based on its influence and the resultant rainfall for Mhlatuzane was derived from the spatially averaged rainfall based on the weights.

A trend analysis was performed on the data using the Mann-Kendall trend test in Microsoft Excel Statistical Software (XLSTAT). The Mann-Kendall test was developed to determine monotonic upward or downward trends in data series (Mann, 1945). The test was conducted at 95% confidence level on the annual rainfall from 1981-2015. Rainfall has an impact on soil erosion hence an increase in rainfall may mean an increase in soil loss and the opposite is true (Esther, 2009). Five-year Moving averages were also calculated for the periods of interest to this study which were 1995, 2000, 2005, 2009 and 2015.

4.4 Land use and Land cover Classification

The first objective of the Study was to map land use and land cover changes in the Mhlatuzane micro-catchment so as to determine their potential impact on soil erosion and subsequently sedimentation. Landsat 4-5 TM images were used for mapping land cover changes for 1995, 2000, 2005 and 2009. When mapping the land cover for 2015, a Landsat 8 image was used. The SWADE – LUSIP began in in the late 90s, so these years were chosen so that mapping could be done from before introduction of the project and through the mid-2000s to present, when activities in the project area intensified and the intensification included construction of the reservoir.

The images were downloaded from the United States Geological Survey Global Visualization Viewer website. Images were downloaded for the month of August in order to get images with low cloud cover for good visualization. The images were then imported in ArcMap combining bands 3, 2, 1 and 4, 3, 2 for Landsat 4-5 TM and Landsat 8 images respectively. The bands were combined specifically in that order using the composite bands function in ArcMap and they represent the Red, Green and Blue bands respectively. These bands are for visualizing an image in natural color composite. Since the researcher was familiar with the study area, the classification method selected was the supervised land cover classification. Before beginning the classification, the dynamic range adjustment (DRA) function under image analysis was used to enhance visualization of the image. Classification was done using a signature of points extracted from the image and assigned classes according to the researcher's knowledge of the area. Six land cover classes were selected namely; water, settlements, forest and shrubs, irrigated area, cultivated area and bare land as these had effects on soil erosion especially in preparing the Support Practice and Management (P-factor) for RUSLE.

4.4.1 Validation of the land cover classification

One of the major problems in classification of multiple uses is when those multiple uses or land covers occur in a single parcel of land (Anderson *et al.*, 2001), for example, bare land occurring in the same land parcel as thatched houses in a rural village as well as agricultural land and forest. Even though the researcher knows the area being classified, there is bound to be errors in the classification especially with images with low spatial resolution. This then necessitates the need for accuracy assessment in order to determine if the classification data can provide useful information or not. In this study, the confusion matrix was used to assess the accuracy of the land cover classification following a guide by Strahler *et al*. (2006).

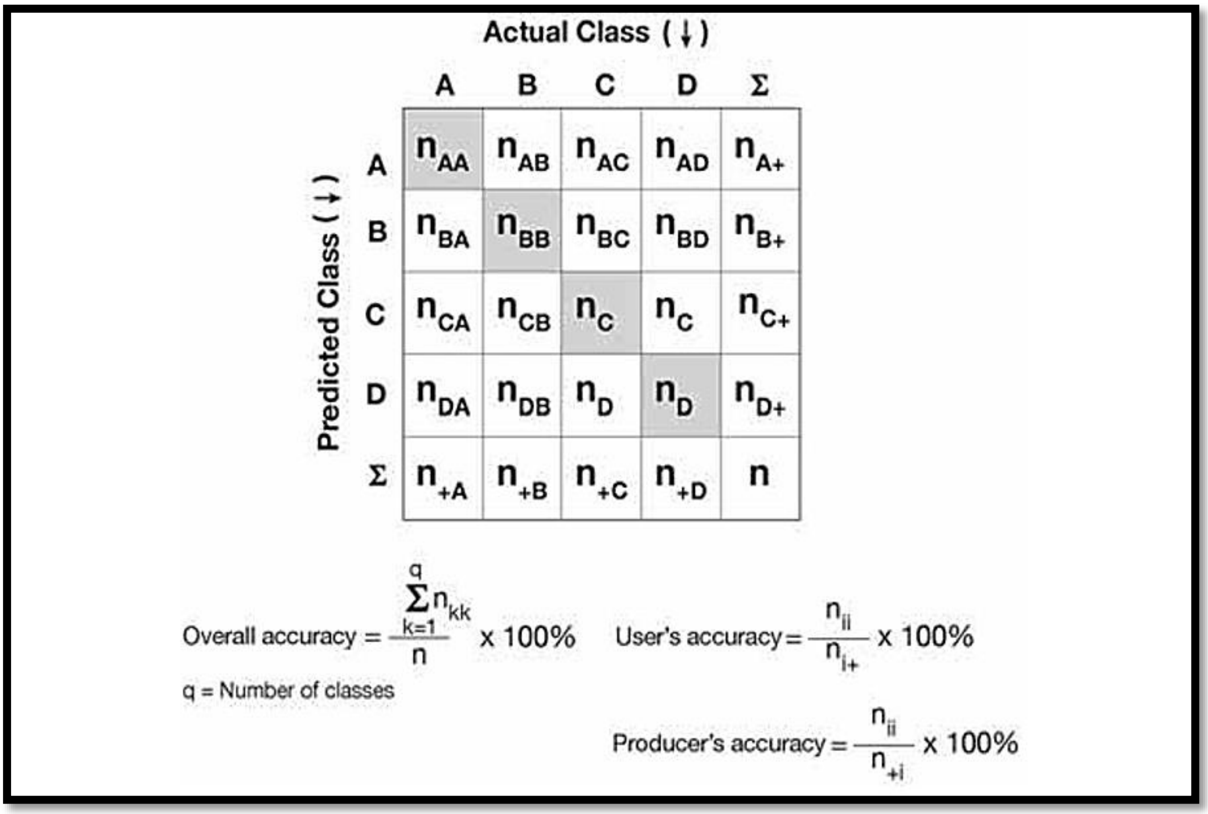

Figure 4-1: A layout of a typical confusion matrix and also shown in the matrix are the equations for computing the producer's and the user's accuracy

4.5 Estimation of Sediment yield of the Mhlatuzane micro-catchment

Soil erosion and sedimentation by water involves the processes of detachment, transportation, and deposition of sediment by raindrop impact and flowing water (Wischmeier and Smith, 1978). The Revised Universal Soil Loss Equation (RUSLE) was used to predict soil erosion at pixel level in the Mhlatuzane sub-basin. This model was chosen because it has proven to work well in areas that are bare and also in Agricultural Fields and the study area is mostly cultivated areas and rural settlements which are characterized by bare soils.

It has also been used by many authors, in combination with GIS and remote sensing to predict soil loss, so there is vast information and guidelines in literature available detailing on the appropriate procedures and formulae to use when predicting soil loss using RUSLE. Remote sensing and GIS techniques were used to prepare the inputs for the model and then to determine soil erosion or sediment yield of the catchment at pixel level. The inputs of the RUSLE model include Rainfall erosivity factor (R), Soil erodibility factor (K), Slope length and steepness factor (LS), Crop management factor (C) and the Support practice factor (P). Thematic maps of these five factors (Figure 4-2) were calculated in ILWIS and then multiplied to produce one soil erosion map for the Mhlatuzane catchment using equation 4-1.

$$A = R \times K \times LS \times C \times P \qquad \textit{Equation 4-1}$$

Where:

A = Annual soil loss (tons $ha^{-1}\ yr^{-1}$)

R = Rainfall runoff factor (MJ mm $ha^{-1}\ h^{-1}$)

K = Soil erodibility factor ($t.ha^{-1} MJ^{-1}\ mm^{-1}$)

LS = Topographic factor (dimensionless)

C = Cover and management factor (dimensionless)

P = Support practice factor (dimensionless)

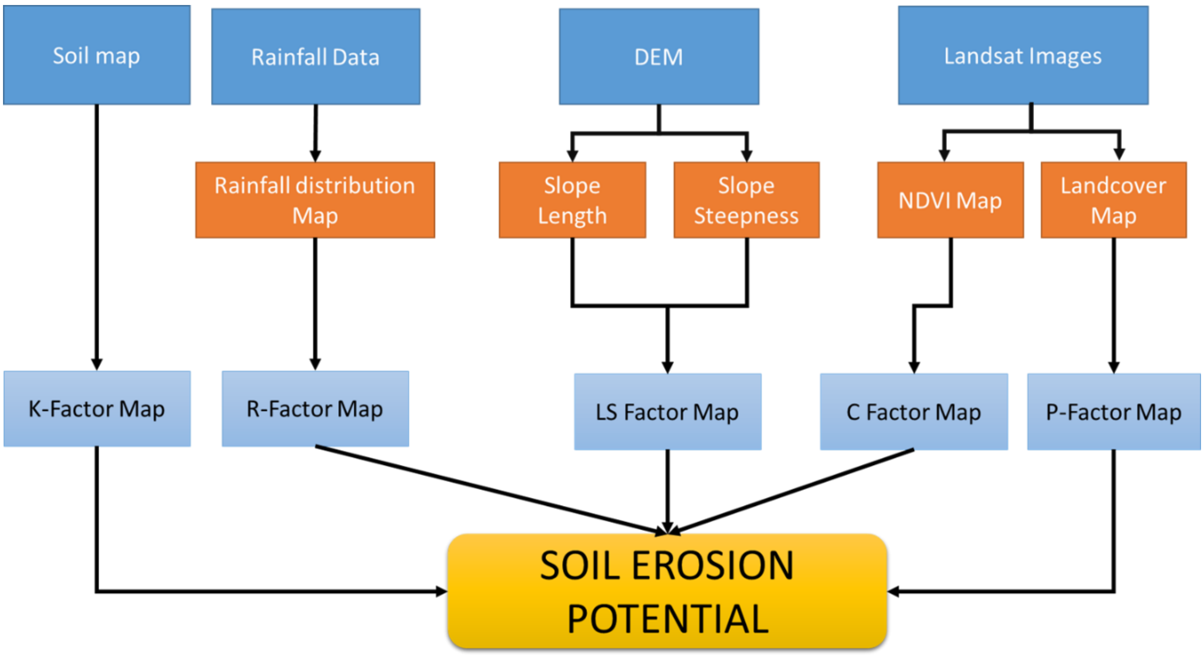

Figure 4-2: Implementation of the RUSLE model in a GIS environment (adopted from Breetzke et al. (2013))

4.5.1 Rainfall erosivity (R-factor)

Rainfall and runoff play an important role in the process of soil erosion, which is usually expressed as the *R* factor. To calculate the *R* factor, long-term precipitation data are needed with high temporal resolution, typically available for only few locations. The RUSLE rainfall-runoff erosivity factor (*R*) for any given period is obtained by summing for each rainstorm the product of total storm energy (E) and the maximum 30-minute intensity (I_{30}). These figures are rarely available at standard meteorological stations hence long-term average R-values are often correlated with more readily available rainfall figures like annual rainfall or the modified Fournier's index (Esther, 2009).

In this study rainfall maps were created in Quantum GIS through the grid interpolation method using the Inverse Distance to a Power (IDP) algorithm. Basically, the monthly rainfall data for the three stations (Sithobela and Khubutha) were summed up for the years 1995, 2000, 2005, 2009 and 2015 to get annual precipitation. Thiessen polygons (Appendix 5), created using the point map for the three stations were used to determine the contribution of each station, showed that the Big Bend rainfall station had no contribution on the Mhlatuzane micro-catchment hence it was excluded in the computations of the R-factor. The rainfall distribution map (mm/yr) from data obtained in the two stations was then be created in Quantum GIS software through the Moving Average interpolation method. The R factor map was then calculated for each year using equation 4-2.

$$R = 38.5 + 0.35\,P \qquad \textit{Equation 4-2}$$

Where:

R = Rain erosivity (Joule.m^{-2})

P = Annual rainfall (mm.$year^{-1}$)

4.5.2 The Soil erodibility (K-factor)

The erodibility (K-factor) determines the susceptibility of soil particles to detachment by raindrop impact and the K values are specific each soil textural class with the appropriate organic matter content (Whichmeier and Smith, 1978). There are various methods of calculating the erodibility factor and one of them is outlined in chapter two with the appropriate equation to use if one has collected ground data on permeability, organic matter content and soil texture. In the absence of ground data, there are various look-up tables published by various authors relating soil type and organic matter content to a K-value. In this study, a look-up table (Table 4-1) published by Stone and Hilborn (2012) was used to determine the K values in tonnes per hectare for the Mhlatuzane catchment.

A detailed soil map for the study area was acquired from the Swaziland Water and Agricultural Development Enterprise (SWADE), GIS department. The map was georeferenced appropriately to enable it for use with other maps for other inputs of the RUSLE model. The attribute table of the soil map had information on the soil type and the areal coverage of that type of soil. A new column with value domain was created on the attribute table and it was labeled K-factor as it contained the K values assigned to each soil class. An attribute map was then created in ILWIS with the column containing the K values used as the attribute to which the new map was identified. The resultant map showed the spatial distribution of the K values in the study area. The average class was used on the organic matter content of the soils.

Table 4-1: K Factor values used to create a Mhlatuzane catchment soil erodibility map (Stone and Hilborn, 2012)

Soil textural class	**K-Factor ton.ha^{-1}.yr^{-1}**		
	More than 2% Organic Matter Content	**Less than 2% Organic Matter Content**	**Average Organic Matter Content**
Coarse sandy loam	0.16	–	0.16
Fine sand	0.13	0.20	0.18
Fine sandy loam	0.38	0.49	0.40
Loam	0.58	0.76	0.67
Loamy fine sand	0.20	0.34	0.25
Loamy sand	0.09	0.11	0.09
Loamy very fine sand	0.56	0.99	0.87
Sand	0.02	0.07	0.04
Sandy clay loam	0.45	–	0.45
Sandy loam	0.27	0.31	0.29
Silt loam	0.83	0.92	0.85
Silty clay	0.58	0.61	0.58
Silty clay loam	0.67	0.79	0.72
Very fine sand	0.83	1.03	0.96
Very fine sandy loam	0.74	0.92	0.79
Clay	0.47	0.54	0.49
Clay loam	0.63	0.74	0.67
Heavy clay	0.34	0.43	0.38

4.5.3 The slope length-gradient (LS-factor)

The LS-factor is an indication of the susceptibility of an area to erosion based on the steepness and length of slope in each spatial location compared to a standard site with 9% steepness and 22.13 m slope length (Whichmeier and Smith, 1978). The sediment transport index (STI) is an equivalence of the LS factor; it accounts for the effect of topography on erosion and reflects the erosive power of the overland flow. A 30 m spatial resolution, DEM covering the study area retrieved from ASTER GDEM website was used to prepare the LS map. DEM hydroprocessing function was used in ILWIS to arrive at the Sediment transport index as outlined in a manual prepared by Gumindoga (2015).

Filling Sinks

This operation was performed before determining the Flow direction in the study area in order to clean up the DEM, so that local depressions (sinks) are removed. The Fill sinks operation removed depressions that consisted of a single pixel. Any pixel with a smaller height value than all of its 8 neighbouring pixels was increased to the smallest value of the 8 neighbouring pixels. The operation also removed depressions that consisted of multiple pixels where a group of adjacent pixels had smaller height values than all pixels that surrounded such a depression.

Calculation of the Flow direction map

Flow direction (FD) is an indication of the flow of water within the catchment and water always flow from the highest elevation to the lowest unless if an external force (pump) is used. In this study, the FD map was computed from the sink-free DEM to determine the flow of water which would later show the outlet of the catchment. The FD map was calculated for each location on 3x3 pixels comparing the center pixel with the neighbouring pixels. The steepest slope algorithm was used to calculate the flow direction map where the direction of flow was towards the steepest pixel in relation to the 8 neighbouring pixel

Calculation of the Flow Accumulation map

The flow direction map calculated in the previous step was used to calculate the flow accumulation map which extracts the drainage pattern of a catchment. Each individual pixel in the flow accumulation map shows the accumulated number of pixels that contribute to that pixel. The values from the flow accumulation map vary spatially with outlets of the largest streams, rivers having the largest values.

After running the flow accumulation operation, the map was displayed using the logarithmic stretch function to enable careful and detailed studying of its value. The values represented the number of upstream pixels contributing to the target pixel or, if multiplied by the pixel area, each value represented the upstream catchment area in raster format. The flow accumulation map covered more than the sub catchment extent so it was crossed with the flow direction map to extract information for only those pixels that fell in the study area. Any map with the correct catchment boundary could be used but for this study the flow direction map was chosen. The resultant map contained information for both the flow direction and flow accumulation so an attribute map was created and flow accumulation was used as the attribute.

Calculating the Topographic/wetness Index map

The topographic index map was calculated for both slope in degrees and slope in percentages. Firstly, the filled-sinks DEM map was used to calculate the height differences in the X-direction and in the Y-direction using the filtering operation in ILWIS. The equations 4-3 and 4-4 were used to calculate the slope in percentages and in degrees respectively.

$$SP = 100 \times HYP \times \frac{DX}{DY} \div PS$$ *Equation 4-3*

$$SD = RADDEG(ATAN) \times \frac{SP}{100}$$ *Equation 4-4*

Where:

SP = Slope in Percentages

SD = Slope in Degrees

HYP = Internal Map calculator functions

DX and DY = height differences in the X and Y direction respectively

ATAN and RADDEG = internal Map calculator functions.

The next step was to calculate the Contributing area (A) for each pixel using the flow accumulation map. Equation 4-5 was typed on the command line in ILWIS to produce a map of the contributing area to be used in computing the topographic index (TI).

A = Flow accumulation x PS *Equation 4-5*

Where:

A = contributing area (m^2)

PS = Pixel size (30 m x 30m = 900m^2)

The LS factor for the Mhlatuzane catchment was then calculated using the equations below, equation 4-6 for slope thickness less than 21% and equation 4-7 for slope thickness greater than 21% (Toxopeus, 1996).

$$LS_1 = \left(\frac{L}{72.6}\right) \times\ 65.41 sin(S) + 4.56\, sin(S) + 0.065) \qquad \textit{Equation 4-6}$$

$$LS_2 = \left(\frac{L}{22.1}\right)^{0.7} \times\ (6.432 sin(S^{0.79})\, cos(S)) \qquad \textit{Equation 4-7}$$

Where:

LS = Slope length and slope steepness factor

L = Slope length in metres

S = Slope steepness in radians

4.5.4 The crop/vegetation and management (C-factor)

The C-factor was determined from satellite data imagery from Landsat TM. Normalized Difference Vegetative Index (NDVI) was used to calculate the C-factor values for the years 1995, 2000, 2005, 2009 and 2015. The NDVI is an indication or vigor in vegetation and it normally ranges from -1 to 1. It is a numerical indicator that uses the visible and near-infrared bands of the electromagnetic spectrum, and is adopted to analyze remote sensing measurements and assess whether the target being observed contains live green vegetation or not. It basically shows the vigor of vegetation on the soil surface detected by satellites. It is expressed as a ratio ranging from -1 to 1 with extreme negative values representing water, values around 0 represent bare soil and values towards 1 represent healthy green vegetation.

In this study, the normalized vegetative was used as the input in the equation to determine the crop factor. Bands 3 and 4 (Red and Near Infra-red respectively) were used for images (1995, 2000, 2005 and 2009) downloaded from the Landsat 4-5 TM satellite. For the 2015 Landsat 8 image, bands 4 and 5 were used for Red and Near Infra-red bands respectively. The red and near infra-red bands were used because vegetation reflects more on the NIR band. The NDVI for the study area was calculated using equation 4-8.

$$NDVI = \frac{NIR - R}{NIR + R} \qquad \textit{Equation 4-8}$$

Where:

NIR = Pixel reflectance value in the Near Infra-red band

R = Pixel reflectance value in the Red band

The NDVI map was then applied in equation 4-9 by Van der Kniff *et al.* (2000) to calculate the crop factor:

$$C = e^{-\alpha \frac{NDVI}{\beta - NDVI}}$$ *Equation 4-9*

C = crop management factor

α = 2

β = 1

4.5.5 Support practice and management (P-factor)

The conservation/support practice factor (P-Factor), in the Universal Soil Loss Equation is the ratio of soil support practice to the corresponding loss with up and down slope culture. Experimental data to quantify the P-Factor for non-crop management practices on forested and rangeland watersheds are usually not available and therefore classification by (Whichmeier and Smith, 1978) was used in this study to calculate the P-factor map.

The classification used land use and landcover information combined with the slope of that spatial location (Table 4-2). A slope map in percentages was calculated in Integrated Land and Water Information Systems (ILWIS) using equation 4-3 presented in sub-section 4.4.3. The slope was then grouped using the slicing function in ILWIS into the slope ranges in Table 4-2. The slope map was then crossed with the Land use/Land cover map for each year then P-factor values were assigned to each pixel (spatial location) with the corresponding slope and land use type, to produce a P-Factor map for the modeled years.

Table 4-2: P-Factor Values used in calculating the P-factor map

Land use type	Slope	P-factor
Agriculture	0 – 5	0.1
	5 – 10	0.12
	10 – 20	0.14
	20 – 30	0.19
	30 – 50	0.25
	50 – 100	0.33
Other Land	**All**	**1.00**

4.6 Selection of the RUSLE Model

The RUSLE model was selected among the many models (Table 4-3) that exist for estimation of soil erosion and subsequently sediment yield of a catchment. This model was chosen because it has been used successfully by many researchers to estimate soil loss around the world including the southern African region (Wall *et al*., 2002b; May and Place, 2005; Ahmad and Verma, 2008; Esther, 2009; Andersson, 2010; Breetzke *et al*., 2013). Therefore there was enough information available on literature to guide the researcher on how to estimate soil loss using the RUSLE combined with GIS especially in Swaziland catchments where there have been limited studies on soil loss with which an already locally approved model could be selected from. Table 4-3 shows some of the most widely used models for estimating soil loss potential.

Table 4-3: Review of the widely used soil erosion risk assessment models

Model	Description	Strengths	Limitations	Sources
Universal Soil Loss Equation (USLE)	Empirically derived model	-Has been found to work well in determining soil loss for disturbed land uses -Has been widely used globally to estimate long term soil loss -Works well with GIS	-Not practical in the estimation of soil loss on event basis -Soil losses or gains from neighbouring areas are not considered -Does not perform well in forested lands	(Renard *et al.*, 2010) (Whichmeier and Smith, 1978)
Revised Universal Soil Loss Equation (RUSLE)	Improved version of the USLE Most widely used model	-Incorporates more data than USLE and corrects errors/fills gaps found in USLE -Much more flexible for use in wider range of environments (globally) -Improved to enable applicability in areas such as forests, rangelands, and disturbed areas	-Lacks the capability of computing deposition along hillslopes, depressions, valleys and channels	(Renard *et al.*, 2010) (Breetzke *et al.*, 2013) (Esther, 2009)
Pan-European Soil Erosion Risk Assessment (PESERA)	Physically based and spatially distributed model	-Can be used with daily rainfall to estimate soil erosion for one storm event -Can also be used well with GIS to estimate erosion at grid level	-Established only for areas related European scale environments -Cannot work with limited amount of data as that leads to anomalies in the predictions	(Kirkby and Irvine, 2003)
Soil Loss Estimation Model for Southern Africa (SLEMSA)	Zimbabwean based Empirical model A modelling technique or framework	-Developed in response to poor applicability of USLE in Zimbabwe -Widely used in African environments -Can make use of limited data and also -improves progressive as more data becomes available -Simplistic in nature and relatively easy to use	-Has a weakness of over-estimation of soil loss values resulting from co-linearity of slope length and steepness factors -Soil loss predictions do not address factors contributing to rill and gully erosion	(Breetzke *et al.*, 2013) (Smith, 1999)
Water Erosion Prediction Project (WEPP)	Physically based Model	-Based on fundamental hydrologic and soil erosion processes -Considers both erosion, deposition and also ephemeral gullies within a field setting	-Has been applied in the US but not much literature is available on its application in African environments	(Smith, 1999) (Ampofo *et al.*, 2001) (Nearing *et al.*, 1989)

4.7 Applicability of RUSLE Model in a Climate Variability/Change Environment

Climate change refers to those changes experienced which are additional to natural weather variability patterns observed over comparative time periods (ECA-SA, 2012). Studies of the anticipated impacts of climate change on land degradation and soil erosion date back to the early 90s (Imeson and Lavee, 1998). Climate change is expected to affect soil erosion based on a variety of factors including precipitation amount and intensity impacts on soil moisture and plant growth, and direct fertilization effects on plants due to greater carbon dioxide concentrations among others (Plangoen *et al*., 2013). According to Wischmeier (1959), the R factor for any given period is obtained by summing, for each rainstorm, the product of total storm energy and the maximum 30 minutes intensity (I_{30}).

The RUSLE model will still be applicable even when conditions change due to climate variability and change. Bosco et al. (2009) have noticed the flexibility advantage RUSLE has over other models like the PESERA and WEPP and this allows setting the equation to adapt it to the environment to be analysed. When applying the RUSLE in changing environment due to climate change it is imperative to improve the data collection for rainfall and rainfall intensity. Rainfall intensity data has to be available at meteorological stations as originally the R-factor is a product of storm energy and 30 minute intensity. The crop factor will also be affected by climate change as an increase in the carbon dioxide concentrations in the atmosphere will yield an increase in crop photosynthetic activity hence improving crop vigor (Plangoen *et al*., 2013). The crop vigor is remotely sensed by satellites hence any changes due to climate change will be noted. Other factors of the RUSLE like the LS factor, K factor and P factor will not be affected much as they are not directly affected by climate variability and change.

4.8 Determination of Sediment Yield

Not all the sediment generated in a catchment ends up in river channels and reservoirs as some gets trapped in depressions and vegetation in the area. Therefore, de Vente *et al.* (2011) emphasizes that it should not be concluded that estimations of sediment generated in a catchment equals the deposition in rivers and reservoirs. This then necessitates the use of Sediment Delivery Ratios (SDRs) that account for the deposition of sediment as it flows from the point of generation towards streams and reservoirs. The SDR is presented as a fraction from

0 – 1.0 and when SDR = 1.0, the transport capacity of the sediment flow is not exceeded and at that point the sediment delivery is directly related to soil erosion (Kinnell, 2004). When SDR is closer to zero, it means that the transport capacity of the catchment is low, sediment is deposited in depressions before it reaches the rivers. In this study the SDR was calculated using the equation 4-10 by the USDA (1983).

$$SDR = 0.5656CA^{-0.11}$$ *Equation 4-10*

Where:

SDR = Sediment Delivery Ratio (dimensionless)

CA = Catchment area (km^2)

Other methods for determining the SDR deals with specific sites where sufficient sediment yield and stream flow data are available (Lu et al., n.d.). Another most widely used method for determining the SDR is the SDR- area power function which is represented as $SDR = \alpha A^{\beta}$, where α and β are empirical parameters (Walling, 1983). The SDR method selected for this study was that which required only catchment area since there was no historical data on sediment yield. After determination of the sediment delivery ratio, the average sediment yield was then calculated using equation 4-11, by Wischmeier and Smith (1978).

$$SR = SDR \times A$$ *Equation 4-11*

Where:

SR = Sediment yield (ton/ha/year)

SDR = Sediment delivery ratio

A = Average soil loss (ton/ha/year)

4.9 Validation of the RUSLE using soil erosion monitoring plots

GIS and remote sensing provides sophisticated methods of determining sediment yield at pixel level and also for a varying temporal scale. However, the data that is obtained through these methods have to be validated with observed ground data. Soil erosion experimentation around the world commonly uses hydrologically defined runoff plots with runoff and soil loss measured at the exit of the plot by collection in a tank system (Ciesiolka *et al.*, 2004). In this study, runoff plots were used to determine soil loss from each rainfall event from the month of January 2016 to March 2016 and the data obtained was then compared with the estimates from GIS and remote sensing using RUSLE. A total of four plots were installed within the catchment to capture the spatial distribution of rainfall and erodibility factors. A conventional rain gauge was installed in each plot in order to measure rainfall as erosion begins with soil detachment by raindrop impact.

In order to ensure safety of the plots and to avoid theft of the material used to set up the plots the plots had to be set up in protected areas (fenced-off areas). Some sites that could have been arguably better than those chosen for the plots were abandoned because of lack of protection for the plots. The sizes of the plots also varied based on the amount of space that was available for the researcher to erect the plots. Detailed information on the plots and the places that they were located in the catchment is shown in Table 4-4.

Table 4-4: Characteristics of the soil erosion monitoring plots

Site Name	**Location**	**Area (m^2)**	**Flow direction**	**Soil type**	**Slope (%)**	**Land use/land cover**
Luhlanyeni	26^0 49’ 52.1” S 31^0 36’ 00.32” E	80	North-East	Sandy Loam (solodized)	13.9	Settlements/Plot by roadside
Gucuka	26^0 48’ 12.0” S 31^0 41’ 32.15” E	96	North-West	Deep pale grey sand (regosolic)	8.9	Forest and Shrubs
Gcekeni Farm	26^0 43’ 48.43” S 31^0 41’ 05.94” E	44	East	Red Clay	12.7	Sugarcane Farm
Mpompotha High School	26^0 53’ 42.7” S 31^0 30’ 46.97” E	63	North	Deep Red Loam (Ferrisolic)	7.3	Dense well Maintained grass cover

Figure 4-3: Installation of the runoff plots (top-left), Raingauge (top-right), Sediment collector (bottom-left) and cover to prevent direct rainfall (bottom-right). (Images taken on 6 January 2016)

The erosion monitoring plots were furnished with 160 litre drums that collected the water and sediment during a storm event. The outlet of the plot was sited at the lowest point and it was connected to the drum by a 75 mm plastic pipe. The drums were covered on top to avoid direct rainfall falling in and diluting the collected samples hence compromising the results by making the sediment concentration seem less than the actual. To delineate each Erosion Plot, 2 mm thick galvanized iron sheets were used and dug least 100mm into the ground and protruded another 100 mm above surface. 300 mm long round bars were used to reinforce the iron sheets on either side to enabling them to resist runoff water from flowing into the plot during heavy storms. Plot 1 (Luhlanyeni site) was installed first as a pilot plot in order to test if it worked well and if adjustments were to be made they would be incorporated in the installation of the other three plots.

Data was collected at the sites after every rainfall event since the make-up of the plots allowed them to measure soil erosion by rain and not from wind. During data collection, the mixture of water and sediment was emptied into another empty drum of the same size, covered and taken to the workshop and allowed 24 hours to settle. After the heavier particles settled, the water would be carefully poured out of the drum into several small 25 litre buckets depending on how much sediment was collected. The concentrate at the bottom would be emptied into a separate bucket then taken to the lab for drying to determine how much soil was eroded from that rainfall event.

The remaining cleaner water would be stirred to mix the sample well and 3 sub-samples taken to determine the concentration and noting the volume of water in the buckets. The mixing ensured that the sub-samples are a representative of the concentration of sediment in the water. The three sub-samples were also taken to the lab to be filtered and oven dried at 105 ^{0}C for 30 minutes to remove any remaining moisture. After drying, the samples were left to cool for 15 minutes then weighed to determine amount of sediment. The sediment from the three representative samples and the concentrate would be summed up to get the soil loss for that storm event. Rainfall was also recorded from the conventional rain gauges and information on when the rain started and when it stopped raining was obtained through informal interviews with the locals that assisted with the research. Such information was necessary in determining the rainfall intensity in mm/hr since it has a bearing on the amount of soil lost in a storm event. A regression analysis was performed in excel using XLSTAT software for the soil loss data and the rainfall intensity in order to determine if the rainfall intensity can be used to estimate

4.10 Grab Sampling

Water samples were taken by scooping (using a 500 ml plastic sampling bottle) at a sampling point, at 300 mm below the water surface as that has an advantage of getting a good mix of sediment and water as opposed to sampling on the surface (Mavima *et al.*, 2011). The sampling points were the outlet of the feeder canal and at a gauging station (GS12) upstream of the Lubovane reservoir. The reason for sampling at a gauging station is that the flow was measured known hence there would be no need to estimate flow in order to determine the flow of sediment past that point. A trial sample was taken at Othandweni Bridge which is located at the point where the Mhlatuzane River discharges into the reservoir and it was found that the sediment concentration differs with a big margin from that of GS 12 upstream. This then necessitated continued sampling at that site. Flow at that point was estimated using the float method of determining velocity and the area was estimated by measuring the depth and the distance from the right bank and left bank for each sampling. The discharge was then calculated using equation 4-12.

$Q = A \times V$ *Equation 4-12*

Where:

Q = Discharge (m^3/s)

A = Cross sectional area (m^2)

V = Stream Velocity (m/s)

4.10.1 Sampling in the Mhlatuzane River

Sampling at GS 12 was done downstream of the weir since the water was turbulent as it flowed across the weir allowing a good mix of water and sediment as recommended by Mavima *et al.* (2011). Samples were taken weekly from the month of January 2016 to end of March 2016. The samples were then taken to the lab for processing. They filtered first using a filter paper to remove excess water then weighed the filter paper was put in a petri-dish of known mass and oven dried for 30 minutes in a laboratory to remove the moisture. After 30 minutes they were removed from the oven and then left to cool for 15 minutes then weighed to get the sediment weight in mg. The sediment concentration was then determined by comparing the sediment weight with the volume of water that was removed by filtering and drying (mg/500ml). The data obtained from the samples taken in the Mhlatuzane River at the Othandweni Bridge was then compared with the observed soil loss and GIS based RUSLE model for estimating the sediment that passes through that point, allowing the RUSLE with the GIS inputs to be applicable in determining sediment that has settled in the Lubovane reservoir.

4.10.2 Sampling in the Feeder Canal

In the canal, samples were taken using the same sized equipment explained in sub-section 4.8 and following the method explained. The sampling in the canal was done to determine the amount of sediment conveyed by the feeder canal from the Great Usuthu River, so that when added to the sediment from the catchment the resultant sediment load flowing into the Lubovane reservoir could be estimated. Suspended sediment was sampled in the canal since there was no equipment available for sampling bedload. Daily discharge data for the FC was obtained from SWADE so as to be able to calculate the concentration of the sediment with the flow that was going into the reservoir. Once samples were taken, the procedure for determining the sediment load was followed as outlined in sub-section 4.8. The sediment concentration obtained from processing the samples in the lab was presented in mg/l. The sediment discharge, Q_s, (kg.s^{-1}) was obtained by multiplying the instantaneous discharge, Q (l.s^{-1}) by the Suspended Sediment Concentration (mg.l^{-1}), (Equation 4-13) which, integrated over time, provided the sediment yield (SY) in tonnes per year (Didoné *et al*., 2015).

$$Q_s = C_s \, x \, Q$$ *Equation 4-13*

Where:

Q_s = sediment discharge (kg.s^{-1})

C_s = the concentration of sediment in the grab sample (mg.l^{-1})

Q = Stream/canal discharge from the rating curve (m^3.s^{-1})

From the sediment concentration the annual deposit of sediment (ADS) was calculated in order to estimate the impact of sediment in the lifespan of the reservoir. The factors that affect the ADS include the gross mean annual runoff (GMAR), the measured sediment concentration (SC), trap efficiency (TE) and the density of sediment (d). Equation 4-14 was used to calculate the ADS (Tumbare, 2013). The trap efficiency for the reservoir was calculated from equation 2-9 in Chapter 2.

$$ADS = \frac{GMAR \times SC \times TE}{d \times 10^8}$$ *Equation 4-14*

$$GMAR = CA \times MAR$$ *Equation 4-15*

Where:

CA = Catchment Area (km^2)

MAR = Mean Annual Runoff (mm/yr)

D = Assumed to be 1.55 ton.m^{-3} where measured values are unavailable.

The MAR of the Mhlatuzane river was obtained from the Hydrology section of the report on the proposed impacts of the LUSIP project on Usuthu and Mhlatuzane downstream flows by Vakakis-International (2000). The potential MAR of the Feeder canal was calculated from the 13.5 m^3/s which is the full conveyance capacity of the canal. Water users downstream of the abstraction point are entitled to 10.8 m^3/s. This allocation was removed from the Usuthu MAR as it is water that is not available for abstraction by the canal. According to the LUSIP water management study by Coyne-et-Bellier (2012), the canal would only be able to abstract water from November to May so the MAR was calculated assuming 7 months of abstraction and 6% losses to evaporation and seepage. The GMAR for Mhlatuzane and the calculated MAR for the canal were added to determine the annual inflow into the reservoir.

4.11 Bathymetric Survey

The soil erosion modeling provided information on the annual average yield of the catchment but not all the sediment generated ends up in the reservoir. Due to the complex process of sediment transportation, some of the sediment ends up in depressions, some trapped by vegetation, buildings and other land surface features (Kinnell, 2004). Also the sediment loading in the dam comes from both the river and the feeder canal. Hydrographic or Bathymetric surveys were then conducted in the reservoir in order to determine the changes in the capacity and geometry of the reservoir due to sedimentation. Hydrographic surveying in reservoirs is a key activity in order to collect data for a variety of purposes like estimation of storage capacity, rate and pattern of sediment deposition, movement of underwater sediment delta and reservoir routing (Munir *et al.*, 2014). Data collected through hydrographic surveying plays a pivotal role in decision making for short and long term planning, operation and management of the reservoir. The Lubovane reservoir is mostly used for agricultural and domestic water supply to the rural communities of the Siphofaneni area.

Depth sounding of the Lubovane reservoir was carried out using a Garmin GPSmap 720 series model Echo-sounder with an inbuilt GPS and a transducer/sonar mounted at back lower parts of the boat. Days when wind was calm and the weather was good were chosen for the survey to avoid excessive waves so that accurate readings were obtained. The device had a display and control touch screen on the dashboard of the boat and it was supplied power from within the electrical system of the boat. The display screen would show the relative position of the boat in relation to prior surveyed points. The mark function was used to mark points along the survey lines from bank to bank. Survey lines were kept at around 50 metres and 10 metres between each marked points. Each marked point recorded the coordinate of that particular point in Latitudes and Longitudes, water depth at that particular point, date and time that point was collected. The marked points and survey parts were stored in an SD card installed in the device so that on the next survey date the survey parts would be displayed to take note of paths that have already been survey so they are not repeated.

The southern African region was hit hard by an El-Nino drought on the hydrological year that the research was conducted. This saw a reduction in the water levels of the Lubovane reservoir. During the days of conducting the study, the dam fluctuated between 66 % and 75% to full capacity which meant that it was covering less area than the area covered at full capacity. On the first day of the survey the reservoir was at 66% to FSL, containing $103.6 x 10^6$ m^3 of water and it covered 10.3 km^2. When full, it covered 13.9 km^2, which meant that there was an area (3.6 km^2) not covered by water. That area could not be covered by the survey since the boat could not measure depth in the dry portions. This is why the survey points in Figure 4-4 do not cover the whole reservoir. The reservoir boundary was digitized when the reservoir was spilling hence the boundary is covering an area greater than 13.9 km^2.

3270 points were taken in total and in very high density in order to limit interpolation errors as much as possible because if the points are sparsely related, the depths between is assumed to be linear during the interpolation. The points were then entered into Microsoft office excel for proper arrangement and exploration of the data. Three columns were created containing the data on latitudes, longitudes and water depth. The sonar is 0.3 m on average below the water surface in calm waters hence that was subtracted from the depths. The readings were then reduce using the dam level on that specific day to determine the elevations of the points below the water surface. Then the data now had X, Y and Z coordinates. A point map was created in ArcGIS software with the new elevations as the Z attribute. The points were explored for consistence and outliers which signaled incorrectly recorded points due to typing errors were corrected to bring the points within the boundary.

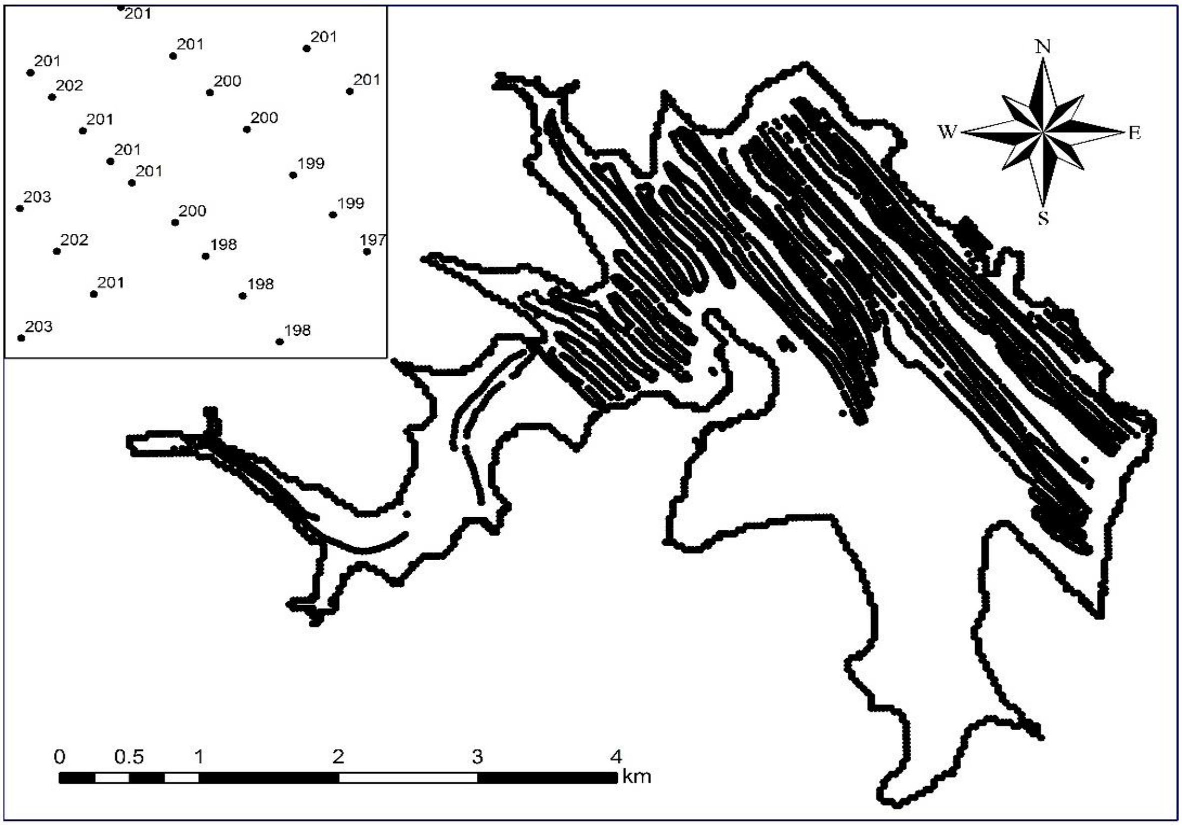

Figure 4-4: Depth points surveyed during the bathymetric survey

The point map was then exported to Quantum GIS software for creation of contours in order to use them for the calculation of the new reservoir volume. The point map was imported into QGIS together with the shapefile for the Lubovane reservoir. The grid interpolation method was used to interpolate the elevations between the different points within the reservoir boundary. The extent of the interpolation was set to be bigger than the reservoir boundary in order to enable coverage of the whole boundary when the contours were created. The interpolated surface was then clipped/masked using the Lubovane reservoir boundary as the mask layer to extract only those pixels falling within the reservoir. The raster extraction tool was used to extract the contours from the boundary which showed the new elevations of different points within the reservoir boundary. Equation 4-16 was used to calculate the different volumes in the areas enclosed by each contour in ArcGIS 10.2 and in turn the cumulative volume to the full supply level.

$$V = \frac{A_1 + (A_1 \times A_2)^{0.5} + A_2}{3}$$ *Equation 4-16*

Where:

V = Volume for each contour or Elevation (m^3)

A_1 and A_2 = Area 1 and Area 2 respectively (m^2)

4.12 Water availability assessment

The key impact of sediment accumulation in reservoirs is the capacity loss which ends up affecting the annual reservoir yields because the amount of water lost through spillway discharges increases as storage capacity is lost (UNESCO, 2011). Reservoir yields refer to the volume of water that can be drawn from the reservoir annually at that specified reliability level. The Lubovane reservoir was constructed to store excess water during the rainy season in order to supply LUSIP farms throughout the dry season (Mhlanga *et al*., 2012; Vakakis-International, 2000), so storage capacity is a vital part in the operation of the reservoir.

4.12.1 Storage loss projections

The average sediment load used in the assessment was that obtained from the bathymetric survey because it accounted for sediment deposited by both the river and canal. Sediment load from the grab sampling/sediment concentration method was not used because only suspended load was analysed so bedload was not accounted for hence it underestimated the annual sediment loading. The sediment loading from RUSLE Model was also not used for the projections of storage loss because it only considered sediment generated only from the Mhlatuzane catchment.

Moreover, Estigoni *et al.* (2014) argues that bathymetric surveys provide a more accurate method of assessing sediment deposition compared to other methods. The annual capacity for the successive years was obtained by subtracting the annual sediment volume deposited in the reservoir from the capacity of the previous year. The accumulation of sediment in the reservoir was assumed to be constant for ease of analysis and prediction. The period chosen for analysis was from 2009 when the reservoir was commissioned to 2080 when the reservoir is expected to silt up if no measures are taken to combat reduce sediment loading.

4.12.2 Calculation of annual loss in yields due to reduction in storage

In this study, the effect of sediment accumulation on storage capacity and yield of the reservoir was predicted using the TB Mitchel method established by Mitchell (1982). This method was developed in Zimbabwe for use in estimating reservoir and catchment yields for semi-arid regions. It was selected because the Usuthu basin, in which the Mhlatuzane micro-catchment is situated, falls under the semi-arid category and. It was developed using reservoirs in Southern Africa so the conditions are similar. The method utilizes the Mean Annual Runoff (MAR), Storage ratio (SR), Evaporation Factor (EF), Volume/Capacity of the reservoirs in the catchment as well as the coefficient of variation (CV). The curves were developed for CVs ranging from 60% to 120% (see Appendix 6). The MAR and CV for the Mhlatuzane catchment and larger Usuthu basin measured at Bulungapoort was obtained from the from the original documents detailing on the designs and feasibility studies of the reservoir (Vakakis-International, 2000). The EF was calculated using equation 4-17 from daily evaporation data obtained from the Big Bend Meteorological station (Appendix 3).

$$EF = S^2 \left[\frac{0.785}{(E \times A)}\right]^3 \qquad \textit{Equation 4-17}$$

Where:

EF = Evaporation factor (Dimensionless)

S = Reservoir storage capacity (10^6 m^3)

E = Annual evaporation (m)

A = Reservoir Surface area at full supply level ($10^6 m^3$)

The curves in the TB Mitchel method were each calculated from multiplying the EF and the MAR. Therefore, the CV and the product of MAR and EF were used to select the appropriate curve from which the yield was estimated. Evaporation is part of the water budget as it contributes to losses hence it is vital in yield assessments. The TB Mitchell curves give a yield ratio which is given by equation 4-18. The potential yield at the appropriate level was then calculated through substituting for the YR and MAR in equation 4-18, leaving Q_G as the only unknown in the equation. The MAR used was the sum of the MAR for Mhlatuzane River and the MAR for the FC.

$YR = \frac{Q_G}{MAR}$ *Equation 4-18*

Where:

YR = Yield Ratio obtained from the TB Mitchell curves (Dimensionless)

Q_G = Annual yield that can be obtained from the reservoir at reliability level (G)

MAR = Mean Annual Runoff (10^6 m^3)

Since the TB Mitchell curves were designed for a 10% risk level (Mitchell, 1982), the obtained yield had to be converted to a 20 % risk level which is normally used in water supply for agriculture in Swaziland and the Lubovane reservoir is primarily used for irrigation. The 20 % yield was calculated from the 10 % yield using equation 4-19.

$Q_{G20} = 1.18Q_{G10} + 0.05(MAR)$ *Equation 4-19*

Where:

Q_{G10} and Q_{G20} = Annual yields at 10% and 20% risk levels respectively (10^6 m^3)

MAR = Mean annual Runoff (10^6 m^3)

4.12.3 Population projections and Water Demand

Upon completion of the LUSIP, a total of 6500 ha and 5000 ha of land will be put under irrigation for LUSIP I and LUSP II respectively. The Lubovane reservoir was designed to supply water for both phases of the project. Apart from provide water for irrigation, the LUSIP water supply system provides potable water for the residents of the benefitting chiefdoms. The chiefdoms include KaShongwe, Gamedze and Ngcamphalala under LUSIP I and Gamula/Mahlabaneni for LUSIP II. Lesibovu and Mpumakudze potable water scheme were left out in the analysis as they have they use boreholes. The combined population for these chiefdoms was 27 234 in 2012 with a growth rate of 2.9% for the project area (Fatoyinbo *et al.*, 2011). The population was projected up to 2080 using the empirical equation 4-20. The growth rate was assumed to be constant throughout the period for ease of analysis.

$$P_t = P_0 (1 + r)^t$$ *Equation 4-20*

Where:

P_t = Population at time t

P_o = Present/Initial population

r = Growth rate

t = time incremental (years)

In the simulations of the water demand, the demand for irrigation was kept constant for the projected years, only the domestic water demand changed because domestic water demand responds to changes in the population. The water demand for irrigation was obtained from the water management study and the feasibility study reports of the LUSIP prepared by Coyne-et-Bellier (2012). The project was divided into four blocks which are the Weir block, Bovane North block, Bovane south block, St. Phillips block and Matata block. The water demand for phase I is $33.7 x 10^6$ m^3, $57.5 x 10^6$ m^3 and $23.2 x 10^6$ m^3 for Bovane north, Bovane south and St. Phillips block respectively with Matata block having an annual demand of $78.5 x 10^6$ m^3 in the second phase of the project. Irrigation is expected to begin in 2019 in the Matata block so its water demand was included in the water demand assessment. The water demand for domestic use was calculated using the World Health Organization guidelines of 50 litres per capita per day (WHO, 1997) for drinking water since Swaziland does not have drinking water standards.

4.13 Data Analysis

Data was analysed using various GIS softwares as well as SPSS and XLSTAT in order to generate useful information from the Data. ILWIS was used mostly to compute the maximum, minimum and average soil loss potential as well as the standard deviation of the data. Quantum GIS was used to perform Grid interpolation and to generate contours for the determination of the capacity of the Lubovane reservoir. Trend analysis was performed on the rainfall data in SPSS to determine whether the rainfall was reducing or increasing with time. Linear regression analysis was done on the rainfall data comparing each station against the other in order to test if the station can be used to fill gaps in the data for the other station. The station in Sithobela had lots of gaps in its data then the Bigbend station was used to predict the rainfall for those missing months. The Bigbend rainfall measuring station was found to have a good relationship with the Sithobela station with an R^2 of 0.98. Equation 4-21 was derived from the regression analysis and it was used to predict the missing values in the rainfall data from the Sithobela rainfall station.

$$S = 1.1073\,(S) + 4.8266 \qquad \textit{Equation 4-21}$$

Where:

S = Predicted monthly rainfall for the Sithobela station (mm)

B = Observed monthly rainfall for the Bigbend station (mm)

CHAPTER FIVE

5. RESULTS AND DISCUSSIONS

This chapter presents the results that were obtained in the study in order to achieve the objectives. The main objective of this study was to determine the sediment yield of the Mhlatuzane sub-basin; hence the sedimentation rates of the Lubovane reservoir so as to determine its implications on the lifespan of the LUSIP with respect to continued availability of water for irrigation and domestic use. The results presented in this chapter include temporal variation of rainfall in the Mhlatuzane micro-catchment assessment of land use and land cover changes, results from sediment concentration for the Mhlatuzane river and the Feeder canal, Results from 3-months of monitoring soil loss through erosion plots, results from the RUSLE model which was used to model soil loss in the catchment as well as results from a bathymetric survey conducted in the reservoir.

5.1 Historical rainfall trends in Mhlatuzane

Figure 5-1 shows observed rainfall trends for the Mhlatuzane micro-catchment for the period, 1981-2015. Historical observed rainfall for the individual stations is presented in Appendix 6b. The Thiessen weights calculated in ArcMap showed that Khubutha rainfall measuring station had the most influence (59%) in the study area, followed by Sithobela with 41% and the Bigbend station was found not to be contributing in the study area in as far as rainfall is concerned. This means that rainfall recorded at the Bigbend station has no bearing on the rainfall received anywhere within the study area.

The rainfall for the two stations (Khubutha and Sithobela) was then considered for the trend analysis. The null hypothesis (H_0) of the analysis was that there is no trend in the data series and the alternative hypothesis was that there is a trend in the data series (see Appendix 6). The p-Value obtained from the analysis was 0.309 which was higher than 0.05 thus we failed to reject the null hypothesis which said there is no trend in the data series. Figure 5-1 visually shows a decreasing trend in the rainfall but according to the Mann-Kendal trend test, the decreasing trend in the data is not significant.

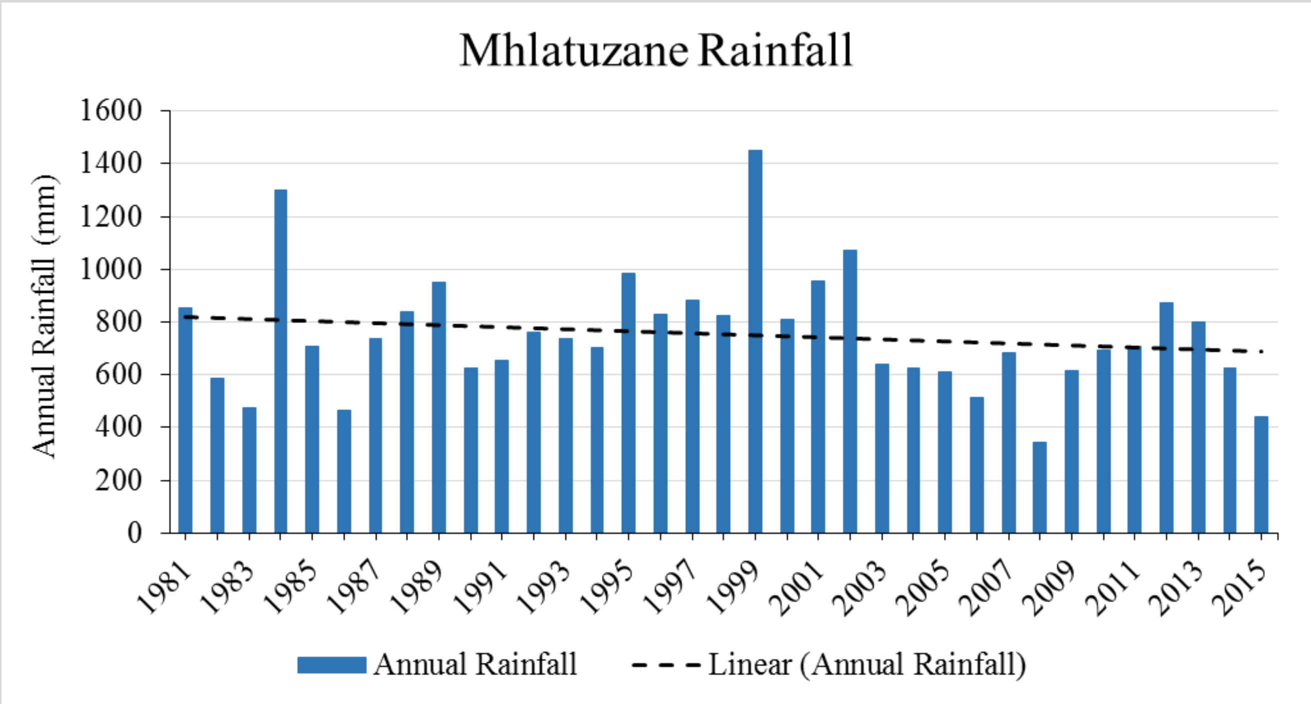

Figure 5-1: Rainfall trends in the Mhlatuzane catchment

The moving average results (Table 5-1) show rainfall averaged for five year intervals (two years before and two years after the year of interest). The years of interest in these study were 1995, 2000, 2005, 2009 and 2015 (as shown in Table 5-1) as they were the years for which sediment yield was modelled using RUSLE. The 5-year moving averages also show that rainfall has been reducing slightly in the micro-catchment with the period around 2005 receiving the lowest rains. It must be noted though that for the year 2015, the average was computed from 2013, 2014 and 2015.

Table 5-1: Five-year moving averages of rainfall in Mhlatuzane micro-catchment

	1995s	**2000s**	**2005s**	**2009s**	**2015s**
Moving average rainfall (mm/yr)	827	814	607	614	622

5.2 Land use Land cover Assessment

5.2.1 Validation of the Land cover Classification

Land cover classification, even though supervised, may possess some errors in the classification where pixels are assigned a class that they do not represent in the real image (Anderson *et al*., 2001). These errors are increased when classifying images of low resolution. Landsat images that were used in this study are 30m spatial resolution which means that the satellites can only identify land surface features more than 30m and be able to distinguish between the features. Below that, it sees the features as the same. To attain near-perfect classification, images with higher spatial resolution are to be used (e.g. SPOT 5 images which can have a resolution of 5m) but those are purchased as opposed to Landsat images which are free. Tables 5-2 & 5-3 present the confusion matrix that was prepared in ArcGIS to assess the land cover classification accuracy.

Table 5-2: Confusion matrix for Land cover classification

	W	SL	IRR	CU	F&S	BL	SUM	Producers accuracy
Water (W)	**52**	0	1	0	0	0	53	**98.1**
Settlements (SL)	8	**24**	1	8	19	17	77	**31.2**
Irrigation (IRR)	0	0	**59**	0	0	0	59	**100.0**
Cultivation (CU)	0	2	0	**14**	0	0	16	**87.5**
Forest and Shrubs (F&S)	0	0	0	5	**24**	0	29	**82.8**
Bare land (BL)	0	3	0	3	0	**6**	12	**50.0**
SUM	60	29	61	30	43	23	**246**	
User's accuracy	**86.7**	**82.8**	**96.7**	**46.7**	**55.8**	**26.1**		**72.4**

Table 5-3: Class and Overall Accuracy

	Class Accuracy (%)	Overall Accuracy (%)
Water	92.4	
Settlements	57.0	
Irrigation	98.4	
Cultivation	67.1	
Forest and Shrubs	69.3	
Bare land	38.0	
Average	**70.4**	**72.8**

The results show that water, irrigation, cultivation, forests and shrubs were well classified whilst bare land and Settlements were poorly classified. Water, irrigation and cultivation were probably easy to identify and classify especially in the 2015 image because of the reservoir and the large areas under sugarcane production downstream of the Lubovane reservoir which fall in the same tile. The Mhlatuzane catchment is predominantly composed of rural settlements which have sparse homesteads as opposed to clustered high density settlements patterns. Some of the homesteads are made of thatched, stick and mud houses which reflect solar radiation/light almost in the same way as bare land. That made it difficult to distinguish between most settlements and bare land hence the poor classification between the two classes. The fortunate part is that in the P-factor calculations in soil erosion assessment, the two classes both encourage overland flow hence they are related so they do not greatly affect the P-factor maps. According to van Vliet *et al.* (2011) accuracy of land cover assessment is considered to be poor below 50%, fair above 50% and good above 70%. The Land cover classification performed in this study was good according to the above mentioned classification.

5.2.2 Land use/Land cover changes

There were some noticeable changes in the land cover and land use patterns over the mapped period (1995, 2000, 2005, 2009 and 2015). Some of the changes have a direct impact on soil erosion and subsequently sedimentation and these include forest coverage, changes in bareland and changes in farming activities. The results showed low coverage of water bodies from 1995 – 2005 and significant amount of water started showing in the 2009 assessment since that is when the dam had started impounding water. The areal coverage of water increased from 0.05% coverage in 2005 to 3% percent coverage in 2009. In 2015 the areal coverage of water decreased to 1.9% of the total catchment. This was because in 2009, the dam was still not utilized since the irrigation infrastructure downstream had not been completed so there was very low drawdown (to compensation flows) as compared to 2015 when the dam now irrigates over 6 500 hectares of land. The decrease in water coverage in 2015 can also be articulated to the low rainfall in 2015 as compared to 2009 which may have resulted in low inflows into the reservoir hence the low water levels in 2015 as compared to 2009.

Forest and shrubs covered about 27% of the total catchment area in 1995 and had a 3% decrease in 2000 and decreased again by 4% consistently towards 2009. There was a 2% increase in forested areas from 2009 to 2015. This might be partly due to that when the reservoir started impounding water, some forested areas were covered by water and also some of the homesteads that were falling within the Probable maximum flood (PMF) of the reservoir were resettled upstream of the dam thus causing deforestation on those areas to allow construction of houses. In 2009, a project Global Environment Facility (GEF) office was opened at LUSIP and as part of their work they implemented a land rehabilitation programme which involved planting trees in the study area (IFAD, 2013) hence that also may have led to the increase in forest and shrubs from 2009 to 2015. The 2009 and 2015 images in Figure 5-2 show that although forest might have been seen to slightly increase but there was a decrease in the concentration of forests in the areas around the water body with settlements and bare land increasing in those areas which is a threat to siltation of the reservoir.

Bare land was covering about 38% of the total catchment area in 1995 and it was moderately increasing towards 2005. It dropped to 29% in 2009 had an alarming increase towards 2015 when it covered about half of the land (49% of total area). This relates to the decrease in forested areas from 27% in 1995 to 19% in 2015 due of deforestation. Since the catchment mostly contains rural settlements, firewood is the common source of fuel that is used hence the deforestation increases. An increase in the population also leads to an increase in the demand for fuel hence increased deforestation. Figure 5-3 shows a summary of the changes in land cover over the years.

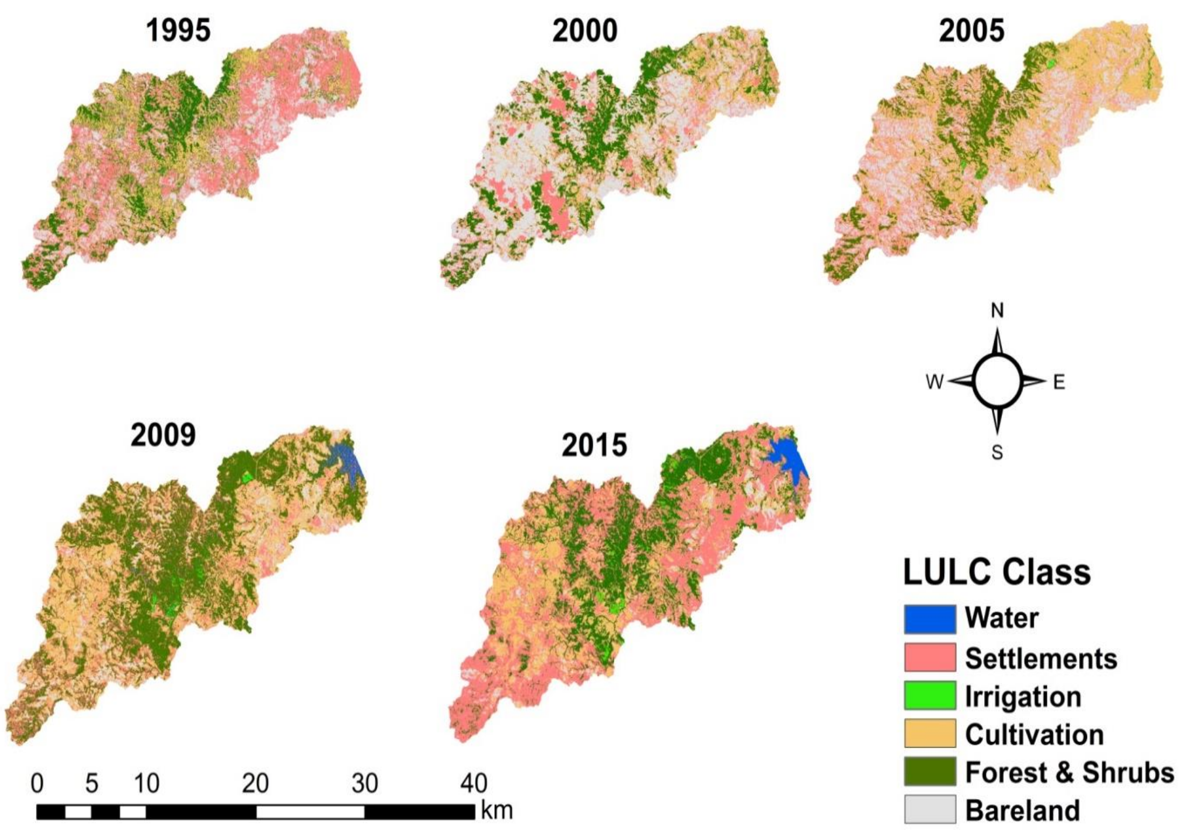

Figure 5-2: Land cover Maps for Mhlatuzane catchment

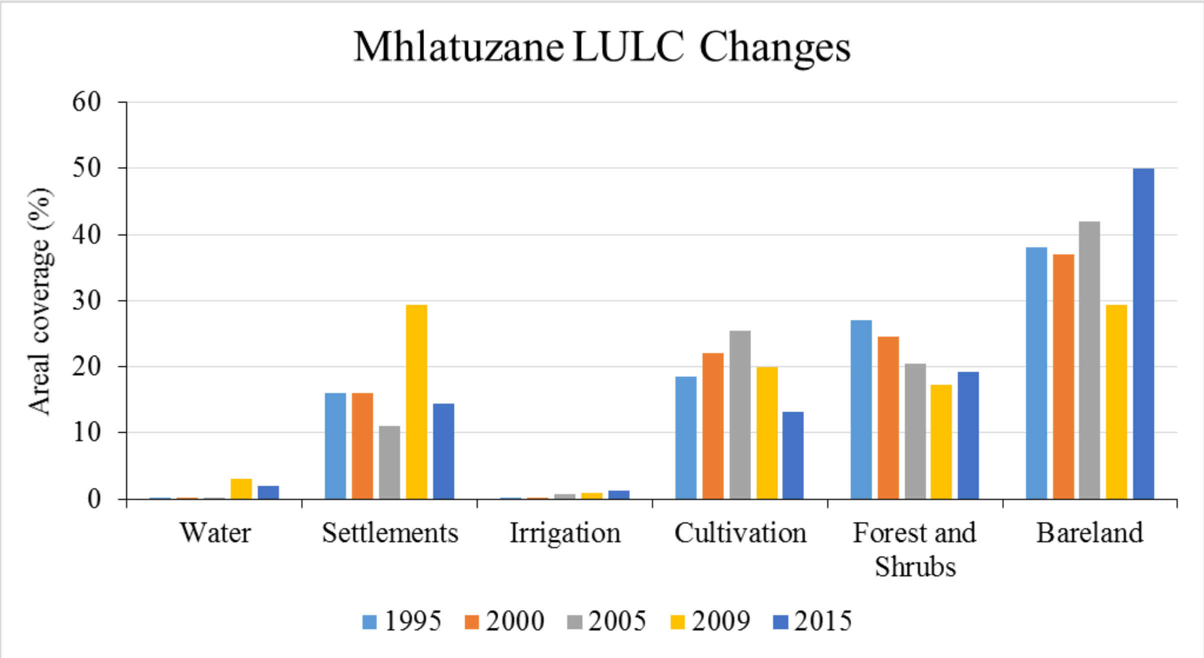

Figure 5-3: Land use and land cover changes in Mhlatuzane micro-catchment

5.3 Soil Erosion Modelling using RUSLE

5.3.1 Validation of RUSLE – Soil erosion monitoring plots

The results (Appendix 7a and 7b) show that observed soil loss had a positive relationship with rainfall, i.e. when rainfall was high, soil loss was also relatively high. However, in some rainfall events, there was relatively high rainfall but soil loss rates were low. These events include plots 2 and 3 (09 March 2016) and also for plot 4 in the last event. This can be attributed to that even though rainfall was high, not much of the rainfall was converted to runoff because of the dense vegetative cover in plot 4 and the gentle slope (Table 4-4). Plot 4 had the least observed soil loss (see Appendix 7b) compared to the other plots mainly because its features encouraged infiltration as opposed to runoff. A test of the relationship between rainfall intensity and soil erosion rates was performed and the results showed an R^2 value of 0.9036 at 95% confidence level (Figure 5-4) which means they had a strong positive relationship. This generally means that an increase in rainfall intensity would lead to an increase in soil erosion. The relationship was not perfect due to the other factors which affect soil erosion other than rainfall erosivity which are the LS factor and C-factor. The analysis considered soil loss recorder in all the four plots distributed within the micro-catchment, sited in areas with varying land cover, slope and soil type.

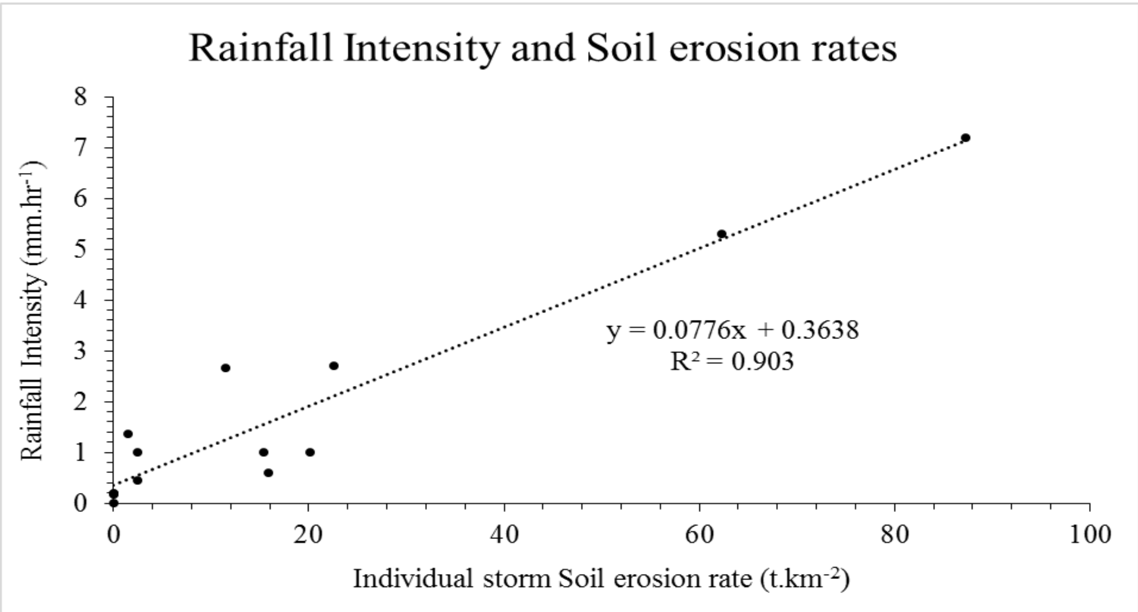

Figure 5-4: Relationship between rainfall intensity and Rates of soil erosion

Plot 1 had higher soil loss on average followed by plot 2, plot 3 and plot 4. This was due to the varying features of the plots in terms of slope and ground cover which affect overland flow. The variations of the plots were meant to capture the different characteristics of the catchment in terms of slope, cover, and soil type and rainfall variability. One factor that had not been linked to the soil loss is the soil type (erodibility class). Plot 1 and plot 2 were placed on sandy loam soils and deep pale grey sand (plaster sand) respectively which are relatively highly erodible soils because of the low cohesion between the particles and yet the particles are too small to allow maximum infiltration as opposed to coarse sand. This then encourages overland flow thus erosion. Plot 3 and 4, placed in Gcekeni farm and Mpompotha had Red clay and Deep red loam soils respectively which are not as erodible as the soils in the other two plots.

Figure 5-5 shows the comparison of the observed and modelled soil loss at pixel level. The 2015 map was chosen for the comparison because it is the one closest to the observed period. The results show that the observed soil loss was lower than the modeled soil loss for 2015 but there was a positive relationship in the observed soil loss and the modeled. The Root Mean Square Error (RMSE) method was used to assess the performance of the model and the RMSE was found to be 2.48. According to Mashingia *et al.* (2013), the RMSE ranges from 0 to infinity and a perfect score is 0. This means that the model prediction in this study was relatively poor. The differences may be attributed to errors in computing some of the parameters of RUSLE, particularly the P-factor which is subject to errors in landcover classification. Also the fact that the modeled soil loss used data for annual basis as the RUSLE model was developed to model annual soil loss (Whichmeier and Smith, 1978), yet the observed soil loss was per storm event and the period of observation was only three months. Increasing the observed data through increasing the number of plots in the catchment and the observation period can enhance model calibration and hence overall model performance.

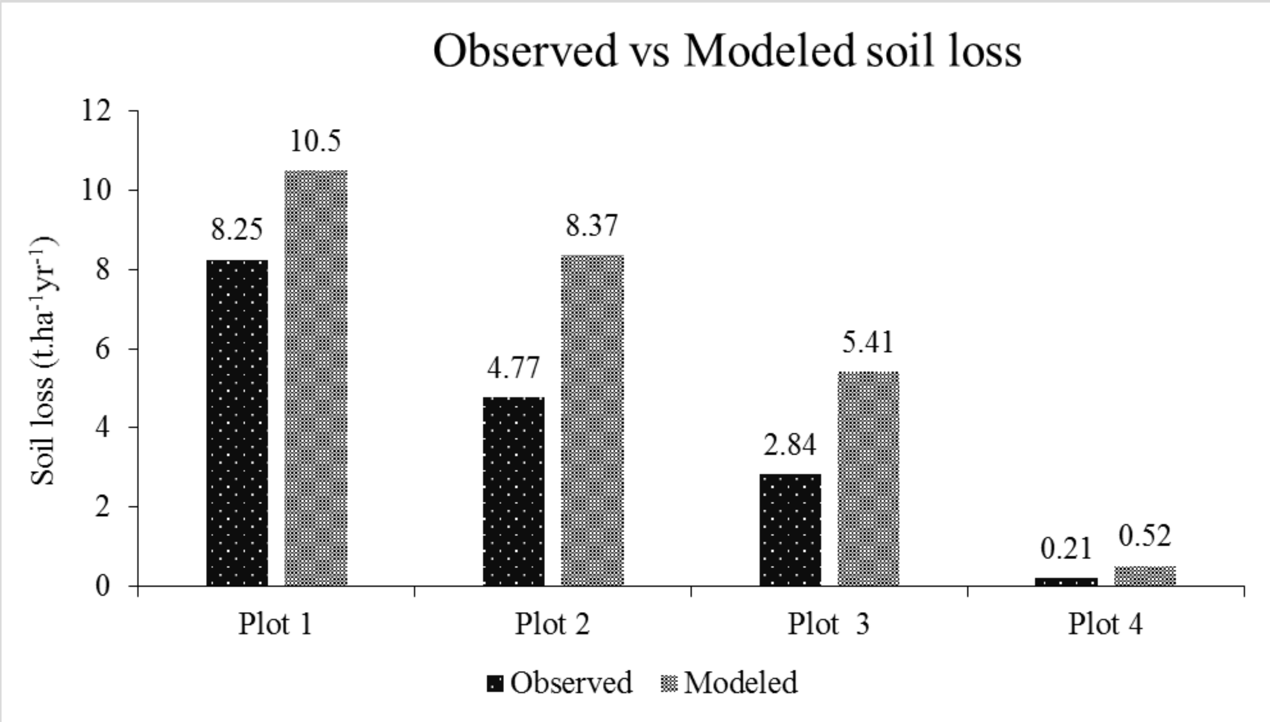

Figure 5-5: Observed and modeled soil loss at pixel level

The average soil loss that was obtained in the catchment when all the data from all the plots was put together and averaged was 4.02 $t.ha^{-1}.yr^{-1}$. The observed soil loss relates with the modelled soil loss using RUSLE combined with GIS and Remote Sensing as most of the area (around 80%) in the catchment was dominated with modelled soil loss in the 0 – 10 $t.ha^{-1}.yr^{-1}$ category. In Ethiopia, where sediment yields are amongst the highest in Africa, a survey of 33 catchments varying in area from 49 to 1622 km^2 was carried out to determine sediment yield of the catchments the range of sediment yields varied from 0.35 to 12.50 t/ha/year with an average value of 3.69 $t.ha^{-1}.yr^{-1}$ (Vakakis-International, 2000).

5.3.2 RUSLE Model Results

The results obtained from the soil erosion modeling using the RUSLE model are presented in this section. The subsections below first present results for the different inputs into the model and the last subsection presents final results of the soil loss hazard maps produced for the successive periods.

5.3.2.1 R-Factor

The rainfall erosivity factor is the measure of the erosive power of rainfall or the potential of raindrops to detach soil particles and cause soil erosion. Figure 5-6 shows the spatio-temporal variations of the R-factor for the study area. The rainfall erosivity calculated from the observed rainfall ranged from 178 to 487 $MJ.mm.ha^{-1}.hr^{-1}.yr$ considering all the years. The individual years observed also had spatial variations in the R-factor depicted by the difference in the minimum and maximum R-factor. The highest variation was experienced in 1995 with a difference of 251 $MJ.mm.ha^{-1}.hr^{-1}.yr$ and 2015 had the lowest variation depicted by the difference of 19.4 $MJ.mm.ha^{-1}.hr^{-1}.yr$ between the maximum and minimum R-factor values.

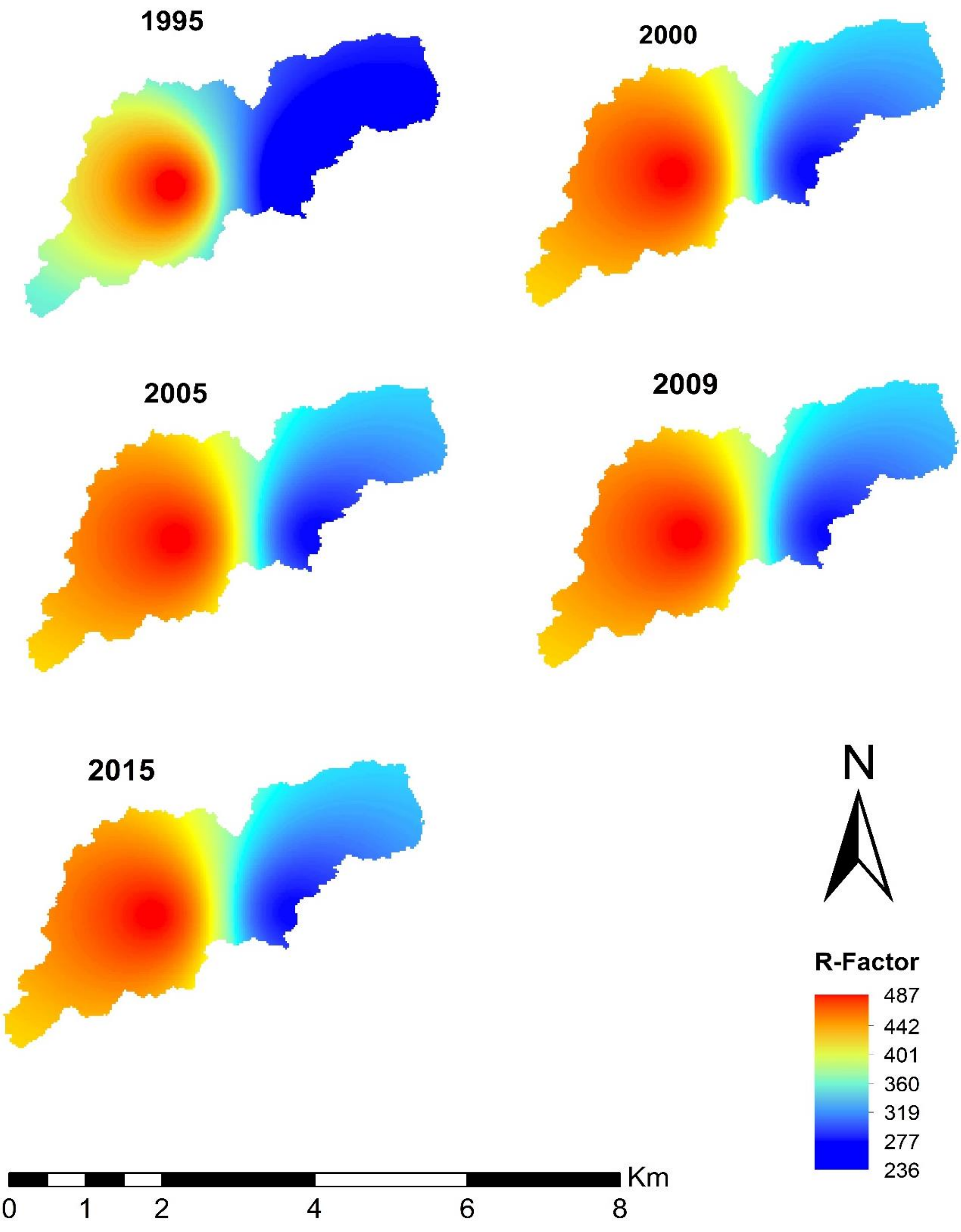

Figure 5-6: Rainfall Erosivity in the Mhlatuzane micro-catchment

Highest erosivity values are in the high altitude areas of Khubutha and Mpompotha where high rains are usually experienced in the micro-catchment and lowest values are on the lower part towards the outlet of the catchment in the North East direction where the Lubovane reservoir is located. The area with high rainfall erosivity also coincided with areas that are steep and the combined effect of the high erosivity and steepness leads to high soil erosion potential. There were temporal variations as well in erosivity values with 1995 having the highest average rainfall erosivity factor of 235.5 $MJ.mm.ha^{-1}.hr^{-1}.yr$ followed by 2000, 2005 and 2009 that had the similar averages of around 243 $MJ.mm.ha^{-1}.hr^{-1}.yr$, with the latest year 2015 receiving the lowest rains and hence low R-factor values on Average (199.9 $MJ.mm.ha^{-1}.hr^{-1}.yr$). Figure 5-7 shows a graphical representation of the temporal variation of the maximum, minimum and average R-factor values within the Mhlatuzane Micro-catchment.

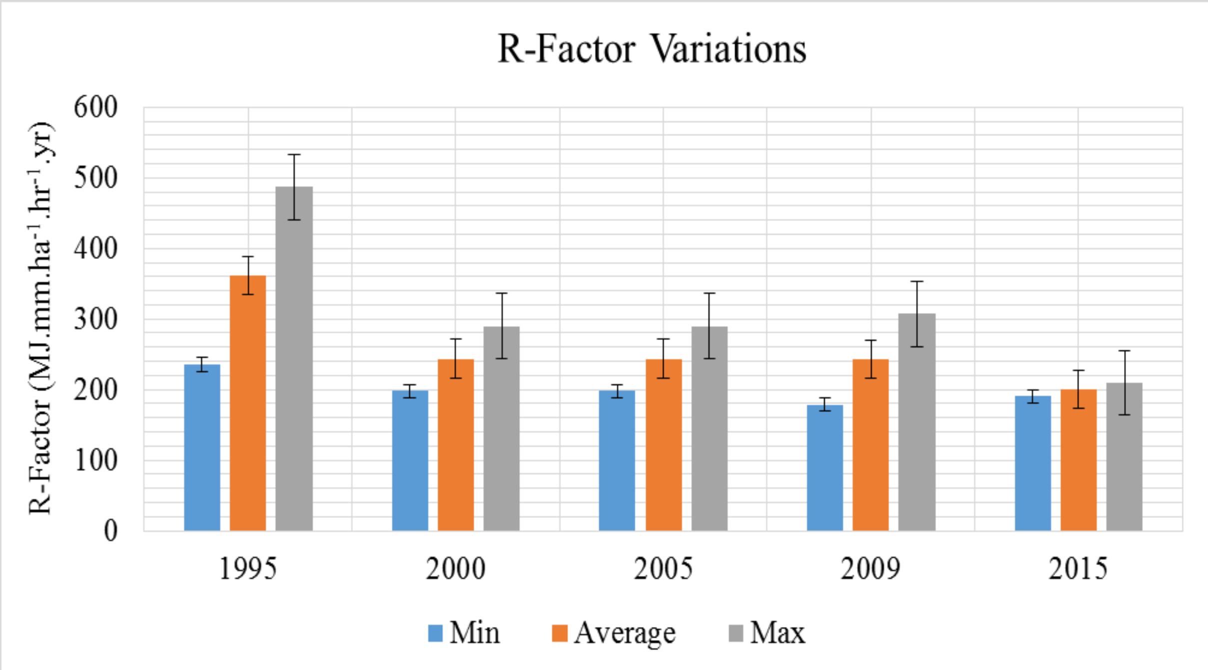

Figure 5-7: Minimum, maximum and average R-Factor values calculated from observed rainfall (Sithobela and Kubuta measuring stations)

5.3.2.2 K-factor

Figure 5-6 shows a K-factor map with the spatial distribution of soil erodibility in the Mhlatuzane micro-catchment where there is a large concentration of sandy loam soils and some alluvial soils (soils with a lot of silt) which are highly erodible. According to the weighting by Stone and Hilborn (2012) that was done to attain the soil erodibility values, 40.5% is covered by soils of low erodibility which is below 0.25 $t.h^{-1}.MJ^{-1}.mm^{-1}$. Soils in the moderate category of 0.25 – 0.5 cover only 19.7% of the catchment and 39.8% is covered by highly erodible soils with K-factor of above 0.5 $t.h^{-1}.MJ^{-1}.mm^{-1}$.

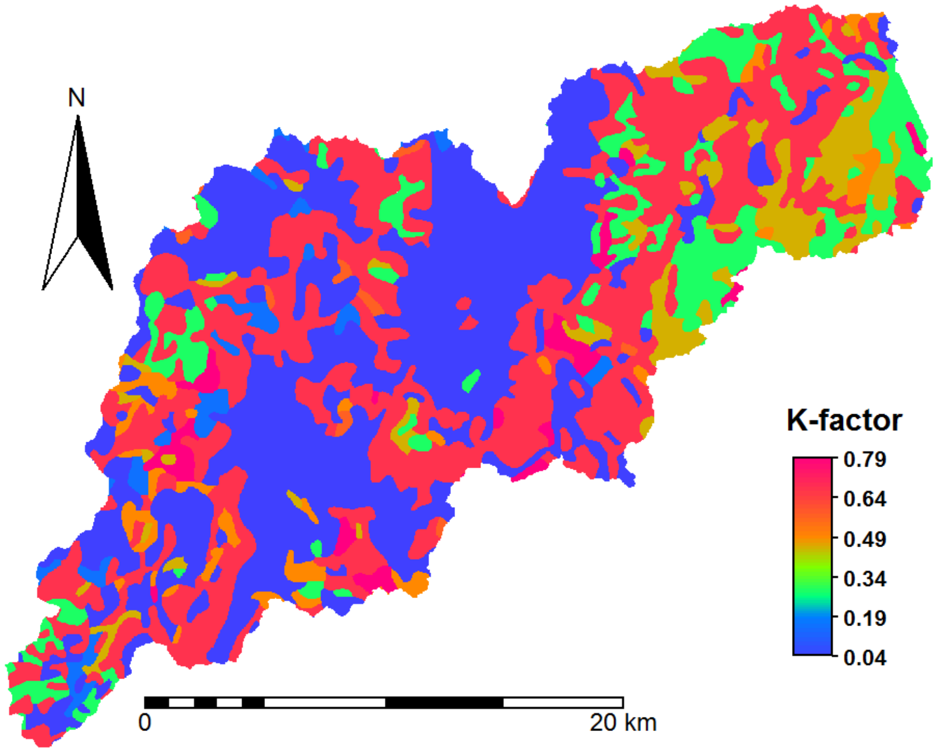

Figure 5-8: Spatial variability of the soil erodibility factor (K)

Highly erodible soils are found in the areas surrounding the reservoir in the Mahlabatsini, Mganyaneni and Othandweni settlements (see study area map in Figure 3-1) and some gullies exist in those places proving that there are signs of severe soil erosion and this poses a great threat to the Lubovane reservoir in as far as sedimentation is concerned. Areas like Sithobela also contain some soils that fall in the high erodibility category while high places like Khubutha, Kaphunga, Mpompotha and those towards Hlatikhulu have soils that are more resistant to soil erosion as shown by the low erodibility values in Figure 5-8.

5.3.2.3 LS-Factor

Minimum and maximum LS-factors in the Mhlatuzane were found to be 0 and 9.7 respectively with an average of 4.8. The results (Figure 5-9 shows low LS factor values around the dam and along the Mhlatuzane River channel. Generally, the results show that the catchment does not have a high concentration of steep areas and most of the areas are gentle undulating. Relatively high LS factor values are found on areas around the mountains of Kaphunga on the far north-western part of the catchment.

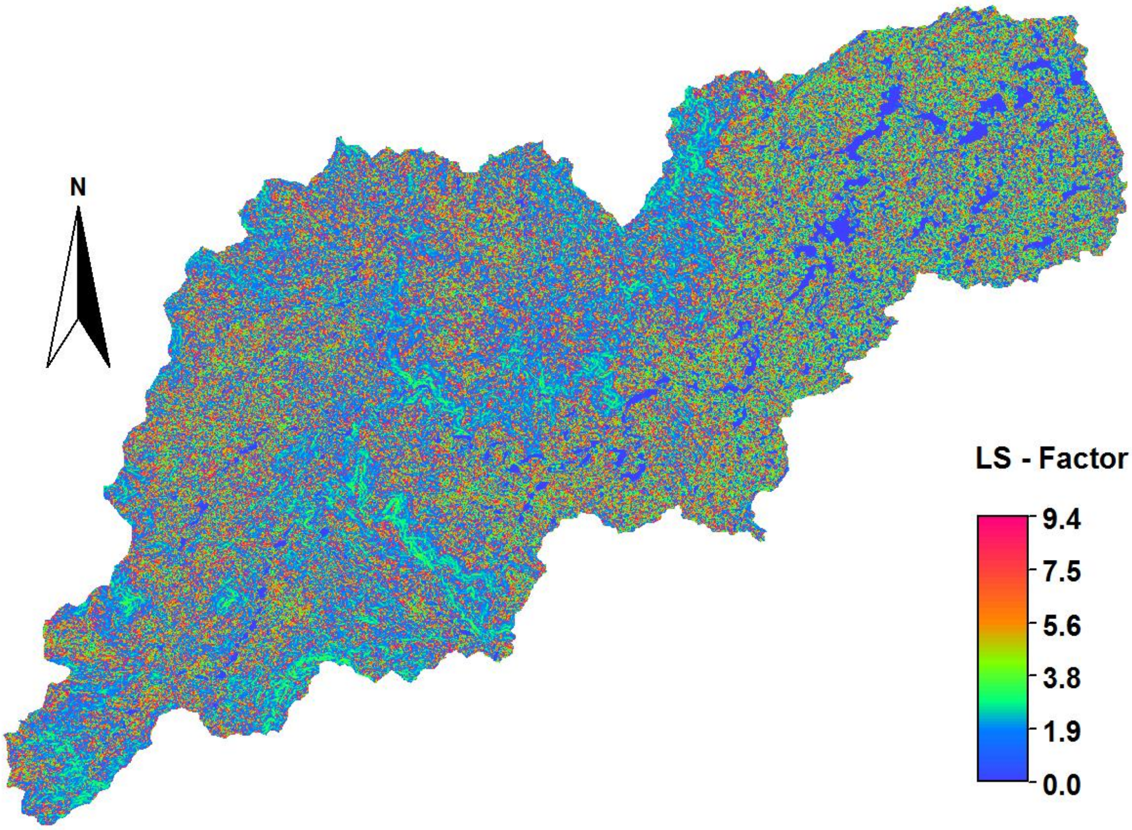

Figure 5-9: The spatial variability of the Slope length and Steepness factor (LS) in the Mhlatuzane micro-catchment

5.3.2.4 C-Factor

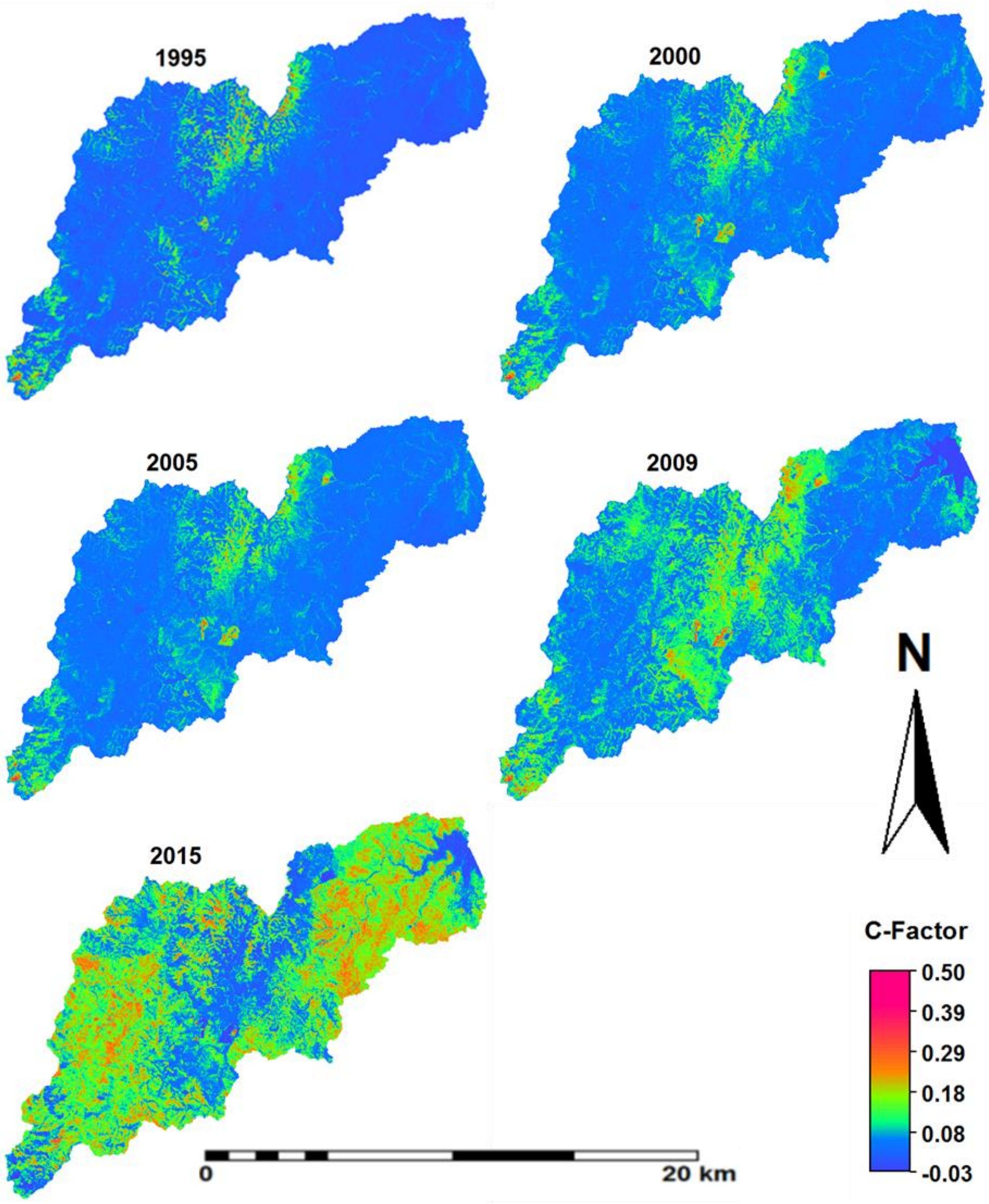

Figure 5-10: Spatial and temporal variations of the Crop cover and management factor in the Mhlatuzane Catchment

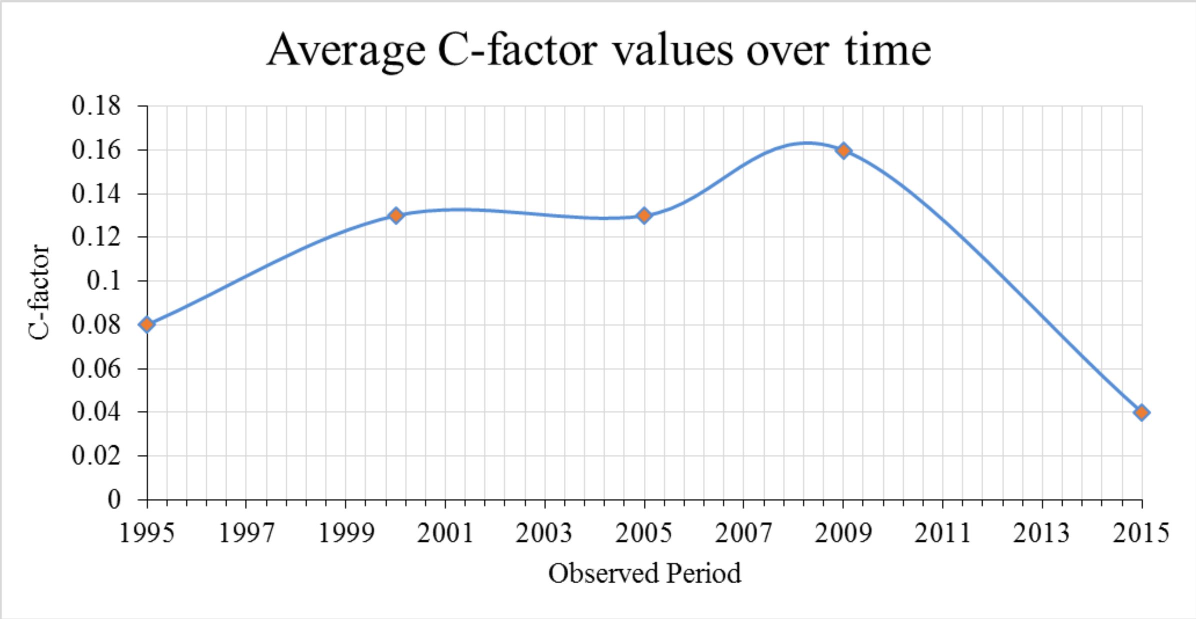

Figure 5-11: Temporal variation of C-factor in the Mhlatuzane micro-catchment

The results (Figures 5-10 & 5-11) of the calculated C-factor values show that the average C-factor in the catchment has been increasing over time from 1995 to around 2008 then it started decreasing through the years towards 2015. This means that the soil was becoming less and less protected from 1995 towards 2008 and then vegetative cover began to increase from 2009 to present. The variations of the C-factor can be attributed to the variations in annual rainfall for the observed years as crop vigor is affected by how much water, crops have received. As the rainfall decreased from 1995 towards 2008, the C-factor increased resulting from the decrease in the NDVI which is a measure of vegetation health and vigor.

Disappearance of vegetation can also be attributed to deforestation as forest and shrubs were noticed to be decreasing from 1995 to 200 (10% decrease) due to clearing of land to allow for settlements and also trees are usually cut to provide wood for fuel. Irrigated areas in the micro-catchment have been low and increasing gradually from 1995 to 2015 hence they contribute less to the C-factor as they account for a very small portion of the micro-catchment.

5.3.2.5 P-Factor

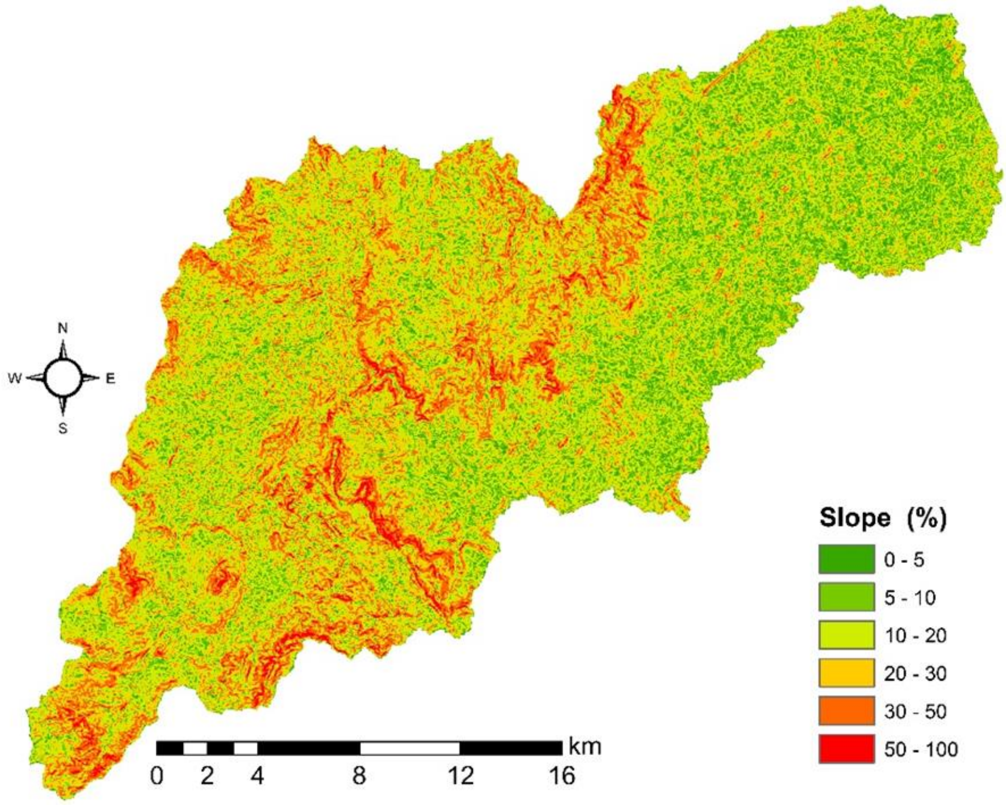

Figure 5-12: Spatial variation in slope measured in percentages within the Mhlatuzane micro-catchment

The slope map result (Figure 5-12) shows the spatial variation of slope in percentages in the Mhlatuzane micro-catchment. Gentle undulating areas are found towards the northeast direction where the reservoir is located. The map shows that steep areas of slope exceeding 50% exist in the micro-catchment and they are concentrated around the Khubutha and Hlatikhulu areas. These are the same areas that are forested (Figure 5-2) in the catchment. The slope map was used with the land cover maps in Figure 5-2 to calculate the P-factor maps shown in Figure 5-13.

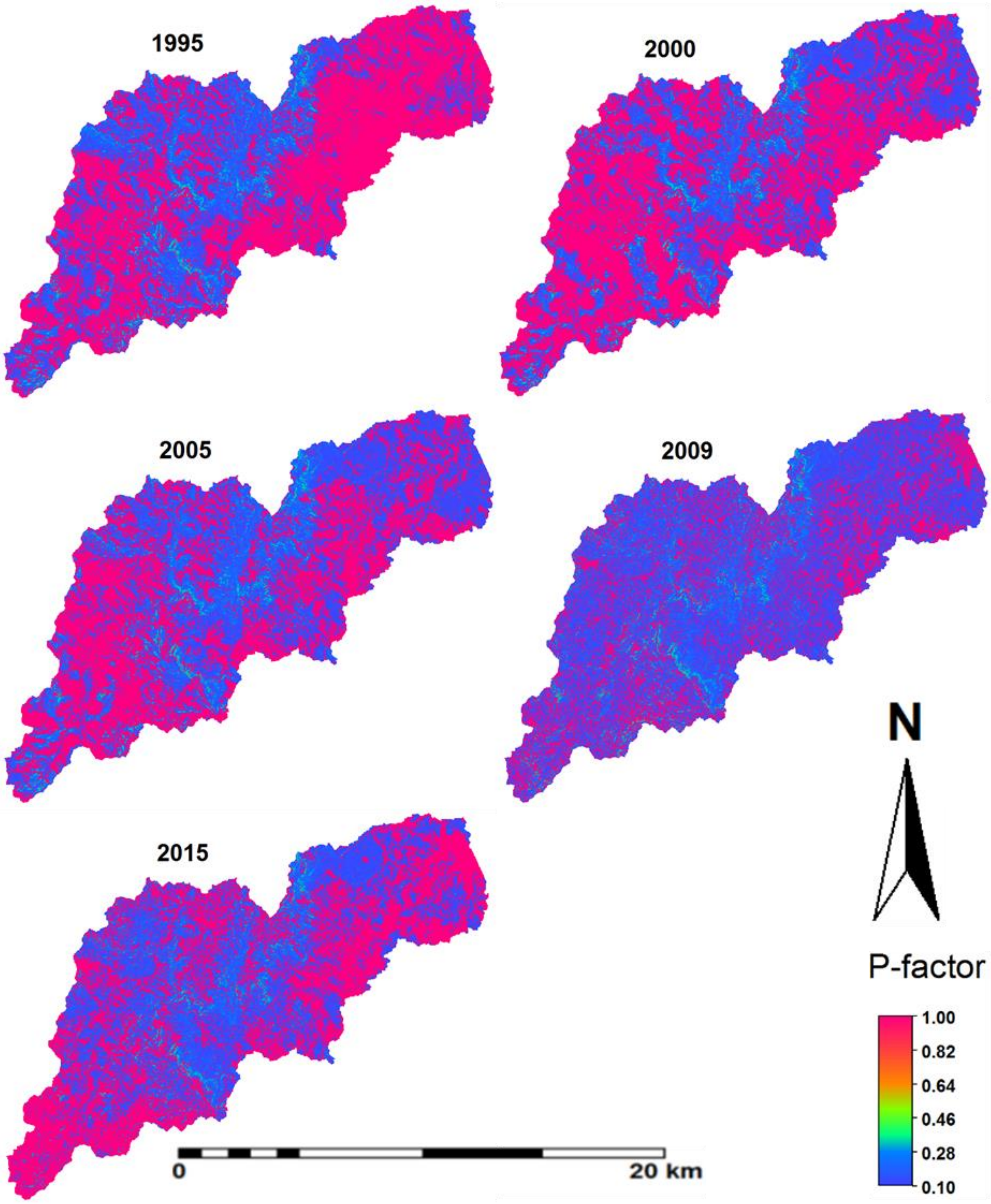

Figure 5-13: Spatial and temporal variations of the support practice factor in Mhlatuzane

The results show that there were a high concentration of P-factor values closer to 1 in 1995 which means there was little being done to prevent soil loss. As the years progressed towards 2009, the concentration of p-values closer to 1 decreased, showing that there were increases in support practices that were being done to prevent soil loss. Such practices in the area include mostly contour ploughing as opposed to ploughing up and down the slope. However, there has been an increase in the p-factor values closer to 1 and it can be attributed to the sudden increase in settlements in the catchment due to the economic activity brought about by the presence of the reservoir.

5.3.3 Potential soil loss in the Mhlatuzane micro-catchment

The results showed that the potential soil loss in the micro-catchment mostly fell in the minimal soil loss potential class (between 70-80%) which ranged from 0 – 10 $t.ha^{-1}.yr^{-1}$ (see Table 5-4). However, from 2005 onwards, the concentration of soil loss potential in the minimal class began decreasing as the area with inactive soil loss potential started increasing (Figure 5-14). The second class to dominate was the Moderate soil loss potential which ranged from above 10 to 50 tonnes per hectare per year. The area dominated by the moderate soil loss potential was fluctuating between 17% and 20% over the years. In the year 2015, the inactive area increased to a 10% coverage from 1.4% in 2009 and this can be articulated to the low rains received in the year 2015 because of the ElNino drought that hit Southern Africa in the 2015/16 hydrological season. The R-Factor in this study was calculated based on the observed rainfall hence a decrease in rainfall results in the decrease in rainfall erosivity and subsequently a low potential for soil loss.

Table 5-4: Areal coverage in percentages of different potential soil loss classes

Potential Soil loss Class	**Range ($t.ha^{-1}.yr^{-1}$)**	**Area covered (%)**				
		1995	**2000**	**2005**	**2009**	**2015**
Inactive	**Less than 0**	0.04	0.06	0.06	1.42	9.95
Minimal	**0- 10**	81.14	78.42	81.94	77.16	70.36
Moderate	**11-49**	18.43	20.67	17.74	18.00	18.62
High	**50-100**	0.37	0.73	0.25	2.85	1.06
Extreme	**>100**	0.03	0.12	0.00	0.56	0.00

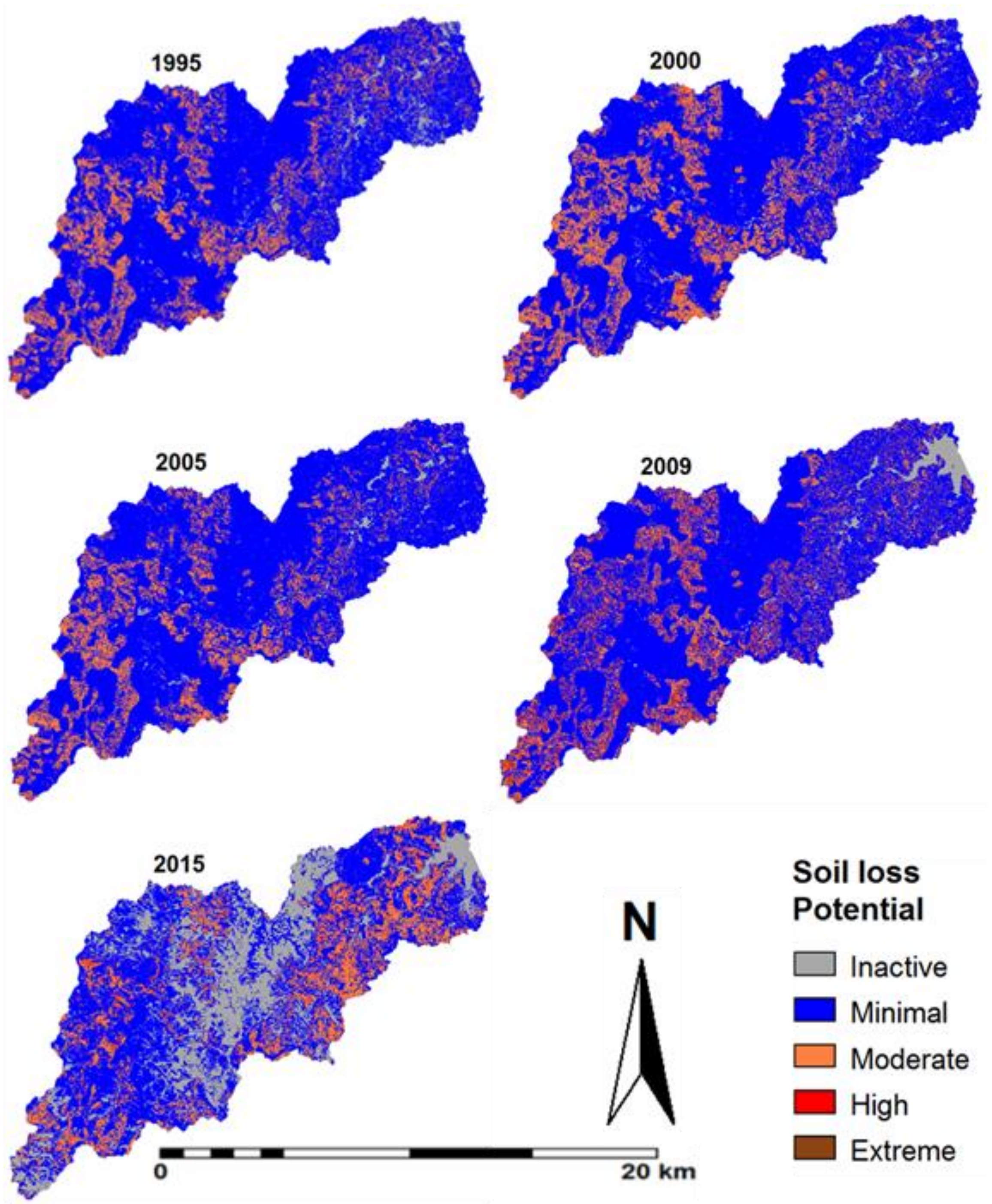

Figure 5-14: Spatial and Temporal changes in potential soil loss

5.3.4 Sediment yield in the Mhlatuzane Micro-Catchment

The SDR for Mhlatuzane micro-catchment was calculated using equation 16 and was found to be 0.3. The SDR is fairly low (closer to 0) meaning that sediment transport in the catchment is inhibited by the transport capacity of the micro-catchment. This suggests that there is an existence of depressions where sediment is deposited before it reaches river and the reservoir. Figure 5-15 shows the temporal variations in modeled sediment yield from the Mhlatuzane micro-catchment.

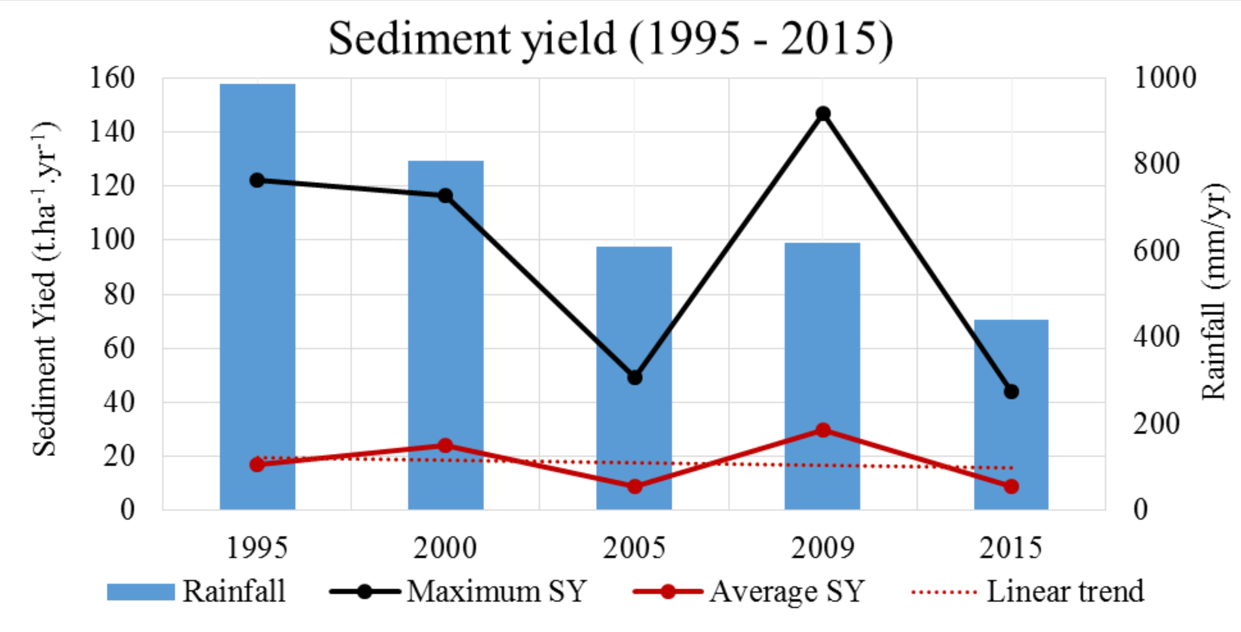

Figure 5-15: Sediment yield variations from 1995 – 2015

The results show that the highest sediment yield occurred in 2009 where the maximum soil loss was 146.48 $t.ha^{-1}.yr^{-1}$ with an average of 30 $t.ha^{-1}.yr^{-1}$. The average sediment yield was in the moderate potential soil loss and the maximum soil loss falls in the extreme range. Sediment yield was high in 2009 because of the occurrence of high c-factor values which resemble a decrease in vegetation vigor meaning that the soil was becoming less and less protected. The year 2009 had the highest c-factor on average of 0.16 against 0.08 (1995) and 0.13 for 2000 and 2005. In the year 2015, the average c-factor values were low (0.04) but the c-factor map (Figure 5-10) which shows both spatial and temporal variation in the c-factor values shows an increase in the concentration of high c-factor values around the Lubovane reservoir and that is a threat to the reservoir as diminishing vegetative cover around those areas leaves the reservoir prone to siltation due to soil erosion.

The sediment yield showed a positive relationship with rainfall on most of the years modeled. As rainfall decreased from 2000 to 2005, the sediment yield also decreased in the Mhlatuzane micro-catchment. However, rainfall remained almost constant for 2005 and 2009 yet sediment yield was high in 2009 and this was because of the decrease in crop vigor, as shown by the high c-factor in 2009 (Figure 5-11), leaving the soil prone to erosion. In 2015, rainfall was low due to the El Nino drought hence the sediment yield was also low. Another reason for the low sediment yield in 2015 was that there was a land rehabilitation project implemented in 2010 by the Global Environment Facility (GEF) in the catchment and it involved afforestation among other activities (IFAD, 2013). The land cover maps (Figure 5-2 and 5-3) have shown a 2% increase in forest and shrubs from 2009 to 2015 and also the c-factor values decreased rapidly towards 2015 from 2009 showing an increase in photosynthetic activity hence crop vigor. The combined effect of increased vegetative cover and low rains contributed largely to the low sediment yield in 2015.

The average sediment yield for the micro-catchment when considering all the mapped years together was 17.64 $t.ha^{-1}.yr^{-1}$. It is to be noted that this value is highly affected by outliers, as most of the area is dominated sediment yield ranging between 0 and 10 $t.ha^{-1}.yr^{-1}$. Tamene et al. (2006) in their study where they analysed the factors that determine sediment yield variability in the highlands of north Ethiopia found sediment yields ranging from 3 – 49 $t.ha^{-1}.yr^{-1}$. The mean annual sediment yield in Ethiopia stood at 19 $t.ha^{-1}.yr^{-1}$ which was above the global average according to the study. The annual sediment loading (considering a 98% TE) to the reservoir from Mhlatuzane micro-catchment sediment yield modeled by RUSLE was found to be 890 800 $t.yr^{-1}$ and the sediment volume when considering a sediment density of 1.55 $t.m^{-3}$ stood at $0.56x10^6$ m^3. If the Mhlatuzane River were the only source of water for the reservoir, the sediment loading would lead to a 0.36% loss in storage due to sedimentation according to the results from RUSLE modeling.

5.4 Sediment concentration

As part of the methodologies to attain the objectives of the study, monitoring of sediment concentration was carried out in the Mhlatuzane River and the Feeder canal as these two channels feed into the reservoir. This subsection presents and discusses sediment concentration results obtained from the three sampling sites.

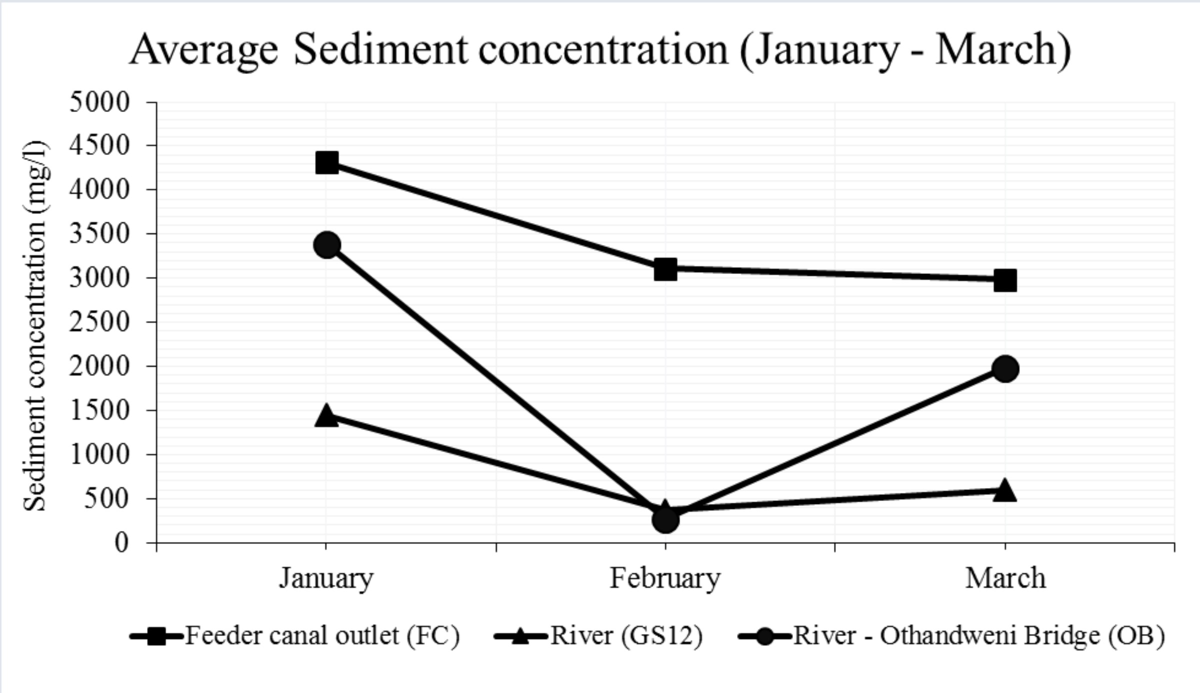

Figure 5-16: Suspended Sediment concentration from the three sampling sites

The results from the grab samples (Figure 5-16) show that sediment concentration (SC) was highest in the Feeder canal outlet when compared to the other two sites in the Mhlatuzane River. The highest sediment concentration observed was in the Mhlatuzane River at Othandweni Bridge (OB) where about 7000 mg/l of sediment was sampled and that was in the morning after a night storm (see Appendix 8). The overall trend on average shows a decrease in SC from January to March. This is mainly because highest rainfall in the micro-catchment is received between December and January and it starts to decrease from February towards the dry season (see Figure 3-2). However, the OB sampling point showed a different trend in the SC where the lowest concentration of sediment on average was in February and then SC increased towards March. This is attributed to that the flows in Mhlatuzane reduced because of rainfall absence such that water was flowing sub-surface hence there was zero concentration in that period and that is what caused the average concentration to go below that of gauging station (GS) 12 in February. On average, FC had the highest sediment concentration of 3436 mg/l followed by sediment concentration at OB and then GS 12 with 2231 and 789 mg/l respectively. GS 12 is about 20 kilometres upstream of the reservoir hence a smaller catchment drains to it as opposed to the OB sampling site which is at the tail of the reservoir and that explains why the sediment load is far less in GS 12. Sediment concentration has been decreasing from January to March.

5.4.1 Mhlatuzane River sediment loading

The Mhlatuzane River had two sites where sediment concentration was monitored, one at a gauging station upstream (GS 12) and another at the point where the river discharges into the dam (Othandweni Bridge). At first the sampling was to be limited to only GS 12 which is about 20km upstream of the Dam, because of the gauging station, it was easy to obtain the flow data for the sampling days. Trial runs were however done on the Othandweni Bridge to compare the sediment and flow and it was found that the flow and the sediment concentration varied greatly when compared to that of GS 12 upstream.

The sediment concentration at the bridge point then became very important as that was the point where the tail of the reservoir was. The sediment concentration observed in the river was 2230.64 mg/l on average. The sediment was then converted from milligrams per litre to kilograms per cubic metre. The MAR for the Lubovane reservoir/Mhlatuzane catchment was then used to calculate the sediment load passing that point annually. The sediment load was found to be 2.98 $t.ha^{-1}.yr^{-1}$ which was lower than the 17 $t.ha^{-1}.yr^{-1}$ modeled using RUSLE. This was somehow expected since the study focused on measuring suspended load due to lack of appropriate equipment and adequate time to measure bedload so the difference can be attributed to sediment that was flowing as bedload during the periods of measurement. Sediment concentration from grab samples using a water bottle is usually 25% less than that determined using integrated suspended samplers (FAO, 2000). The sediment load from the Mhlatuzane river translates to 156 093 $t.yr^{-1}$ and when converted to volume using a mean sediment density of 1.55 $t.m^{-3}$, the result shows that about $0.10x10^6$ m^3 of sediment enters the reservoir each year through the Mhlatuzane river on average.

5.4.2 Feeder Canal sediment loading

The Feeder canal conveys water from the Great Usuthu River and discharges in the Lubovane reservoir. It has three off-takes, all of which are equipped with head control structures meant for two purposes. The main purpose is to allow damming of the water so that it can flow into the off-take pipe even in low flows and the other reason is to trap sediment, mainly bedload. While working with the canal for about 2 years it was noticed that the sediment trapped by this structures gets carried by fast moving water when the canal is flowing at full supply so the structures are not as efficient as they ought to be. Figure 5-17 shows the observed flows in the canal from 2010 to 2015

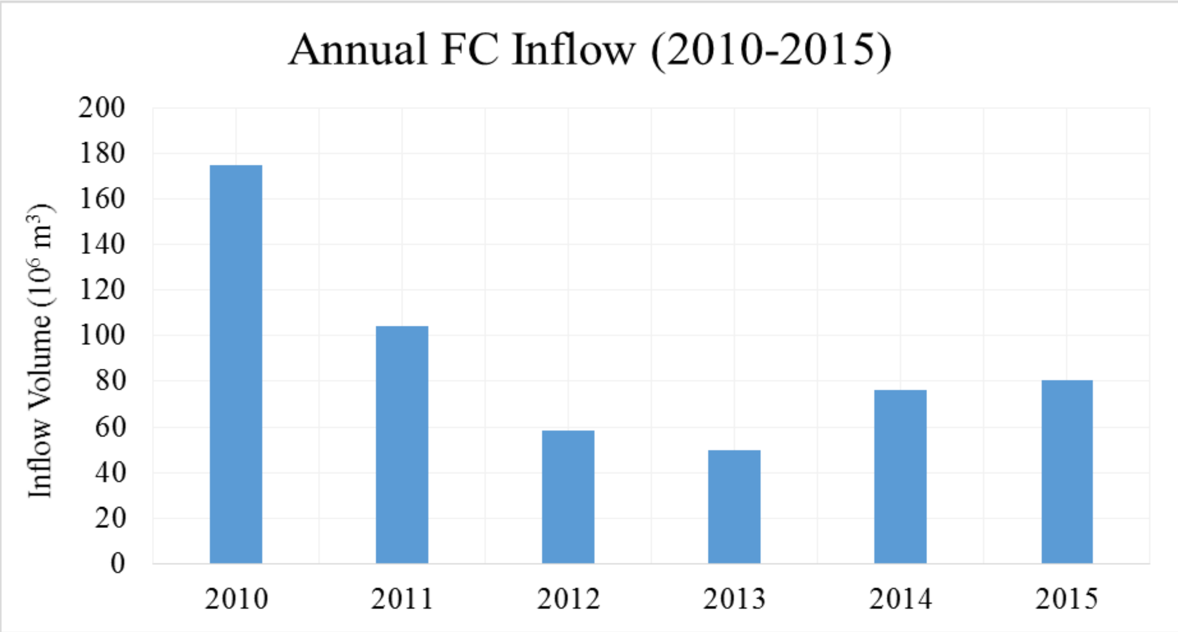

Figure 5-17: Annual Inflow volume for the Feeder canal (January 2010- December 2015)

The annual load of sediment in tonnes per year was computed and found to be 1 121 215.62 tons/yr. The annual deposit of sediment (ADS) from the canal was calculated using the sediment density of 1.55 $t.m^{-3}$ and it was found to be $0.72x10^6$ m^3, which is higher than the ADS from the river. When the sediment load from the canal was combined with that from the Mhlatuzane River it resulted in sediment loading of $0.82x10^6$ m^3 of sediment per year leading to an annual loss in storage capacity of 0.52%.

The trap efficiency of the reservoir was calculated using the Brune's method (Brune, 1953) and was found to be 98.3%. In Zimbabwe, reservoirs of storage ratio of more than 0.1 are assumed to have a 100% trap efficiency and the storage ratio of the Lubovane reservoir when considering the MAR for both the river and the canal is 0.51. According to the data from the sediment concentration, if the sediment loading remains constant, the reservoir will silt in in about 190. It must, however, be noted that the sediment concentration was based on suspended load and not bedload, so the actual sediment loading is expected to be higher than that observed in the study because sediment is transported both along the river bed and in suspension depending on the size of particles.

The sediment loading in the feeder canal constituted more than 80% of the total sediment loading estimated from the suspended sediment concentration observations. This is because, apart from the observed high suspended sediment concentration in the FC, the flows in the feeder canal are also higher than those at Mhlatuzane River hence the flow of sediment in kg/s is higher as well.

5.5 Bathymetric Survey

Water level records for the reservoir date back to 24 November 2008 when first level recorded as 209.37 metres above sea level which was about 27% to full capacity. So, effectively the dam has been in operation for about 7 years. Figure 5-18 presents a Triangulated Irregular Network (TIN) of the reservoir which shows the variance in observed elevations from the deepest point to the spillway level. The deepest point surveyed was 45 m and it was found near the Mhlatuzane Dam. The Golome dam also had deeper portions compared to the other sections in the reservoir. Shallow areas were noticed towards the tail of the reservoir and at the discharge point of the Feeder canal.

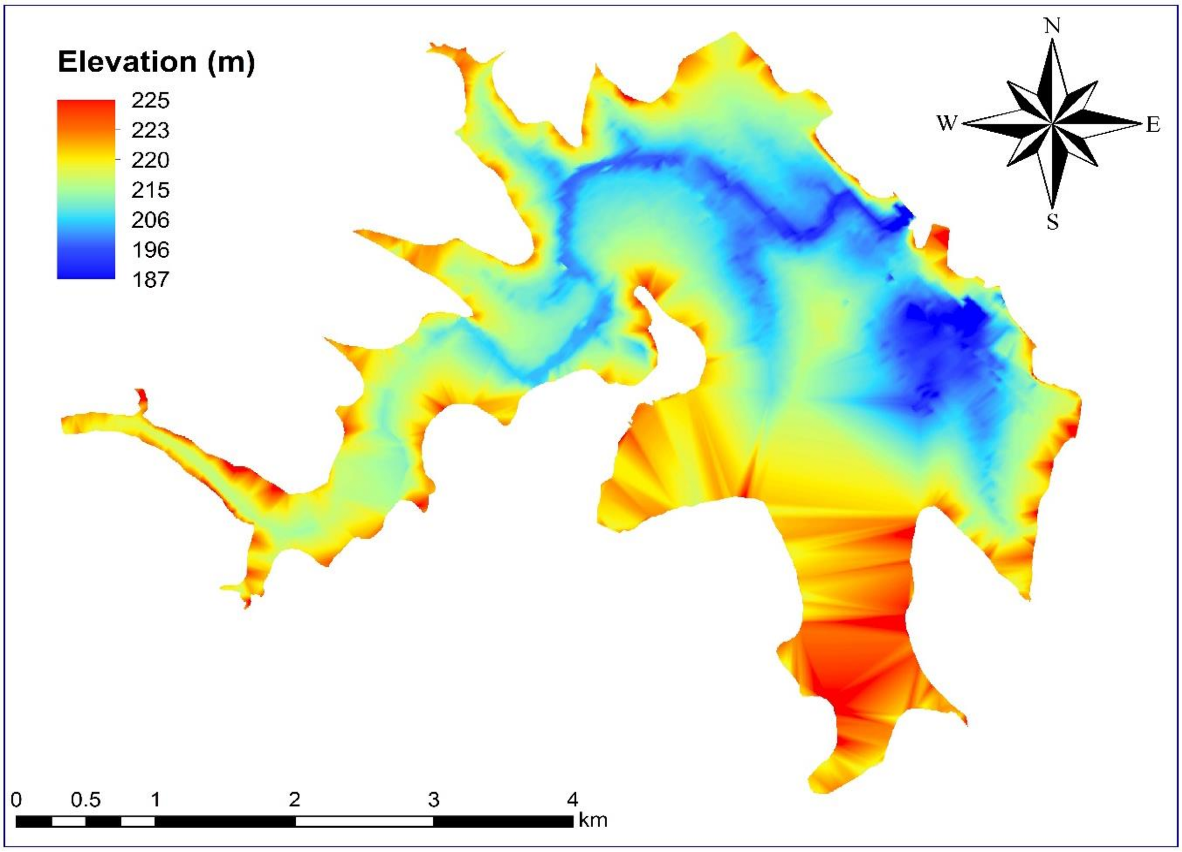

Figure 5-18: Depth profile of the Lubovane reservoir

The results obtained in the study show that there is siltation occurring in the reservoir. The current volume at 224 metres above sea level from the bathymetric survey was found to be $140.14 x 10^6 m^3$ and the original design capacity at full supply level is $154.83 x 10^6 m^3$. This means that there has been a loss of $14.69 x 10^6 m^3$ in storage due to sedimentation over the 7 years that the reservoir has lived. There is then an annual loss rate in capacity of $2.10 x 10^6 m^3.yr^{-1}$, which is 1.36 % loss in storage capacity annually. At this annual sedimentation rate, if no measures to reduce sediment loading are implemented, the Lubovane reservoir will now have a new reduced lifespan of 81 years after which it will have silted up. The design life of the reservoir and the estimated lifespan of the LUSIP is 100 years. A Mid-term evaluation report prepared by Vasudeva (2006) during the construction phase of the dam embankments mentioned the availability of excess trees within the area that would be inundated and recommended that they be removed but they were not removed. This might have tempered with the depth sounding results as the surface of the debris from those trees might have been wrongly assumed to be sediment. This probable error can be identified and corrected after a second bathymetric survey has been conducted and the annual sediment loading is compared with that obtained from the first survey.

Figure 5-19 shows a comparison of the original reservoir level-capacity curve and the new one that has been calculated in light of the sedimentation of the reservoir. Figure 5-20 shows the new level-capacity and level-area curves and they reveal that sediment accumulation does not only affect the capacity but it also causes a reduction in the surface area at each contour (see also Appendix 10a and 10b). The study found that as sediment accumulated at the rate of 1.36% of the total capacity, there has been an annual loss in area at FSL of 0.71%. The loss in area can be articulated to that deposition of sediment starts at the tail of the reservoir where the river discharges hence the more the sediment settling around those areas, the more area is lost. However, with time some of the area at full supply is regained as the sediment subsides and is pushed by the water towards the dam wall.

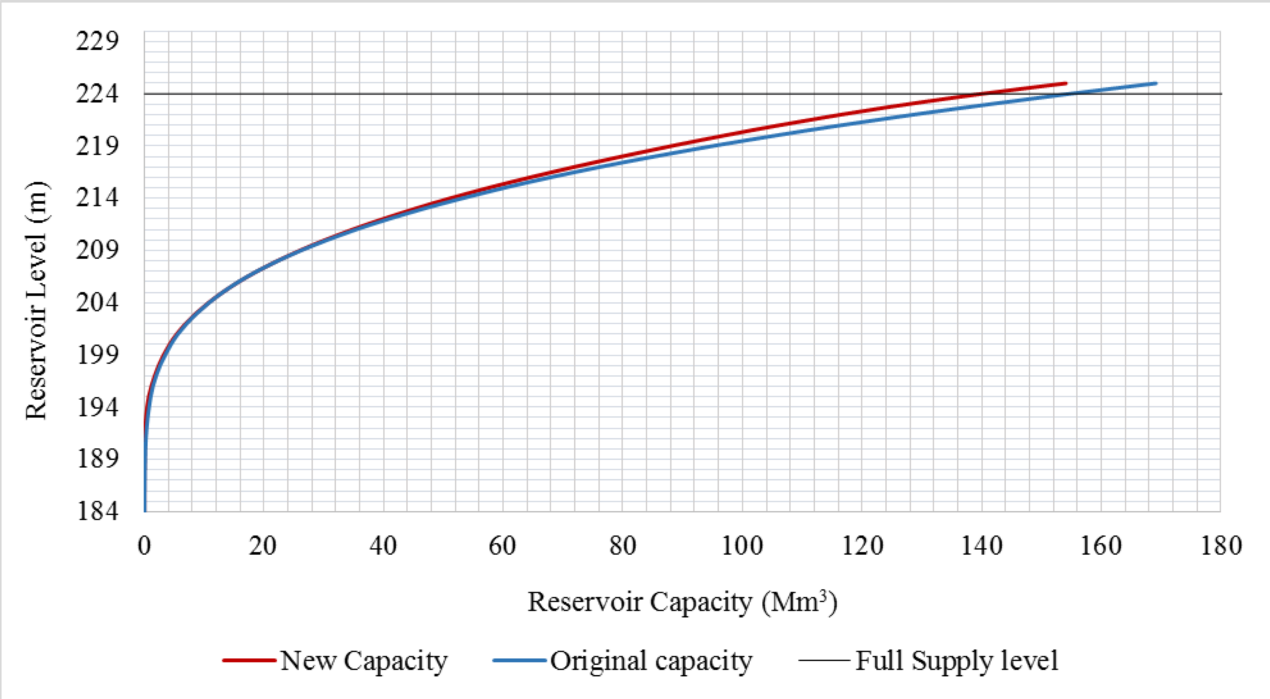

Figure 5-19: Original and New level-capacity curve for the Lubovane Reservoir

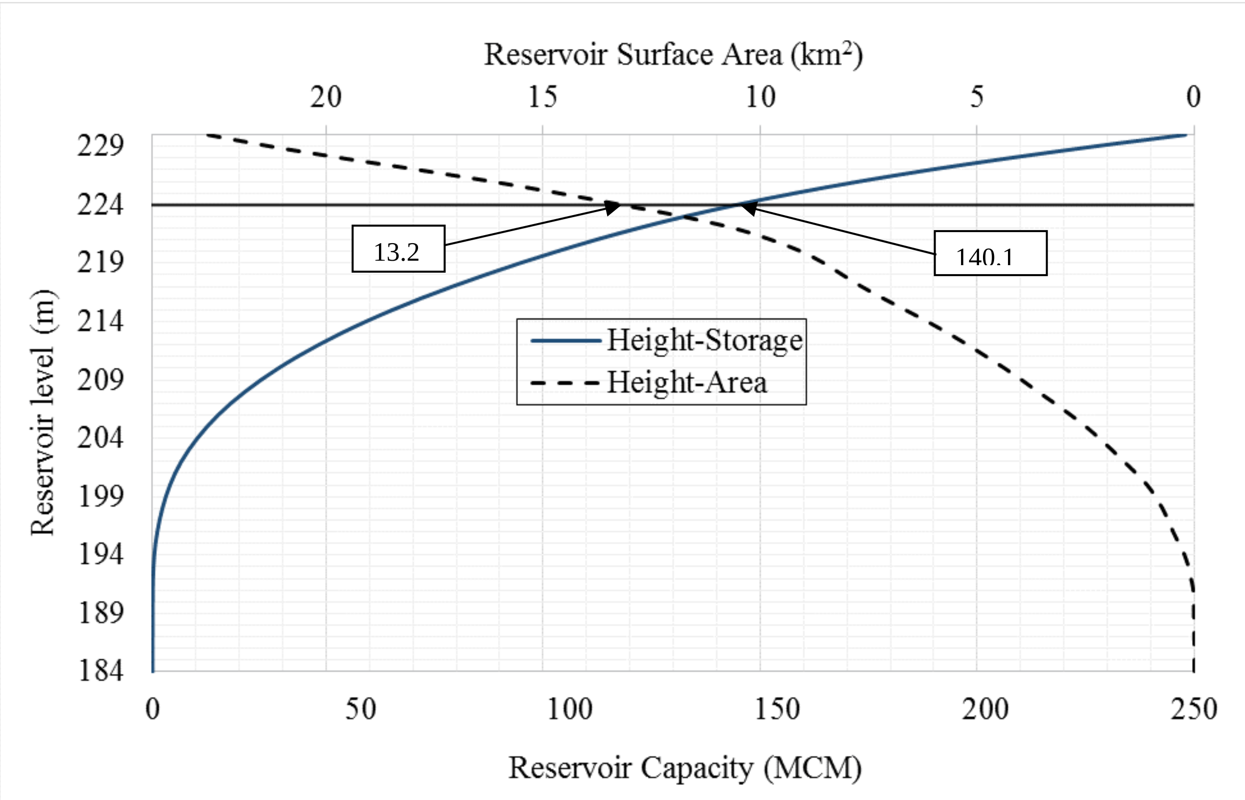

Figure 5-20: The new storage curve for Lubovane Reservoir

The analysis of the sediment concentration data showed that the feeder canal discharges about three quarters of the sediment in the reservoir. The canal conveys water from a larger Usuthu river which has a catchment area of about 12 000 km^2 (Manyatsi and Brown, 2009), with flows that can reach 100 m^3/s hence the sediment concentration and transportation in the Usuthu differs greatly from that of Mhlatuzane river. Table 5-5 presents a summary of the three methods used in the study to assess sedimentation of the Lubovane reservoir.

Table 5-5: Summary of results from all the methods

	Grab Sampling (River + Canal)	RUSLE	Bathymetric Survey
Design Storage Capacity (*10^6 m^3	154.83	154.83	154.83
Current Storage Capacity (*10^{6}m^3)	149.09	150.66	140.13
Designed Lifespan (years)	100	100	100
Current Lifespan (years)	100	100	81
Time remaining until reservoir is silted up (years)	181	253	74
Design Storage ratio	0.51	0.51	0.51
Current Storage Ratio	0.49	0.50	0.46
Annual Deposition of Sediment	0.82	0.56	2.10
Percentage storage lost to sediment to date (%)	3.71	2.53	9.49
Annual percentage loss (%)	0.53	0.39	1.36
Specific Sediment yield (t.km^{-2}.yr^{-1})	-	1764.00	-

The Bathymetric survey method showed high annual sediment deposit determined when compared with the grab sampling method and the RUSLE. This method considered sediment that has already settled in the reservoir, over the years the reservoir has lived, both from sediment loading from the canal and the Mhlatuzane River. This sediment includes particles transported as suspended load and that transported as bedload. The grab sampling method in this study considered only suspended sediment which is partly why the annual sediment loading obtained from the grab sampling method is lower than that from the Bathymetric survey. When comparing the sediment loading from the Mhlatuzane catchment obtained from RUSLE and grab sampling at OB, the grab sampling method also showed lower sediment loading. This then shows that in overall, the grab sampling method underestimated sediment loading because bedload was not sampled. Moreover, sampling with the water bottle might also contributed to the low sediment loading from this method. A study that was conducted by the FAO (2000) to analyze different grab sampling methods found that sampling using a water bottle usually yields sediment concentration that is 25% less than other sophisticated methods like depth integrated samplers.

5.6 Yield Projections and Water Demand

The annual volume of sediment obtained from the bathymetric survey was used to project the available storage up to 2080. If sediment proceeds to accumulate at this rate and no measures are put in place to reduce sedimentation, by 2080 storage will have reduced to about 5.7×10^6 m^3. The results from the yield projections (Figure 5-21) show that, due to the loss in storage capacity of the reservoir, reservoir yields at 20% risk level have been projected to decline by 1.23% annually on average. The changes in yields of the reservoir are variable from year to year. The storage ratio of the reservoir has also been predicted to decline from 0.51 which is the design storage ratio to 0.02 by 2080. The yields of the reservoir are higher than the storage because yields are a function of both storage and MAR, so even if storage reduces, much can still be harvested from the flows in the river and canal.

This reduction in storage ratio means that there will be an increase in losses through spillway discharges during the wet season and thus, the water available for use in the dry season will be reduced. The impacts of the storage loss will even be more felt when the inflows decrease due to climate change and increased evaporation due to temperature increases. In a study conducted by Carlos de Araujo et al. (2006) in Brazil to determine the loss of reservoir volume by sedimentation and its impact on water availability in semi-arid regions of Brazil, storage loss on average was found to be 0.56% annually and the reduction of annual yields was 0.37%.

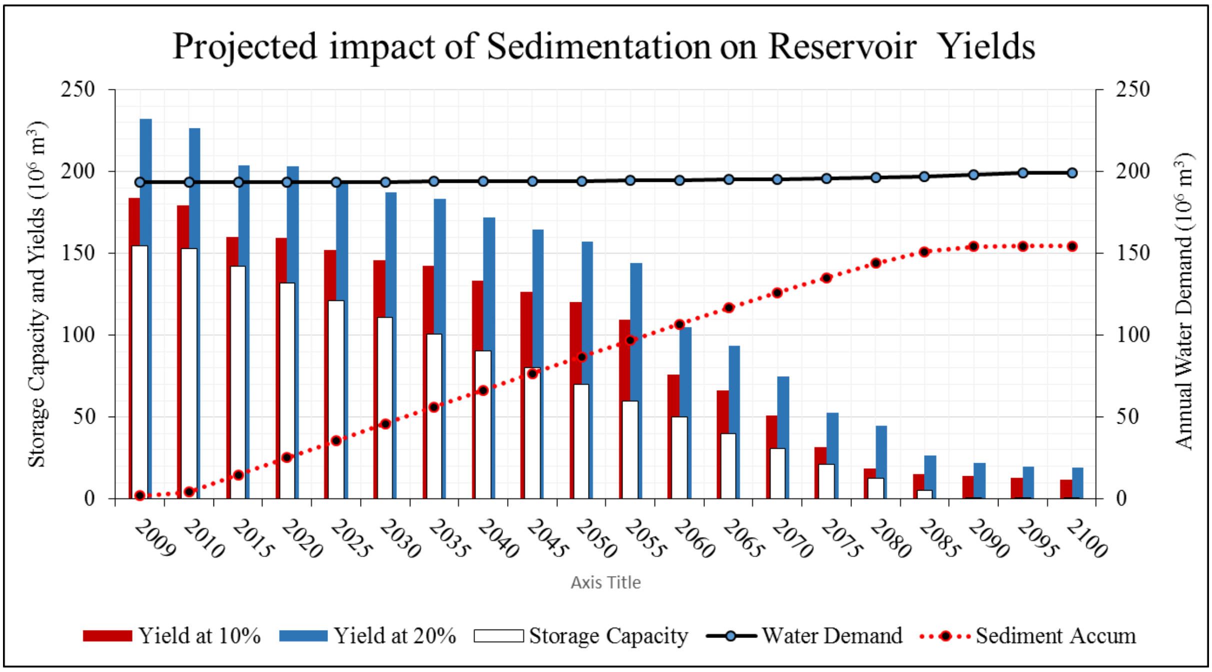

Figure 5-21: Projected impacts of storage capacity loss on reservoir yields against projected water demand

Water demand was analysed and projected into the future in order to determine how it will be affected by the decline in yields. Water demand for both domestic and agricultural use was considered for the analysis. Currently the domestic water demand contributes for less than 1% of the total demand but with the projected population it is expected to contribute about 1.8% by 2080. The water demand for agriculture was kept at a fixed level under the assumption that there will not be addition of land to be irrigated other than the land for which the project was designed for. The results (Appendix 12) show that population will be over 180 000 by 2080, demanding over $3.5 \times 10^6 m^3$ of water annually, assuming that the growth rate remains constant. That means there will be an increase in the water demand from the LUSIP water supply system and the Lubovane reservoir is the major component in the water supply.

In light of sediment accumulation, reduction in annual yields and the gradual increase in water demand, from 2030 the available water will not be able to satisfy the critical demands. This means that there will be need to start reducing the amount of land being irrigated. The yield projections for this study were made under certain assumptions in order to enable ease of analysis. The water demand for irrigation is assumed to be constant in the sense that no additional land will be added for irrigation other than the land considered during design. Another assumption was that no measures will be put in place to mitigate sedimentation rates and that human impacts on soil erosion will not increase or decrease sediment yield of the

Mhlatuzane micro-catchment significantly. The increase of temperatures due to global warming was also assumed that it will not significantly affect evaporation rates in the micro-catchment, even though this is highly unlikely as the micro-catchment is in semi-arid regions.

The annual sedimentation rates (1.36%) obtained in this study are quite high, even above the 1% global average according to the ICOLD (2009). It is therefore very important that sediment reduction measures are implemented in order to ensure reliability of supply. The land rehabilitation efforts by GEF already in place have to be accelerated to reduce sediment yield in the Mhlatuzane micro-catchment. Silt traps also need to be constructed in the upstream tributaries of the Mhlatuzane River and those areas can then be dedicated to sand mining. The sandtrap of the feeder canal has to be seriously optimized, or better yet construction of another sand trapping structure downstream is necessary to reduce sediment loading into the reservoir. It is imperative to also update data by means of continuous bathymetric surveys in order to assess the efficiency of sediment reduction methods.

CHAPTER SIX

6.1 CONCLUSIONS

The main objective of the study was to determine the sediment yield of the Mhlatuzane sub-basin and hence the sedimentation rates of the Lubovane reservoir so as to determine its implications on the lifespan of the LUSI project with respect to continued availability of water for irrigation and domestic use. Several methods were employed to meet the specific objectives of the study and the following conclusions were drawn from the study:

- Significant changes were observed from the study over the years, and those relating directly to soil erosion are changes in bare land and forested areas. There was a 10% decrease in forest and shrubs on average from 1995 to 2015 and also an increase of 11% in bare land. Validation of the land cover classification was done using the confusion matrix and an overall accuracy of 72.8 % which is acceptable, was obtained.
- Sediment yield using RUSLE was found to be 17 $t.ha^{-1}.yr^{-1}$ on average with minimal soil loss (0 - 10 $t.ha^{-1}.yr^{-1}$) covered about 70-80% of the entire catchment in all the years modeled. The observed soil loss from the soil erosion plots was found to be 4.02 $t.ha^{-1}.yr^{-1}$ on average and it was comparable with the modeled soil loss as the observed soil loss was within the class that dominated in the catchment. The sediment yield from the suspended sediment concentration in the Mhlatuzane River was 2.98 $t.ha^{-1}.yr^{-1}$, still within the class range which was dominant in the modeled sediment yield.
- The observed soil loss had a strong positive relationship with rainfall intensity, with an R^2 value of 0.902
- More data on observed soil loss is required to calibrate the RUSLE model in order to make it suitable for use in combination with GIS and remote sensing to model soil erosion in the micro-catchment in future.
- The suspended sediment concentration results showed an annual sediment loading in the reservoir of 1 121 215.62 tons/yr which translated to $0.72x10^6$ m^3, from the feeder canal which had higher sediment concentration and subsequently sediment loading than the Mhlatuzane river. The annual volume of sediment deposited in the reservoir from the sediment concentration (river and canal) was found to be $0.82x10^6$ m^3, leading to 0.53% of storage capacity lost to sedimentation.

- The results from bathymetric survey showed that storage capacity of 14.69×10^6 m^3 (9.5%) has been lost to sedimentation to date, with an annual loss of 1.36%. The lifespan of the reservoir will be reduced to 81 years from the designed 100 years if no measures are implemented to reduce sediment loading.
- The study established that the canal is the main contributor of sediment loading into the reservoir hence the sediment load reduction measures have to be concentrated on it.
- Sediment accumulation was projected and found to decrease reservoir yields at 20% risk level by 1.23% annually and from 2030 onwards, the available water will not be enough to meet critical demands at that risk level if no interventions are effected to reduce sedimentation of the Reservoir.

6.2 RECOMMENDATIONS

- The study recommends that more soil erosion monitoring plots be set up in order to monitor the changes in soil erosion with time, not only in the Mhlatuzane micro-catchment but also in the broader Usuthu catchment to generate useful information for future development.
- It is also recommended that the Department of Water Affairs in Swaziland employs a sediment monitoring program in the main rivers in the country in order to provide information on the sediment flows in the rivers to generate useful information for assessments of sediment loading and future developments.
- Sand trapping in the feeder canal should be optimized in order to reduce the transfer of sediment from the Usuthu River to the reservoir. The current sand trap is not efficient in trapping the silt as the water is turbulent throughout the stretch to the outlet (flow regulating gates). The turbulence results from the force of the water coming in through the pressure channel which is always fully open, as per the recommendations of the operation manual.
- The study recommends the construction of another smaller sand trap about 10km downstream where the velocity of the water would have reduced, allowing adequate settling of larger particles hence reducing the sediment loading into the reservoir.
- It is recommended that the finer material of the sediment removed from the canal be used in the canal servitude to promote grass growth in order to protect the canal and side drains from erosion. The material being transported is mostly from eroded nutrient

rich top soil. The coarser material can be as aggregates to create mortar for repairing cracks, side drains and culverts along the canal stretch.

REFERENCES

Ahmad, I. & Verma, M. K. 2008. Application of USLE Model & GIS in Estimation of Soil Erosion for Tandula Reservoir. *International Journal of Emerging Technology and Advanced Engineering,* 3.

Ampofo, E. A., Muni, R. K. & Bonsu, M. 2001. An Assessment of Sediment Loading into an Agricultural Reservoir in a Semi-Arid Region of Kenya. *West African Journal of Applied Ecology,* 2.

Anderson, J. R., Hardy, E. E., Roach, J. T. & Witmer, R. E. 2001. A Land Use And Land Cover Classification System For Use With Remote Sensor Data. *In:* PECK, D. L. (ed.) *A revision of the land use classification system as presented in U.S. Geological Survey Circular 671* Washington, USA: United States Government Printing Office.

Andersson, L. 2010. *Soil Loss Estimation Based on the USLE / GIS Approach Through Small Catchments - A Minor Field Study in Tunisia.* Master of Science degree in Environmental Engineering / Water Resource Management, Lund University.

Arnoldus, H., Boodt, M. d. & Gabriels, D. 1980. An approximation of the rainfall factor in the Universal Soil Loss Equation. *Assessment of erosion.***,** 127-132.

Blackhurst, R. 2008. *Current and Potential Developments*. *Joint Maputo River Basin Water Resources Study - Mozambique, Swaziland and South Africa.* 8.2-8.4 ed.: Tripartite Permanent Technical Committee (TPTC).

Breetzke, G. D., Koomen, E. & Critchley, W. R. S. 2013. GIS-Assisted Modelling of Soil Erosion in a South African Catchment: Evaluating the USLE and SLEMSA Approach. *InTech Journals***,** 53 - 71.

Brune, G. M. 1953. Trap Efficiency of Reservoirs. *American Geophysical Union,* 34**,** 407 - 419.

Carlos de Araujo, J., Guntner, A. & Bronstert, A. 2006. Loss of reservoir volume by sediment deposition and its impact on water availability in semiarid Brazil. *Hydrological Sciences Journal,* 51**,** 157-170.

Chitata, T., Mugabe, F. T. & Kashaigili, J. J. 2014. Estimation of Small Reservoir Sedimentation in Semi-Arid Southern Zimbabwe. *Journal of Water Resource and Protection,* 6**,** 1017-1028.

Ciesiolka, C. A. A., Yu, B., Rose, C. W., Ghadiri, H., Lang, D. & Rosewell, C. 2004. A simple method for improving soil loss measurement in USLE type experiments. *ISCO 2004 -*

13th International Soil Conservation Organisation Conference - Conserving Soil and Water for Society: Sharing Solutions. Brisbane, Carlifornia, USA.

Collins, F., Jones, D. S., Kowalski, D. G. & Shaw, R. B. 1996. Calculating Revised Universal Soil Loss Equation (RUSLE) Estimates on Department of Defense Lands : A Review of RUSLE Factors and U . S . Army Land Condition-Trend Analysis (LCTA) Data Gaps Center for Ecological Management of Military Lands Department. *Center for Ecological Management of Military Lands, Colorado State University,* 96**,** 9-9.

Coyne-et-Bellier 2012. Lower Usuthu Smallholder Irrigation Project - Water Management Study. Swaziland Water and Agricultural Development Enterprise.

Daffi, R. E. & Ohuchaogu, I. I. 2015. Delineation of River Watershed and Stream Network using Ilwis 3 . 7 . 1 Academic. *International Scientific Research Journal,* 1.

de Vente, J., Verduyn, R., Verstraeten, G., Vanmaercke, M. & Poesen, J. 2011. Factors controlling sediment yield at the catchment scale in NW Mediterranean geoecosystems. *Journal of Soils and Sediments,* 11**,** 690-707.

Didoné, E., Minella, J. & Merten, G. 2015. Quantifying soil erosion and sediment yield in a catchment in southern Brazil and implications for land conservation. *Journal of Soils and Sediments,* 15**,** 2334-2346.

Dube, F. 2011. *Spatial soil erosion hazard assessment and modelling in Mbire District, Zimbabwe: Implications for catchment management.* Master of Science in Integrated Water Resources Management, University of Zimbabwe.

Elwell, H. A. 1978. Modelling soil losses in Southern Africa. *Journal of Agric. Eng. Res,* 23**,** 117-127.

Elwell, H. A. & Stocking, M. A. 1976. Vegetal cover to Estimate Soil Erosion Hazard in Rhodesia. *Geoderma,* 15**,** 61-70.

Esther, M. W. 2009. *Using GIS techniques to determine RUSLE's 'R' and 'LS' factors for Kapingazi River catchment.* Master of Science Degree in Geospatial Information Systems and Remote Sensing, Jomo Kenyatta University of Agriculture and Technology.

Estigoni, M., Matos, A. & Mauad, F. 2014. Assessment of the accuracy of different standard methods for determining reservoir capacity and sedimentation. *Journal of Soils and Sediments,* 14**,** 1224-1234.

FAO 2000. Field measurement of soil erosion and runoff - Chapter 5 Sediment transport. Natural Resources Management and Environment Department - FAO.

Fatoyinbo, F., Ntoampe, K. & Banda, K. 2011. Environmental and Social Management Plan (ESMP) Summary. Lower Usuthu Smallholder Irrigation Project II - (LUSIP II).

Fox, H. R., Moore, H. M., Price, J. P. N., De, D. & Kasri, M. E. L. 1997. Soil erosion and reservoir sedimentation in the High Atlas Mountains , southern Morocco. 233-240.

Gumindoga, W. 2015. GIS-based catchment modeling and DEM hydro-processing: Upper Manyame case study. University of Zimbabwe,.

Hrissanthou, V. 2011. Computation of Lake or Reservoir Sedimentation in Terms of Soil Erosion, Sediment Transport in Aquatic Environments. *InTech Journals*, 332.

Hu, B., Yang, Z., Wang, H., Sun, X., Bi, N. & Li, G. 2009. Sedimentation in the Three Gorges Dam and the future tend of Changjiang (Yangtse River) sediment flux to the sea. *Hydrology and Earth System Sciences*, 13.

ICOLD 2009. Sedimentation and Sustainable use of Reservoirs and River Systems. *In:* COMMITTEE, S. (ed.) *Draft ICOLD Bulletin.* International Commission on Large Dams.

IFAD 2013. Lower Usuthu Sustainable Land Management Project (LUSIP-GEF). *In:* DEPARTMENT, E. A. S. A. D.-P. M. (ed.). International Fund for Agricultural Development.

Jain, M. K. & Kothyari, U. C. 2015. Estimation of soil erosion and sediment yield using GIS. *Hydrological Sciences Journal*, 45, 771 - 786.

Jain, S. K., Singh, P. & Seth, S. M. 2002. Assessment of sedimentation in Bhakra Reservoir in the Western Himalayan egion using Remotely Sensed data. *Hydrological Sciences Journal*, 47, 203-212.

Jebari, S., Berndtsson, R., Bahri, A. & Boufaroua, M. 2010. Spatial soil loss risk and reservoir siltation in semi-arid Tunisia. *Hydrological Siences Journal,*, 55, 121-137.

Kamtukule, S. L. 2008. *nvestigating Impacts of Sedimentation on Water Availability in Small Dams: Case Study of Chamakala II Small Earth Dam in Malawi.* Master of Science Degree in Integrated Water Resources Management, University of Zimbabwe.

Kinnell, P. I. A. 2004. Sediment delivery ratios: a misaligned approach to determining sediment delivery from hillslopes. *Wiley InterScience*.

Kirkby, M. J. & Irvine, B. 2003. Pan-European Soil Erosion Risk Assessment: The PESERA Map. Version 1 ed. Luxembourg: European Soil Bureau Report.

Lin, B., Ho, H., Hsiao, C., Keck, J., Chen, C., Chi, S., Chien, Y. & Tsai, M. Using Multi-scale Sediment Monitoring Techniques to Evaluate Remediation Effectiveness of the

Tsengwen Reservoir Watershed after Sediment Disasters Induced by Typhoon Morakot. the 18th International Conference on Soil Mechanics and Geotechnical Engineering 2013 Paris, France. Technical Committee 102, 571-574.

Lizewski, R. & Bellack, M. 2007. *Water Supply Yield for the Wachusett Reservoir.* Worcester Polytechnic Institute.

Lu, H., Moran, C., Prosse, I. & Sivapalan, M. n.d. Modelling Sediment Delivery Ratio Based on Physical Principles.

Mahabaleshwara, H. & Nagabhushan, H. M. 2014. A Study on Soil Erosion and its Impacts on Floods and Sedimentation. *International Journal of Research in Engineering and Technology,* 03**,** 443-451.

Mann, H. B. 1945. Non-parametric tests against trends. *Econometrica,* 13**,** 245-259.

Manyatsi, A. M. & Brown, R. 2009. National IWRM Survey and Status Report: Swaziland. Global Water Partnership, Southern Africa.

Mashingia, F., Mtalo, F. & Bruen, M. 2013. Validation of remotely sensed rainfall over major climatic regions in Northeast Tanzania. *Physics and Chemistry of the Earth***,** 55-63.

Mavima, G. A., Soropa, G., Makurira, H. & Dzairo, W. 2011. Sedimentation impacts on reservoir as a result of land use on a selected catchment in Zimbabwe. *International Journal of Engineering Science and Technology (IJEST),* 3.

May, L. & Place, C. 2005. A GIS-Based Model of Soil Erosion and Transport. *Freshwater Forum,* 23**,** 48-61.

Mbugua 2009. Using GIS techniques to determine RUSLE'S 'R'and 'LS'factors for Kapingazi river catchment. *Master of Science Research Project Report*.

McPherson, K. R., Freeman, L. A. & Flint, L. E. 2011. Analysis of Methods to Determine Storage Capacity of, and Sedimentation in, Loch Lomond Reservoir, Santa Cruz County, California, 2009. Carlifornia: U.S. Geological Survey Scientific Investigations.

Mhlanga, N. K., Matondo, J. I., Joel, N. & Abul, S. 2012. Evaluation of the Impact of Climate Change on the Inflow to Lubovane Reservoir in Usutu Catchment, Swaziland *Journal of Sustainable Development in Africa,* Volume 14.

Midgley, D. C., Pitman, W. V. & Middleton, B. J. 1994. Surface Water Resources of South Africa 1990. *User's Guide Report.* Pretoria, South Africa: Water Research Commission.

Mitchell, T. B. Potential water yield in semiarid regions. Optimal Allocation of Water Resource (Proceedings of the Exeter Symposium), July 1982 1982. IAHS Publishers.

MNM-Consultants 2002. Report on the Social aspects on the Usuthu River: Swaziland and Mozambique. 3973 KwaNgwanase, South Africa

Mulu, A. & Dwarakish, G. S. 2015. Different Approach for Using Trap Efficiency for Estimation of Reservoir Sedimentation. An Overview. *Aquatic Procedia,* 4**,** 847-852.

Munir, S., Armaghan, M. & Babrus, A. 2014. An Integrated Approach to Hydrographic Surveying of Large Reservoirs—Application to Tarbela Reservoir in Pakistan. *Open Journal of Modern Hydrology,* 4**,** 156-163.

Munthali, K. G., Irvine, B. J. & Murayama, Y. 2011. Reservoir Sedimentation and Flood Control: Using a Geographical Information System to Estimate Sediment Yield of the Songwe River Watershed in Malawi. *Sustainability,* 3**,** 254-269.

Mwendera, E. J. 2006. Rural water supply and sanitation (RWSS) coverage in Swaziland: Toward achieving Millennium Development Goals. *Physics and Chemistry of the Earth,* 31**,** 681-689.

Narasayya, K., Roman, U. C., Sreekanth, S. & Jatwa, S. 2002. Assessment of Reservoir Sedimentation Using Remote Sensing Satellite Imageries.

Nearing, M. A., Foster, G. R., Lane, L. J. & Finkler, S. C. 1989. A process-based soil erosion model for USDA - Water Erosion Prediction Project technology. *Transactions of the ASABE*, 32**,** 1587-1593.

Norton, L. D., Filho, C. C., Cochrane, T. A., Caviglione, J. H., Johanson, L. P. & Marenda, L. D. 2001. Monitoring the Sediment Loading of Itaipu Lake and Modeling of Sheet and Rill Erosion Hazards in the Watershed of Parana River : An Outline of the Project. 321-323.

Pohl, S., Marsh, P. & Bonsal, B. R. 2006. Modelling the impact of Climate Change on Runoff and Annual Water Balance of an Arctic Headwater Basin. *National Hydrology Research Centre,* 60**,** 173-186.

Renard, K. G., Yoder, D. C., Lightle, D. T. & Dabney, S. M. 2010. *Chapter 8: Universal Soil Loss Equation and Revised Universal Soil Loss Equation,* Blackwell Publishing Ltd.

Revel, N. M. T. K., Ranasiri, L. P. G. R., Rathnayake, R. M. C. R. K. & Pathiarana, K. P. P. 2013. Estimation of Sediment Trap Efficiency in Reservoirs - An Experimental Study *European International Journal of Science and Technology,* 2.

Smith, H. J. 1999. Application of Empirical Soil Loss Models in southern Africa: a review. *South African Journal of Plant and Soil,* 16**,** 158-163.

Stone, R. P. & Hilborn, D. 2012. Universal Soil Loss Equation (USLE). 1-8.

Strahler, A. H., Bschetti, L., Foody, G. M., Friedl, M. A., Hansen, M. C., Herold, M., Mayaux, P., Morisette, J. T., Stehman, S. V. & Woodcock, C. E. 2006. *Global Landcover Validation: Recommendations for Evaluation and Accuracy Assessment od Global Landcover maps,* Luxemburg, Office for Official Publications of the European Communities.

Sumi, T. & Hirose, T. 2010. Accumulation of Sediment in Reservoirs. *Encyclopedia of Life Support Systems (EOLSS).*

Suryawan, W. A., Sukri, A. S., Gunawan, Y. & Talanipa, R. 2015. Alternative Management of Erosion and Sediment in Wanggu River Estuary at Kendari City Southeast Sulawesi Province. *Global Journal of Business and Social Science Review,* 03**,** 44-53.

Swaziland 2015. Encyclopedia Britannica Online. *In:* MASSON, J. R. (ed.).

Tamene, L., Park, S. J., Diakau, R. & Vlek, P. L. G. 2006. Analysis of factors determining sediment yield variability in the highlands of north Ethiopia. *Geomorphology,* 76**,** 76-91.

Toxopeus, A. G. 1996. Cibodas: the erosion issue *ILWIS Applications Guide.* International Institute for Aerospace Survey and Earth Sciences (ITC).

Tumbare, M. J. 2013. Sedimentation of small and medium sized dams: discussion issues. *Journal of Engineering, Design and Technology,* 11**,** 112-128.

Tundu, C. 2015. *Analysis of Rivers and Reservoir Sedimentation in Zimbabwe: Case Study of Mazowe.* Master of Science in Water Resources Engineering and Management, University of Zimbabwe.

UNESCO 2011. Sediment Issues & Sediment Management in Large River Basins Interim Case Study Synthesis Report. *In:* INITIATIVE, I. S. (ed.) *Technical Documents in Hydrology.* Beijing: UNESCO office in Beijing & IRTCES.

USDA 1983 *Sedimentation. National Engineering Handbook,* Washington, D.C. , U.S. Department of Agriculture Soil Conservation Service.

Vaezi, A. R., Bahrami, H. A., Sadeghi, S. H. R. & Mahdian, M. H. 2010. Spatial Variability of Soil Erodibility Factor (K) of the USLE in North West of Iran. *Journal of Agriculture, Science and Technology,* 12**,** 241-252.

Vakakis-International 2000. Environmental Impact Assessment Study on the Proposed Lower Usuthu Small-holder Irrigation Development Project - Final Report - Annex C: Hydrology. South Africa.

Van der Kniff, J. M., Jones, R. J. A. & Montanarella, L. 2000. *Soil Erosion risk Assessment in Europe*. *In:* EUROPEAN COMMISSION, E. S. B. (ed.).

van Vliet, J., Bregt, A. K. & Hagen-Zanker, A. 2011. Revisiting Kappa to account for change in the accuracy assessment of land-use change models. *Ecological modelling,* 222**,** 1367-1375.

Vasudeva, P. S. 2006. Lower Usuthu Smallholder Irrigation Project (LUSIP) Swaziland Mid – Term Evaluation Report. South Africa: Intecsa-inarsa.

Wall, G. J., Coote, D. R., Pringle, E. A. & Shelton, I. J. 2002a. *Revised Universal Soil Loss Equation for Application in Canada* Ottawa, Canada, Research Branch, Agriculture and Agri-Food Canada.

Wall, G. J., Wall, G. J., Coote, D. R., Coote, D. R., Pringle, E. a., Pringle, E. a., Shelton, I. J. & Shelton, I. J. 2002b. RUSLEFAC - Revised Universal Soil Loss Equation for Application in Canada: A Handbook for Estimating Soil Loss from Water Erosion in Canada. *Agriculture***,** 117-117.

Walling, D. E. 1983. The sediment delivery problem. *Jornal of Hydrology,* 65**,** 209-237.

Wang, F., Mu, X., Hessel, R., Zhang, W., Ritsema, C. J. & Li, R. 2013. Runoff and Sediment load of the Yan River, China: Changes over the last 60 years. *Hydrology and Earth System Sciences,* 17**,** 2515-2527.

Wang, G., Hapuarachchi, P., Ishidaira, H., Kiem, A. & Takeuchi, K. 2009. Estimation of Soil Erosion and Sediment Yield During Individual Rainstorms at Catchment Scale. *Water Resources Management,* 23**,** 1447-1465.

Whichmeier, W. H. & Smith, D. D. 1978. *Predicting rainfall erosion losses – A guide to conservation planning,* Washington DC, USA., United States Department of Agriculture.

WHO 1997. Guidelines for drinking-water quality. *Surveillance and control of community supplies.* 2nd Edition ed. Geneva: World Health Organization.

Wijesekera, S. & Samarakoon, L. 2001. Extraction of Parameters and Modelling Soil Erosion using GIS in a grid environmnent. *In:* CENTRE FOR REMOTE IMAGING, S. A. P. C., NATIONAL UNIVERSITY OF SINGAPORE (ed.) *22nd Asian Conference on Remote Sensing.* Singapore: Asina Institute of Technology.

Wischmeier, W. H. & Smith, D. D. 1978. Predicting rainfall erosion losses-A guide to conservation planning. *Predicting rainfall erosion losses-A guide to conservation planning*.

Wordofa, G. 2011. *Soil Erosion Modelling Using GIS and RUSLE on the Eurajoki Watershed Finland.* Degree Program in Environmental Engineering, Tampere University of Applied Sciences.

LIST OF APPENDICES

APPENDIX 1: Silt deposits upstream of the Lubovane reservoir in the Mhlatuzane River (left) and the FC discharge point (right)

*Images taken of 5 February 2016

APPENDIX 2: Annual Average rainfall distribution in the Mhlatuzane micro-catchment

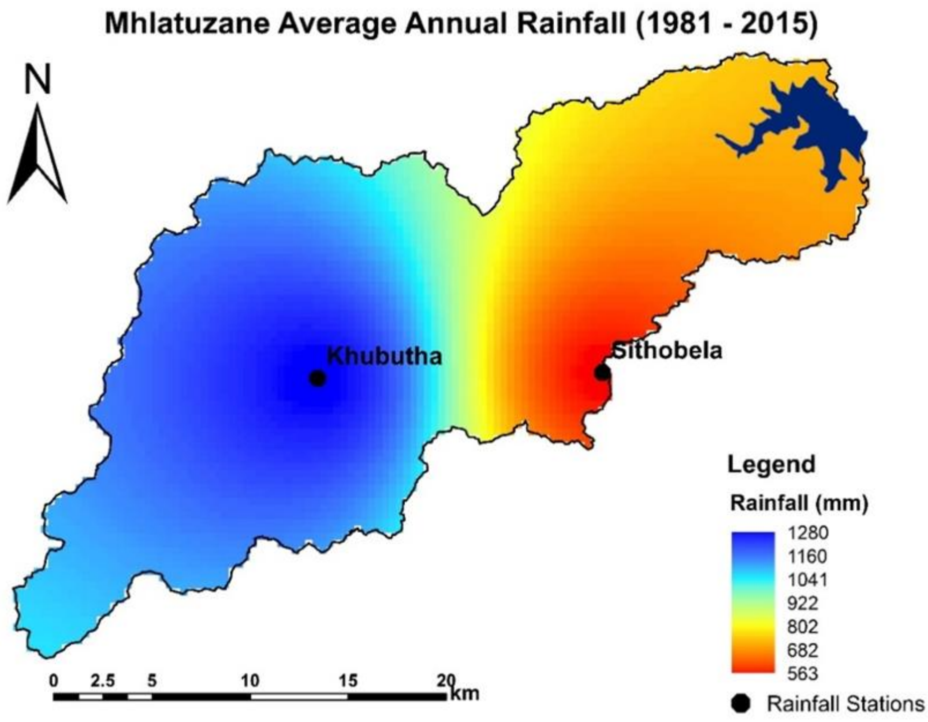

APPENDIX 3: Monthly evaporation rates from the Big Bend Met. Station

Month	Et_o (mm/day)
January	5.8
February	4.8
March	4.3
April	3.2
May	2.5
June	1.9
July	2.4
August	2.9
September	3.7
October	4.2
November	4.2
December	5.8

APPENDIX 4: Annual Rainfall for Khubutha and Sithobela measuring rainfall stations

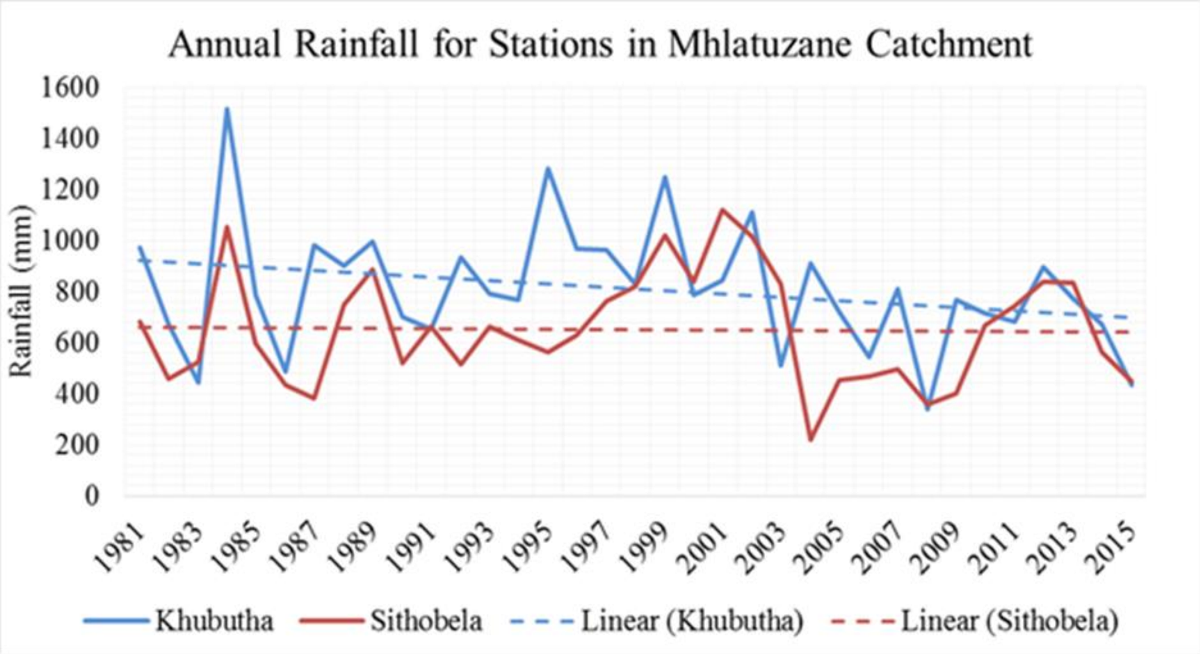

APPENDIX 5: Thiessen polygons showing areal influence of rainfall stations

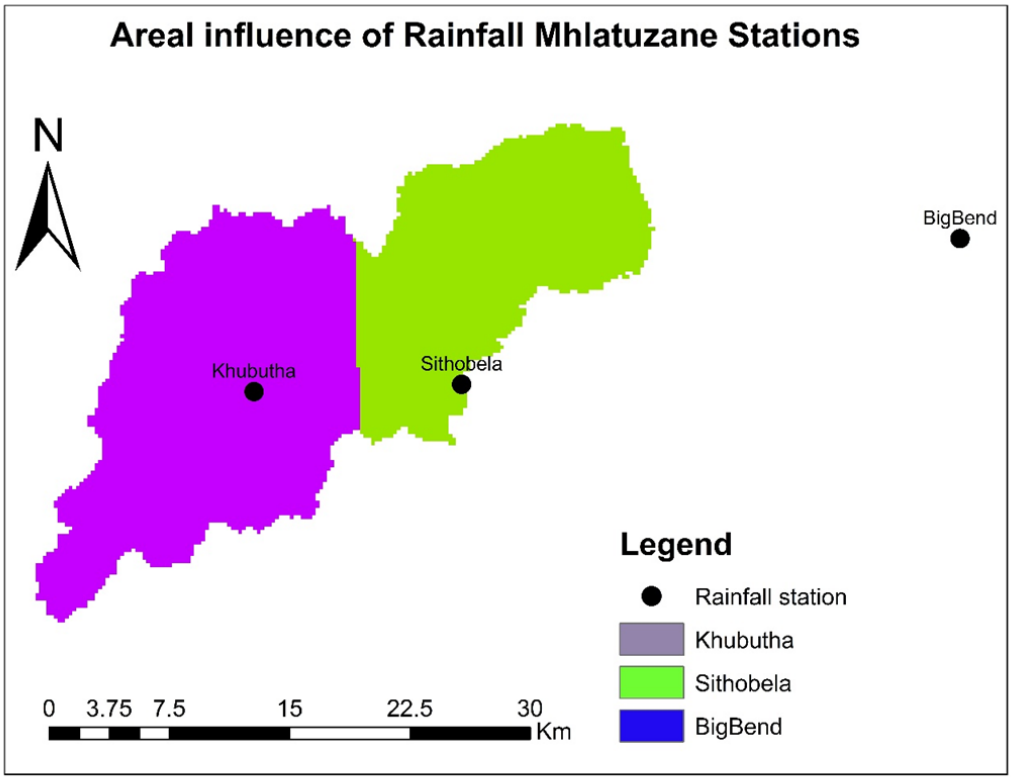

APPENDIX 6: Rainfall Trend analysis results from XLSTAT

XLSTAT 2016.02.27942 - Mann-Kendall trend tests - Start time: 6/19/2016 at 3:08:30 PM

Time series: Workbook = Sithobela Rainfall Data - Annual.xlsx / Sheet = Combined Rainfall / Range = 'Combined Rainfall'!$B$1:$B$36 / 35 rows and 1 column

Date data: Workbook = Sithobela Rainfall Data - Annual.xlsx / Sheet = Combined Rainfall / Range = 'Combined Rainfall'!$A$1:$A$36 / 35 rows and 1 column

Confidence interval (%): 5

Confidence interval (%)(Sen's slope): 5

Summary statistics:

Variable	Observations	Obs. with missing data	Obs. without missing data	Minimum	Maximum	Mean	Std. deviation
Annual Rainfall	35	0	35	345.654	1450.860	753.973	224.871

Mann-Kendall trend test / Two-tailed test (Annual Rainfall):

Kendall's tau	-0.123
S	-73.000
Var(S)	0.000
p-value (Two-tailed)	0.309
Alpha	0.05

The p-value is computed using an exact method.

Test interpretation:

H0: There is no trend in the series

Ha: There is a trend in the series

The risk to reject the null hypothesis H0 while it is true is 30.93%.

APENDIX 7a: Sediment collected per individual storm event from the four erosion monitoring plots

PLOT ID	Dimensions (m)	Plot Area (m^2)	Date collected	Rainfall (mm)	Duration (hrs.)	Sediment collected (g)	Sediment collected per mm of rainfall (g/mm)	Erosion rates (kg/km^2)	Erosion rates (t/km^2)	Erosion rates (t/ha/storm)	Comment
Plot 1	10 x 8	80	15-Jan-16	72	10	6986.90	97.04	87336.25	87.34	0.87	Pilot
Plot 1	10 x 8	80	26-Jan-16	24	24	1609.36	67.06	20117.05	20.12	0.20	
Plot 1	10 x 8	80	22-Feb-16	7	36	0.00	0.00	0.00	0.00	0.00	No Run-off/Soil loss
Plot 2	12 x 8	96	22-Feb-16	11	24	239.20	21.75	2491.67	2.49	0.02	
Plot 3	11 x 4	44	22-Feb-16	2	12	0.00	0.00	0.00	0.00	0.00	No Run-off/Soil loss
Plot 4	9 x 7	63	22-Feb-16	9	48	0.00	0.00	0.00	0.00	0.00	No Run-off/Soil loss
Plot 1	10 x 8	80	09-Mar-16	53	10	4981.39	93.99	62267.38	62.27	0.62	
Plot 2	12 x 8	96	09-Mar-16	38	14	2169.23	57.09	22596.15	22.60	0.23	
Plot 3	11 x 4	44	09-Mar-16	32	12	505.3	15.79	11484.09	11.48	0.11	
Plot 4	9 x 7	63	09-Mar-16	0	0	0	0.00	0.00	0.00	0.00	No Rain
Plot 1	10 x 8	80	15-Mar-16	36	60	1268.3	35.23	15853.75	15.85	0.16	
Plot 2	12 x 8	96	15-Mar-16	20	20	1475.4	73.77	15368.75	15.37	0.15	
Plot 3	11 x 4	44	15-Mar-16	9	9	107.9	11.99	2452.27	2.45	0.02	
Plot 4	9 x 7	63	15-Mar-16	65	48	95	1.46	1507.94	1.51	0.02	

APPENDIX 7b: Observed soil loss from the soil erosion plots (January – March 2016)

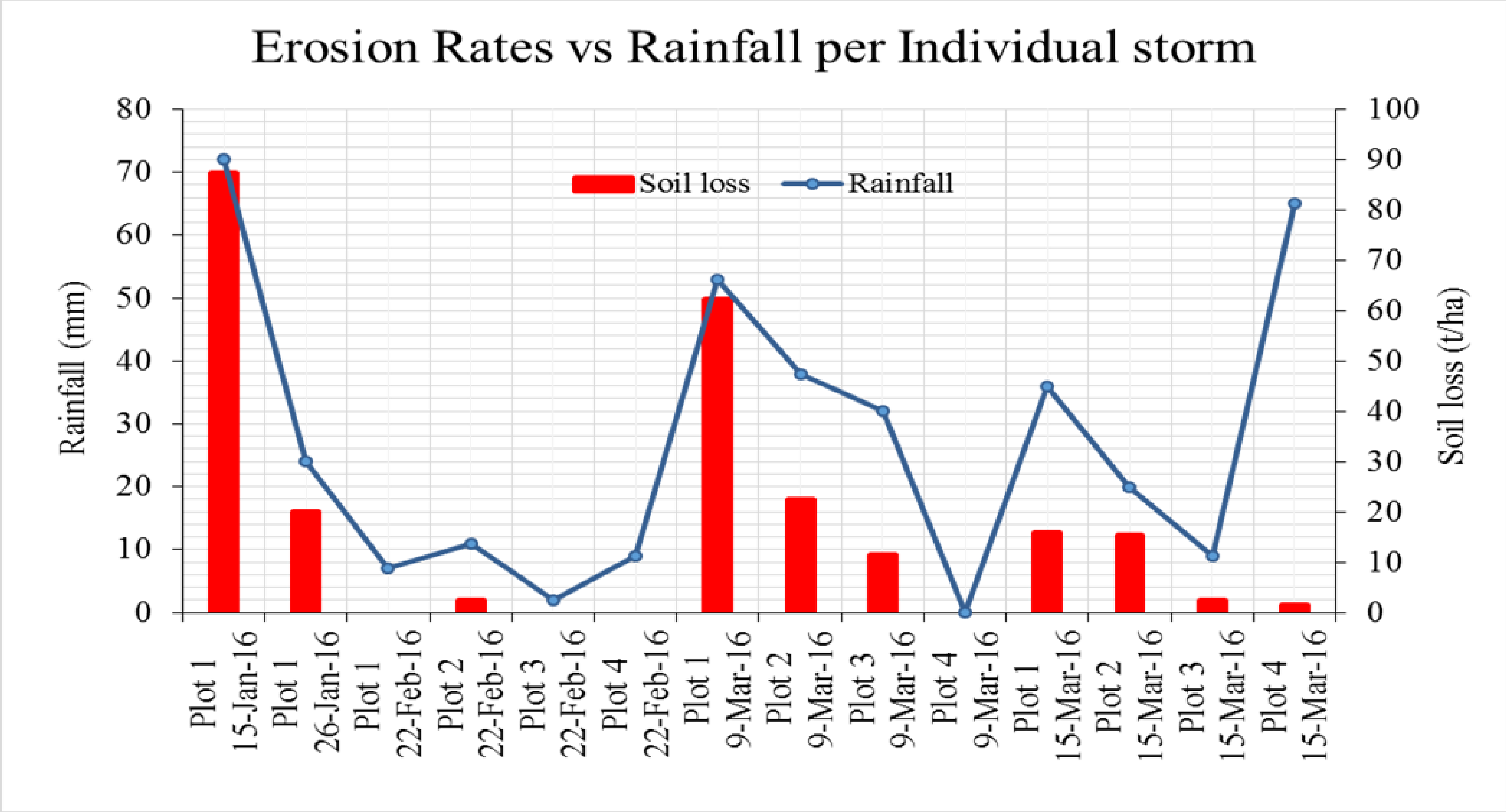

APPENDIX 8: Observed sediment concentration in the Mhlatuzane River and Feeder canal

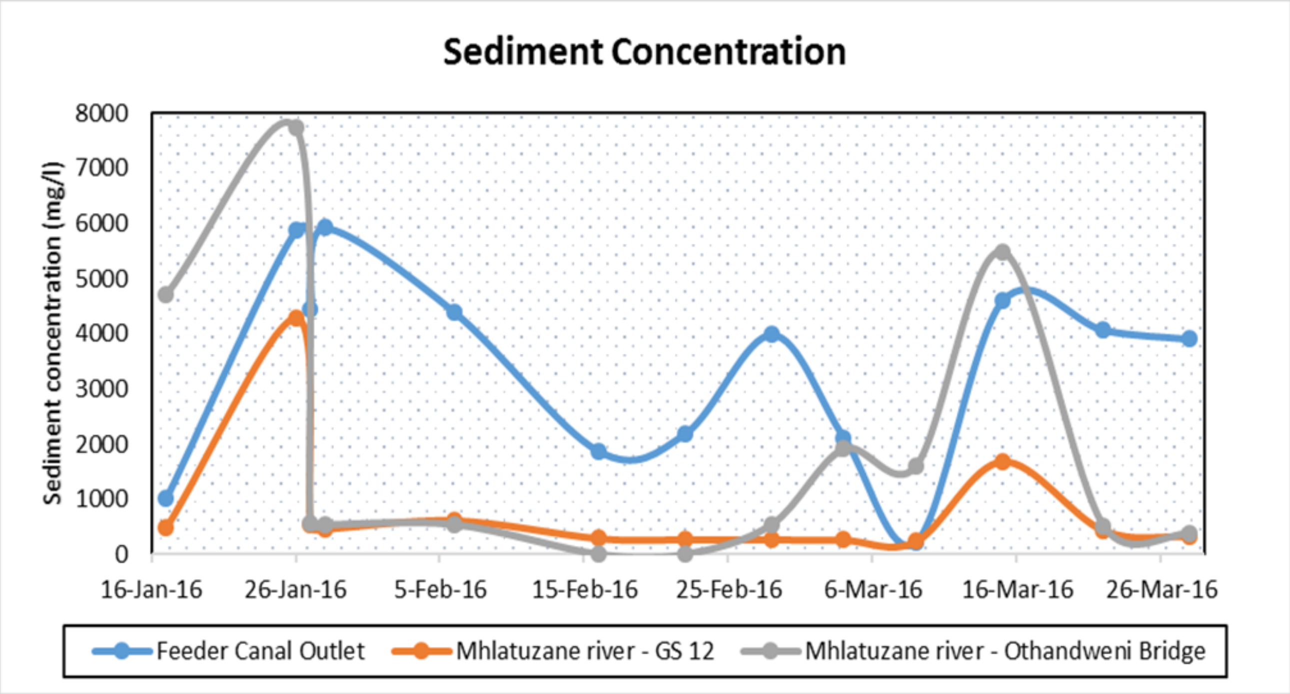

APPENDIX 9: Sample of the 3270 Bathymetric points collected in the reservoir

Waypoint	Lat	Lon	Elevation (m.a.s.l)
532	31.7141	-26.7563	219.18
533	31.71373	-26.756	218.68
534	31.71348	-26.7558	218.08
535	31.71318	-26.7556	217.18
536	31.71303	-26.7554	215.98
537	31.71287	-26.7553	215.28
538	31.71268	-26.7551	214.98
539	31.71242	-26.7549	214.38
540	31.71222	-26.7547	214.18
541	31.71202	-26.7545	213.18
542	31.71188	-26.7543	205.88
543	31.71157	-26.754	212.68
544	31.71125	-26.7537	211.58
545	31.71082	-26.7534	211.38
546	31.71063	-26.7532	209.58
547	31.7104	-26.7531	209.38
548	31.7102	-26.7528	208.38
549	31.70985	-26.7525	206.18
550	31.70953	-26.7522	210.38
551	31.70915	-26.7518	210.78
552	31.709	-26.7516	206.68
553	31.7088	-26.7514	199.28
554	31.70858	-26.7512	199.58
555	31.70838	-26.7509	196.58
556	31.70818	-26.7507	195.08
557	31.70798	-26.7504	192.98
558	31.70778	-26.7502	192.48
559	31.70758	-26.7499	190.78
560	31.70737	-26.7497	191.88

APPENDIX 10a: Original Area-Level-Capacity relationships for the Lubovane Reservoir

Reservoir Level (m)	Reservoir Area (km^2)	Reservoir Storage (Mm^3)	Comment
184	0.00	0.000	
185	0.01	0.005	
186	0.02	0.020	
187	0.02	0.045	
188	0.03	0.075	
189	0.04	0.110	
190	0.05	0.155	
191	0.10	0.230	
192	0.15	0.355	
193	0.20	0.530	
194	0.25	0.755	
195	0.30	1.030	
196	0.45	1.405	
197	0.60	1.930	
198	0.76	2.610	
199	0.91	3.445	
200	1.00	4.400	
201	1.33	5.565	
202	1.60	7.030	
203	**1.87**	**8.765**	Dead Storage
204	2.15	10.775	
205	2.42	13.060	
206	2.85	15.695	
207	3.27	18.755	
208	**3.70**	**22.240**	Minimum Operating level
209	4.13	26.155	
210	4.56	30.500	
211	5.11	35.335	
212	5.66	40.720	
213	6.21	46.655	
214	6.76	53.140	
215	7.31	60.175	
216	8.01	67.835	
217	8.71	76.195	
218	9.40	85.250	
219	10.10	95.000	
220	10.79	105.445	

221	11.57	116.625	
222	12.35	128.585	
223	13.12	141.320	
224	**13.90**	**154.830**	Full Supply Level
225	14.68	169.120	
226	15.54	184.230	
227	16.40	200.200	
228	17.37	217.085	
229	18.13	234.835	
230	**18.99**	**253.395**	Crest Level

APPENDIX 10b: New Area-Level-Capacity relationships for the Lubovane Reservoir

Elevations (m)	New Area	New Capacity	Comment
184	0.000	0.000	
185	0.002	0.002	
186	0.004	0.005	
187	0.007	0.011	
188	0.011	0.020	
189	0.015	0.032	
190	0.020	0.049	
191	0.029	0.073	
192	0.083	0.128	
193	0.138	0.236	
194	0.233	0.417	
195	0.363	0.709	
196	0.498	1.138	
197	0.608	1.688	
198	0.743	2.359	
199	0.904	3.179	
200	1.097	4.173	
201	1.351	5.388	
202	1.632	6.875	
203	**1.910**	**8.644**	Dead Storage
204	2.200	10.700	
205	2.509	13.045	
206	2.862	15.723	
207	3.233	18.765	
208	**3.617**	**22.186**	Minimum Operating Level
209	3.989	25.983	
210	4.382	30.163	

211	4.804	34.750	
212	5.231	39.758	
213	5.681	45.211	
214	6.162	51.128	
215	6.669	57.535	
216	7.186	64.456	
217	7.677	71.885	
218	8.116	79.778	
219	8.540	88.101	
220	9.064	96.883	
221	9.760	106.280	
222	10.629	116.459	
223	11.814	127.636	
224	**13.217**	**140.141**	Full Supply Level
225	14.660	154.080	
226	16.210	169.508	
227	17.895	186.550	
228	19.647	205.327	
229	21.288	225.807	
230	22.744	247.833	

APPENDIX 11: T.B. Mitchel Yield Curves used for estimating yields

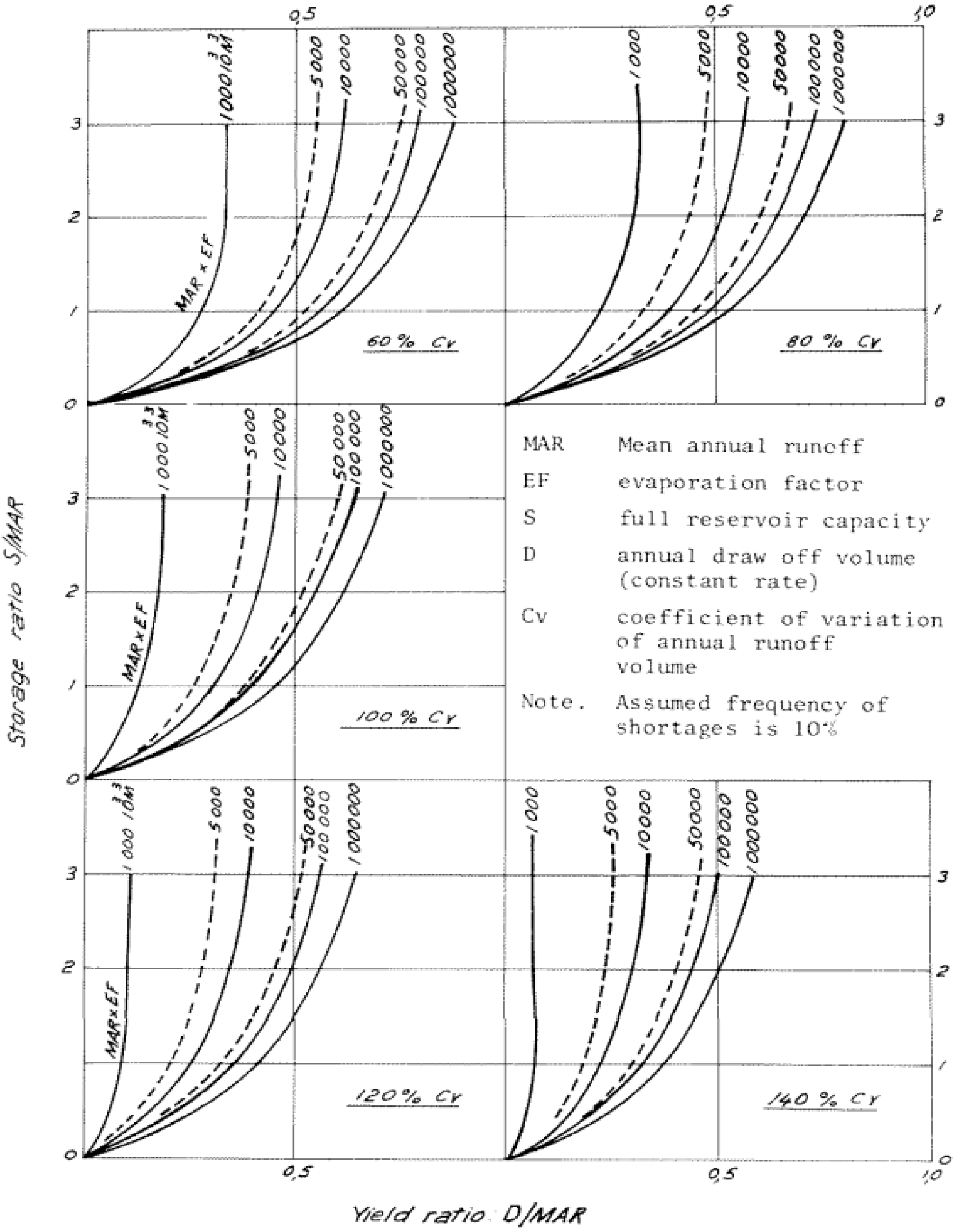

APPENDIX 12: Projected population in the LUSIP project development area

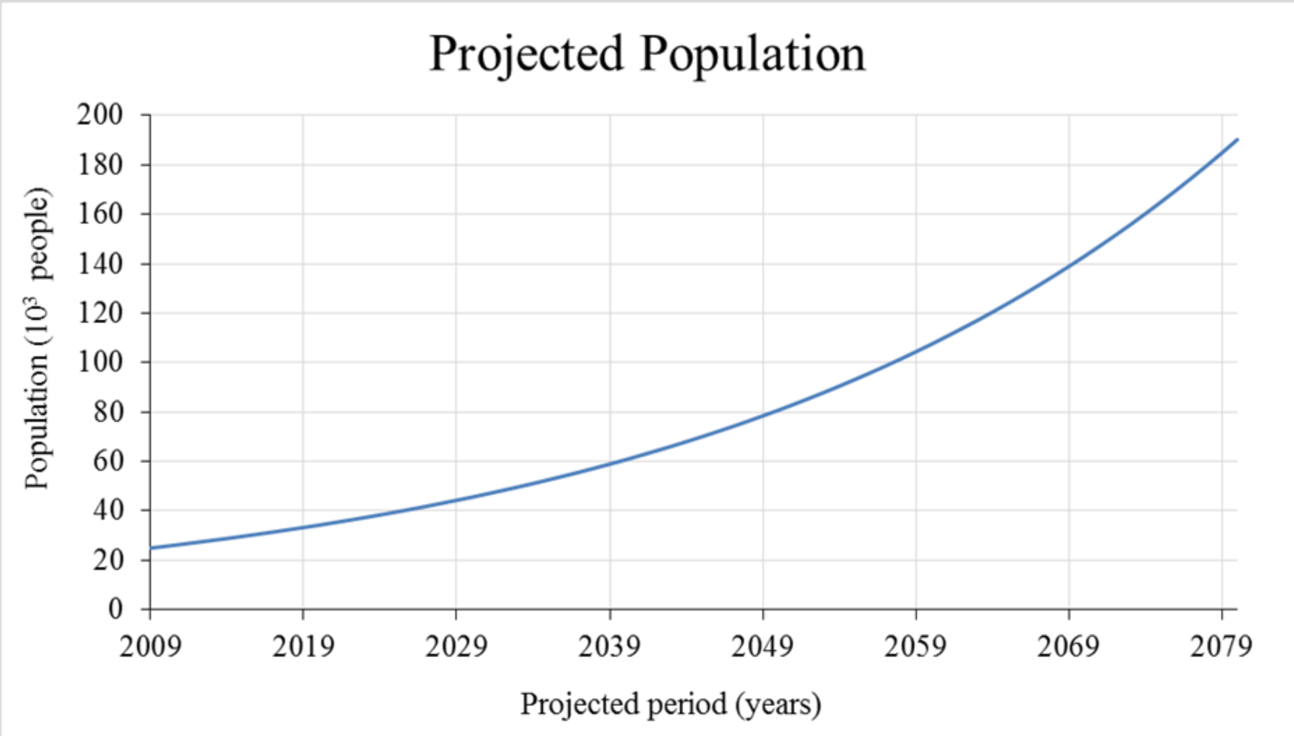

APPENDIX 13: Projected annual domestic and agricultural water demand